Course of lectures on magnetism of lanthanide ions under varying ligand and magnetic fields

RWTH Aachen University, February, 18-21, 2008

Heiko Lueken
Institute of Inorganic Chemistry

Contents

1 Magnetic properties of free lanthanide ions: an overview

1.1 Electronic structure and Hund's rules

The 4f electrons of free Ln ions are influenced by nuclear attraction, interelectronic repulsion (H_{ee}) and spin-orbit coupling (H_{SO}), where $H_{\mathrm{ee}} > H_{\mathrm{SO}}$. To determine the free ion ground multiplet $^{2S+1}L_J$ the following scheme is helpful (N: no. of 4f electrons):

Ln^{3+}	Ce	Pr	Nd	*Pm*	Sm	Eu	Gd	Tb	Dy	Ho	Er	Tm	Yb	Lu
N	1	2	3	4	5	6	7	8	9	10	11	12	13	14
m_s	$+\frac{1}{2}$	$+\frac{1}{2}$	$+\frac{1}{2}$	$+\frac{1}{2}$	$+\frac{1}{2}$	$+\frac{1}{2}$	$+\frac{1}{2}$	$-\frac{1}{2}$	$-\frac{1}{2}$	$-\frac{1}{2}$	$-\frac{1}{2}$	$-\frac{1}{2}$	$-\frac{1}{2}$	$-\frac{1}{2}$
m_l	$+3$	$+2$	$+1$	0	-1	-2	-3	$+3$	$+2$	$+1$	0	-1	-2	-3

1. The term with maximum S lies lowest in energy ($\sum_i m_{s,i} = M_S \rightarrow S$).
2. For a given spin multiplicity, the term with highest L lies lowest in energy ($\sum_i m_{l,i} = M_L \rightarrow L$).
3. For less than half-filled subshells, the level with the lowest value of J lies lowest ($J = |L - S|$), while the highest J lies lowest when a subshell is more than half full ($J = L + S$).

Examples:

Pr^{3+} $[4\mathrm{f}^2]$: $S = 1$, $L = 5$, $J = 4$; $(^3H_4)$

Dy^{3+} $[4\mathrm{f}^9]$: $S = \frac{5}{2}$, $L = 5$, $J = \frac{15}{2}$; $(^6H_{15/2})$

1.2 Energetic effects

The energy splittings of the electronic states of a magnetic system [1] are produced by H_{ee}, H_{SO}, the ligand field (H_{LF}), interatomic exchange interactions (H_{ex}), and the applied magnetic field (H_{mag}). The following scheme shows the order of H_{ee}, H_{SO}, and H_{LF}.

$3\mathrm{d}^{\mathrm{N}}$	H_{ee}	$>$	H_{LF}	$>$	H_{SO}	weak field
	H_{LF}	$>$	H_{ee}	$>$	H_{SO}	strong field
	H_{LF}	$\approx$	H_{ee}	$>$	H_{SO}	intermediate field
$4\mathrm{f}^{\mathrm{N}}$	H_{ee}	$>$	H_{SO}	$>$	H_{LF}	(a)
	H_{ee}	$>$	H_{SO}	$\gg$	H_{LF}	(b)

(a) strong field lanthanide system ; (b) weak field lanthanide system

Table 1 gives approximate sizes of the corresponding energy splittings, including H_{ex} and H_{mag}.

---

[1] Localised electrons are presupposed.

Table 1 Effects acting on d and f electrons.

Effect		System	Energy equivalent wavenumber/cm$^{-1\,a)}$
Electron-electron interaction	H_{ee}	3d, 4d, 5d 4f, 5f	$3\mathrm{d} > 4\mathrm{d} > 5\mathrm{d} \approx 10^{4\ b)}$ $4\mathrm{f} > 5\mathrm{f} \approx 10^{4\ b)}$
Ligand-field potential	H_{LF}	3d, 4d, 5d 4f 5f	$3\mathrm{d} < 4\mathrm{d} < 5\mathrm{d} \approx 2 \times 10^{4\ b)}$ $\approx 10^2$ $\approx 10^3$
Spin-orbit coupling	H_{SO}	3d, 4d, 5d 4f, 5f	$3\mathrm{d} < 4\mathrm{d} < 5\mathrm{d} \approx 10^{3\ b)}$ $4\mathrm{f} < 5\mathrm{f} \approx 10^{3\ b)}$
Exchange interaction	H_{ex}	nd 4f nd–4f	$\leq 10^2$ < 1 < 10
Magnetic field	H_{mag}		≈ 0.5 (1 T)

$^{a)}$ Conversion to other units, see Table 34 (Appendix).
$^{b)}$ Approximate value according to ref. [1].

Inspecting Table 1, two points are important for 4f ions: (i) H_{ex} is at least two orders of magnitude smaller than H_{LF} (and H_{SO}). (ii) H_{mag} has to be chosen carefully on account of comparable magnitude of H_{ex} and H_{mag}. Therefore, in order to detect H_{ex}, H_{LF} should be modelled most exactly and H_{mag} should be very weak.

1.3 Magnetic behaviour of Ln ions

The variation of χ_{m}, μ (permanent magnetic moment corresponding with the Curie constant C), μ_{eff} (effective Bohr magneton number[2]), $\chi_{\mathrm{m}}T$, $\boldsymbol{M}_{\mathrm{m}}$ as a function of T and B_0 serves to characterize the low-lying electronic states of the magnetic systems.

1.3.1 Ground multiplet thermally isolated ($\Delta E(J, J-1) \gg k_{\mathrm{B}}T$)

Neglecting H_{LF}, Hund's formula eq. (1)

$$\boxed{\mu \approx g_J\sqrt{J(J+1)}\,\mu_{\mathrm{B}}} \qquad (\text{except} \quad 4\mathrm{f}^4, 4\mathrm{f}^5, 4\mathrm{f}^6 \quad \text{systems}) \tag{1}$$

applies, where J is the total angular momentum of the ground multiplet and g_J the Landé factor

$$g_J = 1 + \frac{J(J+1) + S(S+1) - L(L+1)}{2J(J+1)}. \tag{2}$$

$S, L,$ and J correspond to the total spin angular momentum, the total orbital angular momentum and the total angular momentum, respectively, of the ground multiplet.

---

[2] Note that the empirical number μ_{eff} has no connexion with the permanent moment μ except when Curie's law is obeyed [2].

A graph showing the variation μ_{eff} *vs.* T is recommended for 4f/5f systems $^{3)}$. According to Kramers' rule [4], ions with an odd number of 4f electrons (half integral values of J) have always a degenerate ground state obeying the Curie law at low temperature (regardless the symmetry of H_{LF}, but presupposed that (i) solely the ligand field (LF) ground state is occupied and (ii) cooperative magnetic effects are absent). For an even number of f electrons, degenerate as well as singlet ground states can be found depending on the symmetry of H_{LF}. A singlet ground state produces temperature independent paramagnetism (TIP) at low temperature.

Going to 5f electron systems, H_{SO} and H_{LF} increase according to the larger effective nuclear charge and according to the fact that 5f electrons are more accessible for ligands. No simple approximation can be made. So, the only possibility to predict the magnetic behaviour for 5f ions are computational methods.

1.3.2 Ground multiplet thermally not isolated ($\Delta E(J, J-1) \approx k_{\text{B}}T$)

$$\text{General equation:} \quad \chi_{\text{m}} = \mu_0 \frac{N_{\text{A}}\mu_{\text{B}}^2}{3k_{\text{B}}T} \frac{\sum\limits_{J=L-S}^{L+S} (2J+1)\Lambda_J \exp\left\{-\frac{\lambda_{LS}}{2}\frac{J(J+1)}{k_{\text{B}}T}\right\}}{\sum\limits_{J=L-S}^{L+S} (2J+1) \exp\left\{-\frac{\lambda_{LS}}{2}\frac{J(J+1)}{k_{\text{B}}T}\right\}} \tag{3}$$

$$\text{where} \quad \Lambda_J = g_J^2\, J(J+1) + 2(g_J-1)(g_J-2)\frac{k_{\text{B}}T}{\lambda_{LS}} \quad \text{and} \quad \lambda_{LS} = \pm\frac{\zeta}{2S}$$

The g_J values are given by eq. (2) (exception: $g_J = L+2$ for $J = 0$). The term spin-orbit coupling parameter λ_{LS} is positive for ions with less than half-full subshell and negative for ions with more than half-full subshell.

Example 1.1 4f ^{6} ($\text{Sm}^{2+}, \text{Eu}^{3+}$)

$$\begin{aligned}
\chi_{\text{m}} &= \mu_0 \frac{N_{\text{A}}\mu_{\text{B}}^2}{3k_{\text{B}}T}\mu_{\text{eff}}^2 \quad \text{where} \\
\mu_{\text{eff}}^2 &= Z^{-1}\Bigg\{144\frac{k_{\text{B}}T}{\zeta} + \left(\frac{27}{2} - 9\frac{k_{\text{B}}T}{\zeta}\right)\exp\left(-\frac{\zeta}{6k_{\text{B}}T}\right) \\
&\quad + \left(\frac{135}{2} - 15\frac{k_{\text{B}}T}{\zeta}\right)\exp\left(-\frac{\zeta}{2k_{\text{B}}T}\right) + \left(189 - 21\frac{k_{\text{B}}T}{\zeta}\right)\exp\left(-\frac{\zeta}{k_{\text{B}}T}\right) \\
&\quad + \left(405 - 27\frac{k_{\text{B}}T}{\zeta}\right)\exp\left(-\frac{5\zeta}{3k_{\text{B}}T}\right) + \left(\frac{1485}{2} - 33\frac{k_{\text{B}}T}{\zeta}\right)\exp\left(-\frac{5\zeta}{2k_{\text{B}}T}\right) \\
&\quad + \left(\frac{2457}{2} - 39\frac{k_{\text{B}}T}{\zeta}\right)\exp\left(-\frac{7\zeta}{2k_{\text{B}}T}\right)\Bigg\} \qquad \text{and} \\
Z &= \Bigg\{1 + 3\exp\left(-\frac{\zeta}{6k_{\text{B}}T}\right) + 5\exp\left(-\frac{\zeta}{2k_{\text{B}}T}\right) + 7\exp\left(-\frac{\zeta}{k_{\text{B}}T}\right) \\
&\quad +9\exp\left(-\frac{5\zeta}{3k_{\text{B}}T}\right) + 11\exp\left(-\frac{5\zeta}{2k_{\text{BT}}}\right) + 13\exp\left(-\frac{7\zeta}{2k_{\text{B}}T}\right)\Bigg\}
\end{aligned} \tag{4}$$

---

[3] We recommend this plot or alternatively μ_{eff}^2 *vs.* T instead of the $\chi_{\text{m}}T$ *vs.* T plot for two reasons: (i) The number μ_{eff} has the same numerical value in the SI and CGS-emu system, (ii) μ_{eff} is easily compared with the lanthanide's corresponding free-ion value $\mu_{\text{eff}} = g_J\sqrt{J(J+1)}$ [5].

Eq. (4) is calculated with $g_J = 3/2$ for the multiplets $J = 1, 2, 3, 4, 5, 6$, $g_J = 5$ for $J = 0$, and $\lambda_{LS} = \zeta/6$.

Table 2: Lanthanide ions: term symbol (ground state), one-electron spin-orbit coupling parameter $\zeta_{4\mathrm{f}}$ [cm^{-1}], g_J, $g_J J$, $g_J[J(J+1)]^{1/2}$ and $\mu_{\mathrm{eff}}^{\exp}(295\,\mathrm{K})$ [7]

Ln^{3+}	$4\mathrm{f}^N$	$^{2S+1}L_J$	$\zeta_{4\mathrm{f}}{}^{a)}$	g_J	$g_J J$	$g_J[J(J+1)]^{1/2}$	$\mu_{\mathrm{eff}}^{\exp\,b)}$
$\mathrm{La}^{3+c)}$	$4\mathrm{f}^0$	$^1S_0$				0	
Ce^{3+}	$4\mathrm{f}^1$	$^2F_{5/2}$	625	6/7	15/7	2.535	2.3–2.5
Pr^{3+}	$4\mathrm{f}^2$	$^3H_4$	758	4/5	16/5	3.578	3.4–3.6
Nd^{3+}	$4\mathrm{f}^3$	$^4I_{9/2}$	884	8/11	36/11	3.618	3.4–3.5
Pm^{3+}	$4\mathrm{f}^4$	$^5I_4$	1000	3/5	12/5	2.683	$2.9^{d)}$
Sm^{3+}	$4\mathrm{f}^5$	$^6H_{5/2}$	1157	2/7	5/7	0.845	1.6
Eu^{3+}	$4\mathrm{f}^6$	$^7F_0$	1326	0	0	0	3.5
Gd^{3+}	$4\mathrm{f}^7$	$^8S_{7/2}$	1450	2	7	7.937	7.8–7.9
Tb^{3+}	$4\mathrm{f}^8$	$^7F_6$	1709	3/2	9	9.721	9.7–9.8
Dy^{3+}	$4\mathrm{f}^9$	$^6H_{15/2}$	1932	4/3	10	10.646	10.2–10.6
Ho^{3+}	$4\mathrm{f}^{10}$	$^5I_8$	2141	5/4	10	10.607	10.3–10.5
Er^{3+}	$4\mathrm{f}^{11}$	$^4I_{15/2}$	2369	6/5	9	9.581	9.4–9.5
Tm^{3+}	$4\mathrm{f}^{12}$	$^3H_6$	2628	7/6	7	7.561	7.5
Yb^{3+}	$4\mathrm{f}^{13}$	$^2F_{7/2}$	2870	8/7	4	4.536	4.5
$\mathrm{Lu}^{3+b)}$	$4\mathrm{f}^{14}$	$^1S_0$				0	

[a)] The relation between ζ_{4f} and λ_{LS} of the Russell-Saunders ground term is given by $\lambda_{\mathrm{LS}} = \pm(\zeta_{4\mathrm{f}}/2S)$, where (+) and (−) sign correspond to $N \leq 2l+1$ and $N \geq 2l+1$, respectively.

[b)] Definition: $\chi_{\mathrm{m}} = \mu_0\, N_A\, \mu_{\mathrm{B}}^2\, \mu_{\mathrm{eff}}^2/(3\, k_{\mathrm{B}} T)$.

[c)] diamagnetic

[d)] observed for Nd^{2+} compounds.

Problems

1. Verify the Russell-Saunders ground multiplets for Nd^{2+} and Er^{3+} given in Table 2.
2. Evaluate the susceptibility equation for a free p^1 system perturbed by spin-orbit coupling. (Hint: Apply eq. (3). Note that for the single-electron system $\lambda_{LS} \equiv \zeta$. Solutions are given in section 5.)

2 Theory of free lanthanide ions

2.1 Functions

Schrödinger equation (spin ignored):

$$\Big[-\frac{\hbar^2}{2m_e}\nabla^2 - e\hat{V}(r)\Big]\psi(\boldsymbol{r}) = E\psi(\boldsymbol{r}) \tag{5}$$

For convenience the eigenfunctions (atomic orbitals) are given in spherical polar coordinates:

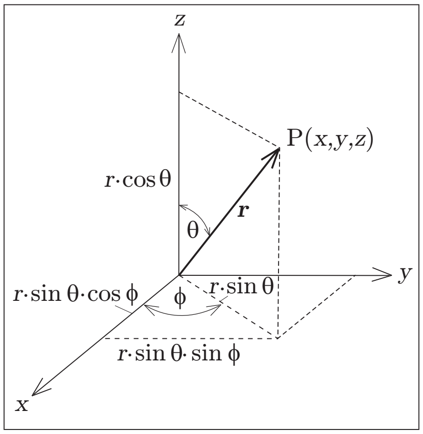

$$\begin{aligned} x &= r\cdot\sin\theta\cdot\cos\phi \\ y &= r\cdot\sin\theta\cdot\sin\phi \\ z &= r\cdot\cos\theta \end{aligned} \tag{6}$$

$$\begin{aligned} r^2 &= x^2+y^2+z^2 \\ \cos\theta &= z/r \\ \tan\phi &= y/x \end{aligned} \tag{7}$$

Fig. 1: Relation between cartesian coordinates and spherical polar coordinates

$$\psi(\boldsymbol{r}) = \psi_{n,l,m_l}(r,\theta,\phi) = \underbrace{R_{n,l}(r)}_{\text{radial f.}}\ \underbrace{Y^l_{m_l}(\theta,\phi)}_{\text{angular f.}} = R_{n,l}(r)\,\Theta^l_{m_l}(\theta)\sqrt{\frac{1}{2\pi}}\,e^{im_l\phi}$$

The functions $Y^l_{m_l}(\theta,\phi)$ are spherical harmonics specified by the quantum numbers l and m_l (Table 3). Real functions (Table 4) are gained by linear combinations

$$\begin{array}{rcll} \frac{1}{\sqrt{2}}\left[-\psi_{n,l,m_l}+\psi_{n,l,-m_l}\right] &=& \frac{1}{\sqrt{\pi}}R_{n,l}(r)\Theta^l_{-m_l}(\theta)\,\cos m_l\phi & m_l \text{ odd} \\ \frac{1}{i\sqrt{2}}\left[-\psi_{n,l,m_l}-\psi_{n,l,-m_l}\right] &=& \frac{1}{\sqrt{\pi}}R_{n,l}(r)\Theta^l_{-m_l}(\theta)\,\sin m_l\phi & m_l \text{ odd} \\ && & \\ \frac{1}{\sqrt{2}}\left[\psi_{n,l,m_l}+\psi_{n,l,-m_l}\right] &=& \frac{1}{\sqrt{\pi}}R_{n,l}(r)\Theta^l_{m_l}(\theta)\,\cos m_l\phi & m_l \text{ even} \\ \frac{1}{i\sqrt{2}}\left[\psi_{n,l,m_l}-\psi_{n,l,-m_l}\right] &=& \frac{1}{\sqrt{\pi}}R_{n,l}(r)\Theta^l_{m_l}(\theta)\,\sin m_l\phi & m_l \text{ even} \end{array} \tag{8}$$

For a complete description of the wave function, the spin has to be taken into consideration. Ignoring spin-orbit coupling, the total function (*spin orbital*) reads

$$\psi(r,\theta,\phi;\sigma) = \psi(r,\theta,\phi)\,\psi(\sigma) \quad \text{where} \quad \sigma = \pm\tfrac{1}{2}. \tag{9}$$

Table 3: Spherical harmonics for $l = 0, 1, 2, 3$

l	m_l	$Y^l_{m_l}(\theta,\phi)$ [a]	$Y^l_{m_l}(x,y,z)$
0	0	$\left(\frac{1}{4\pi}\right)^{1/2}$	$\left(\frac{1}{4\pi}\right)^{1/2}$
1	0	$\left(\frac{3}{4\pi}\right)^{1/2}\cos\theta$	$\left(\frac{3}{4\pi}\right)^{1/2}\frac{z}{r}$
	±1	$\mp\left(\frac{3}{8\pi}\right)^{1/2}\sin\theta\, e^{\pm i\phi}$	$\mp\left(\frac{3}{8\pi}\right)^{1/2}\frac{x\pm iy}{r}$
2	0	$\left(\frac{5}{16\pi}\right)^{1/2}(3\cos^2\theta-1)$	$\left(\frac{5}{16\pi}\right)^{1/2}\frac{3z^2-r^2}{r^2}$
	±1	$\mp\left(\frac{15}{8\pi}\right)^{1/2}\cos\theta\sin\theta\, e^{\pm i\phi}$	$\mp\left(\frac{15}{8\pi}\right)^{1/2}\frac{z(x\pm iy)}{r^2}$
	±2	$\left(\frac{15}{32\pi}\right)^{1/2}\sin^2\theta\, e^{\pm i2\phi}$	$\left(\frac{15}{32\pi}\right)^{1/2}\frac{(x\pm iy)^2}{r^2}$
3	0	$\left(\frac{7}{16\pi}\right)^{1/2}(5\cos^3\theta-3\cos\theta)$	$\left(\frac{7}{16\pi}\right)^{1/2}\frac{z(5z^2-3r^2)}{r^3}$
	±1	$\mp\left(\frac{21}{64\pi}\right)^{1/2}\sin\theta(5\cos^2\theta-1)e^{\pm i\phi}$	$\mp\left(\frac{21}{64\pi}\right)^{1/2}(x\pm iy)\frac{(5z^2-r^2)}{r^3}$
	±2	$\left(\frac{105}{32\pi}\right)^{1/2}\cos\theta\sin^2\theta\, e^{\pm i2\phi}$	$\left(\frac{105}{32\pi}\right)^{1/2}\frac{z(x\pm iy)^2}{r^3}$
	±3	$\mp\left(\frac{35}{64\pi}\right)^{1/2}\sin^3\theta\, e^{\pm i3\phi}$	$\mp\left(\frac{35}{64\pi}\right)^{1/2}\frac{(x\pm iy)^3}{r^3}$
4	0	$\left(\frac{9}{256\pi}\right)^{1/2}(35\cos^4\theta-30\cos^2\theta+3)$	$\left(\frac{9}{256\pi}\right)^{1/2}\frac{(35z^4-30z^2r^2+3r^4)}{r^4}$
	±1	$\mp\left(\frac{45}{64\pi}\right)^{1/2}\sin\theta(7\cos^3\theta-3\cos\theta)\, e^{\pm i\phi}$	$\mp\left(\frac{45}{64\pi}\right)^{1/2}(x\pm iy)\frac{(7z^3-3zr^2)}{r^4}$
	±2	$\left(\frac{45}{128\pi}\right)^{1/2}\sin^2\theta(7\cos^2\theta-1)\, e^{\pm i2\phi}$	$\left(\frac{45}{128\pi}\right)^{1/2}(x\pm iy)^2\frac{(7z^2-r^2)}{r^4}$
	±3	$\mp\left(\frac{315}{64\pi}\right)^{1/2}\sin^3\theta\cos\theta\, e^{\pm i3\phi}$	$\mp\left(\frac{315}{64\pi}\right)^{1/2}\frac{z(x\pm iy)^3}{r^4}$
	±4	$\left(\frac{315}{512\pi}\right)^{1/2}\sin^4\theta\, e^{\pm i4\phi}$	$\left(\frac{315}{512\pi}\right)^{1/2}\frac{(x\pm iy)^4}{r^4}$

[a] Phase factors correspond to the CONDON-SHORTLEY convention: −1 for odd positive m_l and +1 otherwise.

Table 4: Real orthonormal linear combinations of the spherical harmonics $Y^l_{m_l}(\theta, \phi)$ for $l = 1, 2, 3$.

l	function	designation
1	$\left(\frac{3}{4\pi}\right)^{1/2} \cos\theta = \left(\frac{3}{4\pi}\right)^{1/2} \frac{z}{r}$	p_z
	$\left(\frac{3}{4\pi}\right)^{1/2} \sin\theta\cos\phi = \left(\frac{3}{4\pi}\right)^{1/2} \frac{x}{r}$	p_x
	$\left(\frac{3}{4\pi}\right)^{1/2} \sin\theta\sin\phi = \left(\frac{3}{4\pi}\right)^{1/2} \frac{y}{r}$	p_y
2	$\left(\frac{5}{16\pi}\right)^{1/2} (3\cos^2\theta - 1) = \left(\frac{5}{16\pi}\right)^{1/2} \frac{3z^2 - r^2}{r^2}$	d_{z^2}
	$\left(\frac{15}{4\pi}\right)^{1/2} \cos\theta\sin\theta\cos\phi = \left(\frac{15}{4\pi}\right)^{1/2} \frac{xz}{r^2}$	d_{xz}
	$\left(\frac{15}{4\pi}\right)^{1/2} \cos\theta\sin\theta\sin\phi = \left(\frac{15}{4\pi}\right)^{1/2} \frac{yz}{r^2}$	d_{yz}
	$\left(\frac{15}{16\pi}\right)^{1/2} \sin^2\theta\cos 2\phi = \left(\frac{15}{16\pi}\right)^{1/2} \frac{x^2 - y^2}{r^2}$	$\mathrm{d}_{x^2-y^2}$
	$\left(\frac{15}{16\pi}\right)^{1/2} \sin^2\theta\sin 2\phi = \left(\frac{15}{4\pi}\right)^{1/2} \frac{xy}{r^2}$	d_{xy}
3	$\left(\frac{7}{16\pi}\right)^{1/2} (5\cos^3\theta - 3\cos\theta) = \left(\frac{7}{16\pi}\right)^{1/2} \frac{z(5z^2 - 3r^2)}{r^3}$	f_{z^3}
	$\left(\frac{21}{32\pi}\right)^{1/2} \sin\theta(5\cos^2\theta - 1)\cos\phi = \left(\frac{21}{32\pi}\right)^{1/2} \frac{x(5z^2 - r^2)}{r^3}$	f_{xz^2}
	$\left(\frac{21}{32\pi}\right)^{1/2} \sin\theta(5\cos^2\theta - 1)\sin\phi = \left(\frac{21}{32\pi}\right)^{1/2} \frac{y(5z^2 - r^2)}{r^3}$	f_{yz^2}
	$\left(\frac{105}{16\pi}\right)^{1/2} \cos\theta\sin^2\theta\ \sin 2\phi = \left(\frac{105}{4\pi}\right)^{1/2} \frac{xyz}{r^3}$	f_{xyz}
	$\left(\frac{105}{16\pi}\right)^{1/2} \cos\theta\sin^2\theta\ \cos 2\phi = \left(\frac{105}{16\pi}\right)^{1/2} \frac{z(x^2 - y^2)}{r^3}$	$\mathrm{f}_{z(x^2-y^2)}$
	$\left(\frac{35}{32\pi}\right)^{1/2} \sin^3\theta\cos 3\phi = \left(\frac{35}{32\pi}\right)^{1/2} \frac{x(x^2 - 3y^2)}{r^3}$	$\mathrm{f}_{x(x^2-3y^2)}$
	$\left(\frac{35}{32\pi}\right)^{1/2} \sin^3\theta\sin 3\phi = \left(\frac{35}{32\pi}\right)^{1/2} \frac{y(3x^2 - y^2)}{r^3}$	$\mathrm{f}_{y(3x^2-y^2)}$

2.2 Angular momenta

2.2.1 Orbital angular momentum

Classical definition of the angular momentum $\boldsymbol{l}$ (Fig. 2):

$$\boldsymbol{l} = \boldsymbol{r} \times \boldsymbol{p}. \tag{10}$$

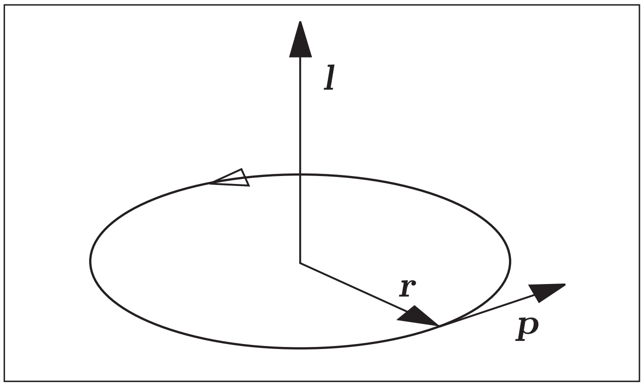

Fig. 2: Definition of the angular momentum

$$\begin{aligned} \boldsymbol{l} &= l_x\boldsymbol{i} + l_y\boldsymbol{j} + l_z\boldsymbol{k} \\ &= (yp_z - zp_y)\boldsymbol{i} + (zp_x - xp_z)\boldsymbol{j} + (xp_y - yp_x)\boldsymbol{k} \end{aligned} \tag{11}$$

Length of the angular momentum vector:

$$|\boldsymbol{l}|^2 = l_x^2 + l_y^2 + l_z^2. \tag{12}$$

Quantum mechanical operators $\hat{l}_x$, $\hat{l}_y$, $\hat{l}_z$ are derived by substituting the position operator and the linear momentum operator for the corresponding classical quantity, i. e.

$$q \longrightarrow \hat{q} = q\,\times \qquad p_q \longrightarrow \hat{p}_q = \frac{\hbar}{i}\frac{\partial}{\partial q} \qquad (q = x, y, z; \quad i = \sqrt{-1})$$

$$\hat{l}_x = \hat{y}\hat{p}_z - \hat{z}\hat{p}_y; \qquad \hat{l}_y = \hat{z}\hat{p}_x - \hat{x}\hat{p}_z; \qquad \hat{l}_z = \hat{x}\hat{p}_y - \hat{y}\hat{p}_x \tag{13}$$

$$\hat{l}_x = \frac{\hbar}{i}\left(\hat{y}\frac{\partial}{\partial z} - \hat{z}\frac{\partial}{\partial y}\right); \quad \hat{l}_y = \frac{\hbar}{i}\left(\hat{z}\frac{\partial}{\partial x} - \hat{x}\frac{\partial}{\partial z}\right); \quad \hat{l}_z = \frac{\hbar}{i}\left(\hat{x}\frac{\partial}{\partial y} - \hat{y}\frac{\partial}{\partial x}\right) \tag{14}$$

Commutation relations

$$\boxed{[\hat{l}_x, \hat{l}_y] = i\hbar\hat{l}_z; \qquad [\hat{l}_y, \hat{l}_z] = i\hbar\hat{l}_x; \qquad [\hat{l}_z, \hat{l}_x] = i\hbar\hat{l}_y}, \tag{15}$$

Operator $\hat{l}_z$ in spherical polar coordinates:

$$\hat{l}_z = \frac{\hbar}{i}\frac{\partial}{\partial \phi} \tag{16}$$

$\hat{l}_z$ acts on the ϕ depending part of the atomic orbitals (Table 3):

$$\begin{aligned} \hat{l}_z \,\big|\, l\, m_l \,\big\rangle &= l_z \,\big|\, l\, m_l \,\big\rangle = m_l\hbar \,\big|\, l\, m_l \,\big\rangle \quad \text{Dirac notation} \\ \big\langle\, l\, m_l \,\big|\hat{l}_z\big|\, l\, m_l \,\big\rangle &= m_l\,\hbar\, \underbrace{\big\langle\, l\, m_l \,\big|\, l\, m_l \,\big\rangle}_{1} \end{aligned}$$

$$\begin{aligned}\text{generally}\quad \hat{H}\,\Psi &= E\,\Psi, \ (\Psi \ \text{normalised eigenfunction of } \hat{H})\\ \int \Psi^* \hat{H}\,\Psi\,d\tau &= E \underbrace{\int \Psi^*\,\Psi\,d\tau}_{1} = E\\ \int \Psi^* \hat{H}\,\Psi\,d\tau &\equiv \langle\Psi|\hat{H}|\Psi\rangle \quad \text{matrix element (Dirac notation)}\end{aligned}$$

Application of $\hat{l}_z$:

$$\begin{aligned}\hat{l}_z \left|\, 2\,2 \right\rangle &= R_{n,2}(r)\frac{\hbar}{i}\frac{\partial Y_2^2(\theta,\phi)}{\partial\phi}\\ &= R_{n,2}(r)\frac{\hbar}{i}\frac{\partial}{\partial\phi}\left[\left(\frac{15}{32\pi}\right)^{1/2}\sin^2\theta\, e^{i2\phi}\right]\\ &= R_{n,2}(r)\frac{\hbar}{i}\left(\frac{15}{32\pi}\right)^{1/2}\sin^2\theta\,\frac{\partial e^{i2\phi}}{\partial\phi}\\ &= R_{n,2}(r)i2\frac{\hbar}{i}\left(\frac{15}{32\pi}\right)^{1/2}\sin^2\theta\, e^{i2\phi} = 2\hbar \left|\, 2\,2 \right\rangle\end{aligned}$$

$$\hat{\boldsymbol{l}}^2 \left|\, l\, m_l \right\rangle = l(l+1)\hbar^2 \left|\, l\, m_l \right\rangle \tag{17}$$

Shift operators:

$$\hat{l}_+ = \hat{l}_x + i\hat{l}_y; \qquad \hat{l}_- = \hat{l}_x - i\hat{l}_y. \tag{18}$$

Reverse operations:

$$\hat{l}_x = \frac{1}{2}(\hat{l}_+ + \hat{l}_-); \qquad \hat{l}_y = \frac{1}{2i}(\hat{l}_+ - \hat{l}_-). \tag{19}$$

$$\boxed{\begin{aligned}\hat{l}_z \left|\, l\, m_l \right\rangle &= m_l\,\hbar \left|\, l\, m_l \right\rangle\\ \hat{\boldsymbol{l}}^2 \left|\, l\, m_l \right\rangle &= l(l+1)\,\hbar^2 \left|\, l\, m_l \right\rangle\\ \hat{l}_\pm \left|\, l\, m_l \right\rangle &= \sqrt{l(l+1) - m_l(m_l \pm 1)}\,\hbar \left|\, l\, m_l \pm 1 \right\rangle.\end{aligned}} \tag{20}$$

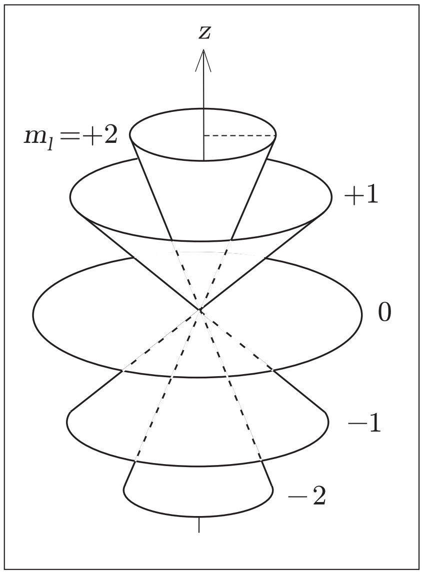

Fig. 3: Specified orientation of $\boldsymbol{l}$ ($l = 2$) with regard to the component l_z while l_x and l_y are unspecified

2.2.2 Spin

Spin orbital of a one-electron system:

$$\psi(\boldsymbol{r})\,\psi(\sigma) = \psi_{n,l,m_l}(r,\theta,\phi)\,\psi(\sigma) = \underbrace{R_{n,l}(r)\,Y^{l}_{m_l}(\theta,\phi)}_{\text{atomic orbital}}\;\psi(\sigma)$$

Spin function: $\psi(\sigma) \equiv |\,s\,m_s\,\rangle \begin{cases} m_s = \frac{1}{2}: & \alpha \\ m_s = -\frac{1}{2}: & \beta \end{cases}$

$$\boxed{\begin{array}{rcl} \hat{\boldsymbol{s}}^2\,\big|\,s\,m_s\big\rangle & = & s(s+1)\,\hbar^2\,\big|\,s\,m_s\big\rangle \quad \text{with} \quad s=\frac{1}{2} \\ \hat{s}_z\,\big|\,s\,m_s\big\rangle & = & m_s\hbar\,\big|\,s\,m_s\big\rangle \quad \text{with} \quad m_s = \pm\frac{1}{2} \\ \hat{s}_\pm\,\big|\,s\,m_s\big\rangle & = & \sqrt{s(s+1)-m_s(m_s\pm 1)}\;\hbar\,\big|\,s\,m_s\pm 1\big\rangle \end{array}} \tag{21}$$

where $\hat{\boldsymbol{s}}^2 = \hat{s}_x^2 + \hat{s}_y^2 + \hat{s}_z^2;\quad \hat{s}_+ = \hat{s}_x + i\hat{s}_y;\qquad \hat{s}_- = \hat{s}_x - i\hat{s}_y$

$\hat{s}_x = \frac{1}{2}(\hat{s}_+ + \hat{s}_-);\quad \hat{s}_y = \frac{1}{2i}(\hat{s}_+ - \hat{s}_-)$

Problems

3. Use the spherical harmonics in Table 3 and construct the real functions $\mathrm{d}_{x^2-y^2}$ and d_{xy} with the help of eqs. (8). Verify the results with the data given in Table 4.

2.3 Quantum-mechanical procedures

2.3.1 Operators

Postulate 1. The state of a system is fully described by the wavefunction $\Psi(\boldsymbol{r}_1, \boldsymbol{r}_2, \ldots, t)$.
Postulate 2. Observables are represented by operators chosen to satisfy the commutation relation

$$\hat{q}\hat{p}_q - \hat{p}_q\hat{q} = [\hat{q}, \hat{p}_q] = i\hbar \qquad (q = x, y, z;\quad i = \sqrt{-1}) \tag{22}$$

Example 2.1 *Verification of the commutation relation*

$$\hat{x} = x\,\times \quad \text{and} \quad \hat{p}_x = \frac{\hbar}{i}\frac{\mathrm{d}}{\mathrm{d}x}$$

$$\begin{array}{rcl} \hat{x}\hat{p}_x\Psi & = & x\dfrac{\hbar}{i}\dfrac{\mathrm{d}\Psi}{\mathrm{d}x} \\ \hat{p}_x\hat{x}\Psi & = & \dfrac{\hbar}{i}\dfrac{\mathrm{d}(x\Psi)}{\mathrm{d}x} = \dfrac{\hbar}{i}\left(\Psi + x\dfrac{\mathrm{d}\Psi}{\mathrm{d}x}\right) \\ (\hat{x}\hat{p}_x - \hat{p}_x\hat{x})\Psi & = & -\dfrac{\hbar}{i}\Psi = i\hbar\Psi \end{array}$$

Tab. 5: Classical and quantum-mechanical forms of E_{kin} and E_{pot}

quantity	D[a]	classical	quantum-mechanical
E_{kin}	1	$\frac{m_\mathrm{e}v_x^2}{2} = \frac{p_x^2}{2m_\mathrm{e}}$	$\frac{\hat{p}_x^2}{2m_\mathrm{e}} = \frac{1}{2m_\mathrm{e}}\left(\frac{\hbar}{i}\frac{\mathrm{d}}{\mathrm{d}x}\right)^2 = -\frac{\hbar^2}{2m_\mathrm{e}}\frac{\mathrm{d}^2}{\mathrm{d}x^2}$
	3	$\frac{p^2}{2m_\mathrm{e}}$	$-\frac{\hbar^2}{2m_\mathrm{e}}\left(\frac{\partial^2}{\partial x^2}+\frac{\partial^2}{\partial y^2}+\frac{\partial^2}{\partial z^2}\right) = -\frac{\hbar^2}{2m_\mathrm{e}}\nabla^2$ [b]
E_{pot} [c]	1	$-eV(x)$	$-e\hat{V}(x) = -eV(x)\cdot$
	3	$-eV(\boldsymbol{r})$	$-e\hat{V}(\boldsymbol{r}) = -eV(\boldsymbol{r})\cdot$

---

[a] Dimension.

[b] ∇ is the Nabla operator.

[c] Valid for one electron with charge $-e$ in the potential V.

2.3.2 Perturbation theory

1. *Non-degenerate states*

$$\hat{H}^{(0)}\Psi_n^{(0)} = E_n^{(0)}\Psi_n^{(0)} \qquad \text{unperturbed system} \tag{23}$$

Hamilton operator of the perturbed system:

$$\hat{H} = \hat{H}^{(0)} + \lambda\hat{H}^{(1)}$$

Schrödinger equation of the perturbed system:

$$\hat{H}\Psi_n = E_n\Psi_n; \qquad \text{find} \quad E_n, \Psi_n \tag{24}$$

Series expansion of Ψ_n und E_n:

$$\Psi_n = \Psi_n^{(0)} + \lambda\Psi_n^{(1)} + \lambda^2\Psi_n^{(2)} + \ldots \tag{25}$$

$$E_n = E_n^{(0)} + \lambda E_n^{(1)} + \lambda^2 E_n^{(2)} + \ldots . \tag{26}$$

Insert the series into eq. (24):

$$(\hat{H}^{(0)} + \lambda\hat{H}^{(1)})(\Psi_n^{(0)} + \lambda\Psi_n^{(1)} + \lambda^2\Psi_n^{(2)} + \ldots) = (E_n^{(0)} + \lambda E_n^{(1)} + \lambda^2 E_n^{(2)} + \ldots)(\Psi_n^{(0)} + \lambda\Psi_n^{(1)} + \lambda^2\Psi_n^{(2)} + \ldots),$$

Ordering of the terms with regard to powers of λ:

$$\hat{H}^{(0)}\Psi_n^{(0)} + \lambda\big(\hat{H}^{(1)}\Psi_n^{(0)} + \hat{H}^{(0)}\Psi_n^{(1)}\big) + \lambda^2\big(\hat{H}^{(1)}\Psi_n^{(1)} + \hat{H}^{(0)}\Psi_n^{(2)}\big) + \ldots = E_n^{(0)}\Psi_n^{(0)} + \lambda\big(E_n^{(1)}\Psi_n^{(0)} + E_n^{(0)}\Psi_n^{(1)}\big) + \lambda^2\big(E_n^{(2)}\Psi_n^{(0)} + E_n^{(1)}\Psi_n^{(1)} + E_n^{(0)}\Psi_n^{(2)}\big) + \ldots .$$

$$\begin{array}{llcl} \lambda^0 & \hat{H}^{(0)}\Psi_n^{(0)} & = & E_n^{(0)}\Psi_n^{(0)} \qquad (27)\\ \lambda^1 & (\hat{H}^{(0)}-E_n^{(0)})\Psi_n^{(1)} & = & (E_n^{(1)}-\hat{H}^{(1)})\Psi_n^{(0)} \qquad (28)\\ \lambda^2 & (\hat{H}^{(0)}-E_n^{(0)})\Psi_n^{(2)} & = & E_n^{(2)}\Psi_n^{(0)}+(E_n^{(1)}-\hat{H}^{(1)})\Psi_n^{(1)} \qquad (29)\\ \vdots & & \vdots & \end{array}$$

The first-order correction to the energy $E_n^{(1)}$
(premultiply both sides of eq. (28) with $\Psi_n^{(0)*}$ and integrate)

$$\underbrace{\int \Psi_n^{(0)*}\hat{H}^{(0)}\Psi_n^{(1)}d\tau - E_n^{(0)}\int \Psi_n^{(0)*}\Psi_n^{(1)}d\tau}_{0} = E_n^{(1)} - \int \Psi_n^{(0)*}\hat{H}^{(1)}\Psi_n^{(0)}d\tau$$

$$\boxed{E_n^{(1)} = \langle n|\hat{H}^{(1)}|n\rangle} \qquad (30)$$

The first-order correction to the wavefunction:

$$\boxed{\Psi_n^{(1)} = -\sum_{m\neq n}\frac{\langle m|\hat{H}^{(1)}|n\rangle}{E_m^{(0)}-E_n^{(0)}}\,\Psi_m^{(0)}} \qquad (31)$$

The second-order correction to the energy:

$$\boxed{E_n^{(2)} = -\sum_{m\neq n}\frac{\left|\langle m|\hat{H}^{(1)}|n\rangle\right|^2}{E_m^{(0)}-E_n^{(0)}}} \qquad \text{(see Fig. 4)} \qquad (32)$$

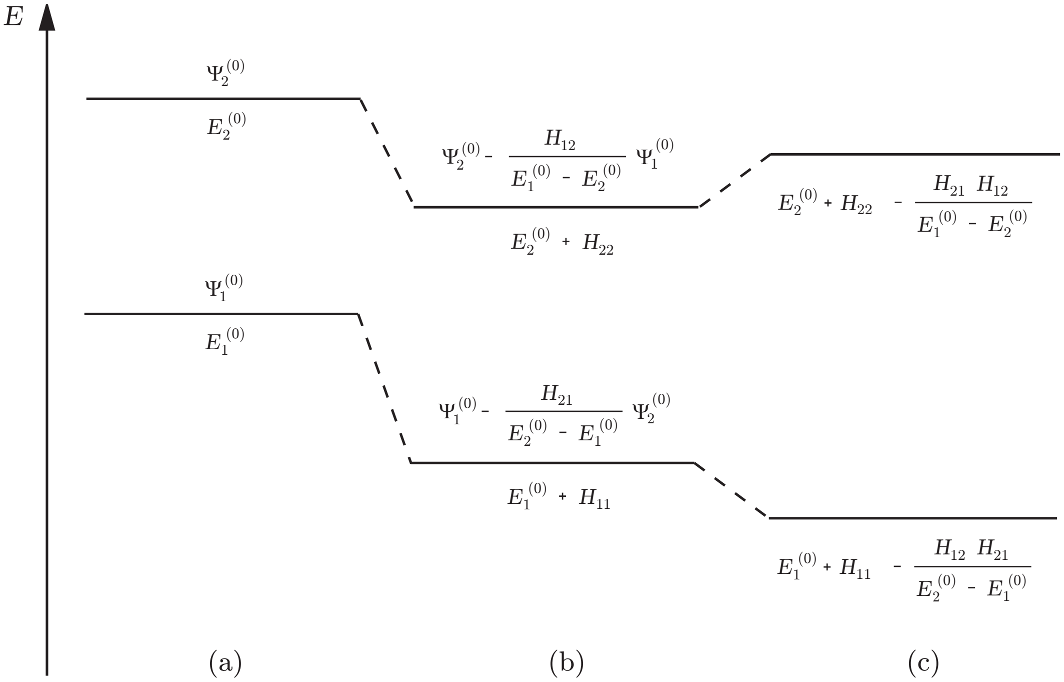

Fig. 4: Illustration of the possible effects of a perturbation on two non-degenerate levels; (a) 0^{th},(b) 1^{st},(c) 2^{nd} order

2. *Degenerate states*

Eq. (30) – (32) apply also in this case; additionally: determination of the correct zeroth-order wavefunctions (see Fig. 5)

Example: doubly degenerate pair of states

$$\hat{H}^{(0)}\Psi^{(0)}_{n,i} = E^{(0)}_n\Psi^{(0)}_{n,i} \qquad (i = 1, 2) \tag{33}$$

$$\Psi^{(0)}_n = u_1\Psi^{(0)}_{n,1} + u_2\Psi^{(0)}_{n,2} \tag{34}$$

The 'correct' linear combinations are those which correspond to the perturbed functions for $\lambda \to 0$.

Determination of u_1 and u_2:

Substituting eq. (34) in eq. (25); eq. (28) now reads:

$$\big(\hat{H}^{(0)} - E^{(0)}_n\big)\Psi^{(1)}_n = \big(E^{(1)}_n - \hat{H}^{(1)}\big)\big(u_1\Psi^{(0)}_{n,1} + u_2\Psi^{(0)}_{n,2}\big) \tag{35}$$

Multiply with $\Psi^{(0)*}_{n,1}$ and $\Psi^{(0)*}_{n,2}$, respectively and integrate:

$$\begin{aligned} u_1\big(H_{11} - E^{(1)}_n\big) + u_2H_{12} &= 0 \\ u_1H_{21} + u_2\big(H_{22} - E^{(1)}_n\big) &= 0 \end{aligned} \qquad \text{where} \quad H_{ij} = \int \Psi^{(0)*}_{n,i}\,\hat{H}^{(1)}\,\Psi^{(0)}_{n,j}\,d\tau = \langle i|\hat{H}^{(1)}|j\rangle$$

To find the non-trivial solutions of this pair of equations, the determinant of the coefficients of the constants u_1 and u_2 must disappear:

$$\begin{vmatrix} H_{11} - E^{(1)}_n & H_{12} \\ H_{21} & H_{22} - E^{(1)}_n \end{vmatrix} = 0; \qquad \begin{array}{ll} H_{11}, H_{22}: & \text{diagonal elements} \\ H_{12}, H_{21}: & \text{off-diagonal elements} \end{array} \tag{36}$$

$$E^{(1)}_{n(1,2)} = \big(H_{11} + H_{22}\big)/2 \pm \sqrt{(H_{11} - H_{22})^2/4 + |H_{12}|^2}$$

$$u_{1(1,2)}(H_{11} - E^{(1)}_{n(1,2)}) + u_{2(1,2)}H_{12} = 0; \qquad x_{(1,2)} = \frac{u_{1(1,2)}}{u_{2(1,2)}} = -\frac{H_{12}}{H_{11} - E^{(1)}_{n(1,2)}}$$

Normalisation:

$$x^2_{(1,2)}u^2_{2(1,2)} + u^2_{2(1,2)} = 1 \quad \Rightarrow \quad \begin{cases} u_{2(1,2)} = \dfrac{1}{\sqrt{x^2_{(1,2)} + 1}} \\ u_{1(1,2)} = x_{(1,2)}u_{2(1,2)} = \dfrac{x_{(1,2)}}{\sqrt{x^2_{(1,2)} + 1}} \end{cases}$$

Correct zeroth-order wavefunctions for the energy $E^{(1)}_{n(1,2)}$:

$$\Psi^{(0)}_{n(1,2)} = u_{1(1,2)}\Psi^{(0)}_{n,1} + u_{2(1,2)}\Psi^{(0)}_{n,2}$$

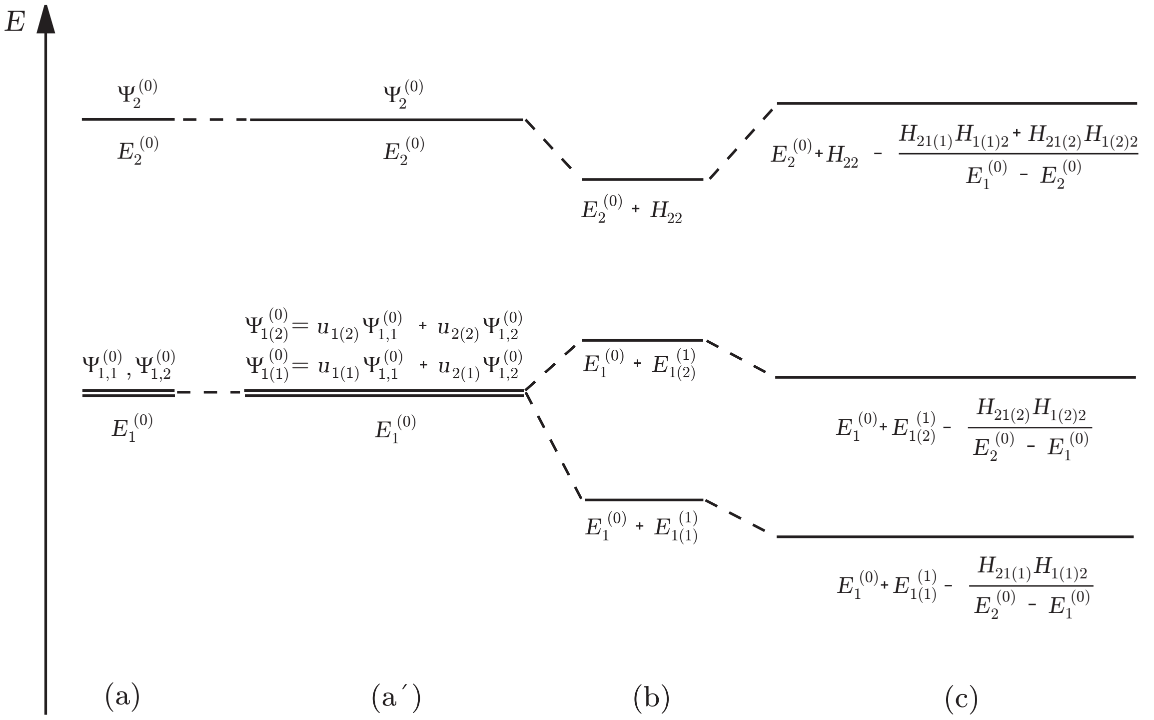

Fig. 5: Illustration of the possible effects of a perturbation on a doubly degenerate ground state and a non-degenerate excited state; (a) 0^{th}, (a') correct 0^{th}, (b) 1^{st},(c) 2^{nd} order

Alternative procedure to solve 2×2 determinants (*cf.* [11], p. 119):

General solution for 2×2 determinants:

$$\begin{vmatrix} H_{11} - E & H_{12} \\ H_{12} & H_{22} - E \end{vmatrix} = 0. \qquad \tan 2\alpha = 2H_{12}/(H_{11} - H_{22})$$

$$E = \begin{cases} H_{11} - H_{12}\cot\alpha; & \Psi_1 = \sin\alpha\psi_1 - \cos\alpha\psi_2 \\ H_{22} + H_{12}\cot\alpha; & \Psi_2 = \cos\alpha\psi_1 + \sin\alpha\psi_2 \end{cases} ; \; H_{ij} = \langle\psi_i|\hat{H}^{(1)}|\psi_j\rangle \tag{37}$$

2.4 Applications

2.4.1 Spin-orbit coupling ($\mathbf{p}^1$, $\mathbf{f}^1$, $\mathbf{f}^{13}$)

Example 2.2 *p^1 system*

$$\hat{H}_{\mathrm{SO}} = \xi(r)\,\hat{\boldsymbol{l}}\cdot\hat{\boldsymbol{s}} \qquad \text{where} \qquad \xi(r) = -\frac{e}{2m_{\mathrm{e}}^2c^2}\,\frac{1}{r}\,\frac{\partial V(r)}{\partial r}. \tag{38}$$

p^1 system: $l = 1$, $s = \frac{1}{2}$, $j_1 = l - s = \frac{1}{2}$ and $j_2 = l + s = \frac{3}{2}$ (see Figs. 6 and 7, Table 6)

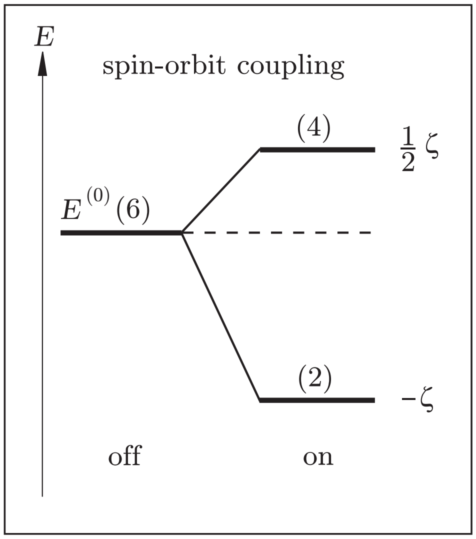

Fig. 6: Splitting of the p^1 levels by spin-orbit interaction (ζ: one-electron spin-orbit coupling constant)

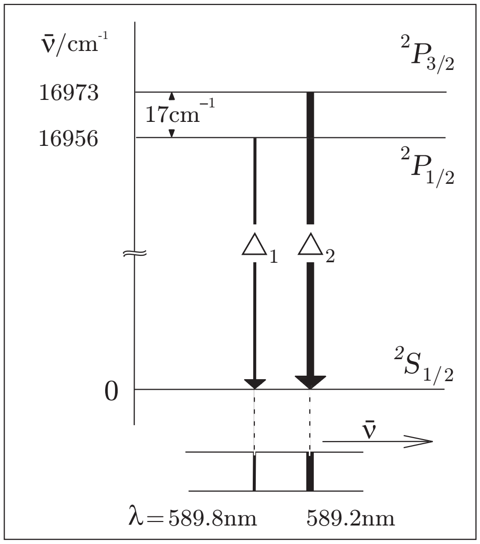

Fig. 7: Term scheme of the sodium atom

Unperturbed states sixfold degenerate

$$\hat{H}^{(0)}\psi_i^{(0)} = E^{(0)}\psi_i^{(0)} \qquad (i = 1, 2, \ldots, 6).$$

Eq. (35) reads in this case:

$$(\hat{H}^{(0)} - E^{(0)})\psi^{(1)} = (E^{(1)} - \hat{H}^{(1)})\big(u_1\psi_1^{(0)} + \ldots + u_6\psi_6^{(0)}\big). \tag{39}$$

Premultiplication with $\psi_1^{(0)*}$ and integration result in:

$$\underbrace{\int \psi_1^{(0)*}\big(\hat{H}^{(0)} - E^{(0)}\big)\psi^{(1)}d\tau}_{0} = \int \psi_1^{(0)*}\big(E^{(1)} - \hat{H}^{(1)}\big)\big(u_1\psi_1^{(0)} + \ldots + u_6\psi_6^{(0)}\big)d\tau$$

$$\begin{aligned} 0 \;=\; & u_1E^{(1)}\int \psi_1^{(0)*}\,\psi_1^{(0)}d\tau + \ldots + u_6E^{(1)}\int \psi_1^{(0)*}\,\psi_6^{(0)}d\tau \\ & -u_1\int \psi_1^{(0)*}\,\hat{H}^{(1)}\,\psi_1^{(0)}d\tau - \ldots - u_6\int \psi_1^{(0)*}\,\hat{H}^{(1)}\,\psi_6^{(0)}d\tau. \end{aligned} \tag{40}$$

Using the abbreviation $\int \psi_i^{(0)*} \hat{H}^{(1)} \psi_j^{(0)} d\tau \equiv H_{ij}$ we obtain a system of six equations:

$$\begin{aligned}
0 &= u_1\big(H_{11} - E^{(1)}\big) + u_2 H_{12} + \cdots + u_6 H_{16} \\
0 &= u_1 H_{21} + u_2\big(H_{22} - E^{(1)}\big) + \cdots + u_6 H_{26} \\
\vdots & \qquad\qquad\qquad \vdots \\
0 &= u_1 H_{61} + u_2 H_{62} + \cdots + u_6\big(H_{66} - E^{(1)}\big)
\end{aligned} \tag{41}$$

Non-trivial solutions for the coefficients of $u_1, u_2, \ldots, u_6$:
Calculation of the integrals H_{ij}

$$\int \big(\psi_{n,l,m_l}(r,\theta,\phi)\,\psi_{m_s}(\sigma)\big)^* \,\hat{H}_{SO}\,\psi_{n,l,m_l'}(r,\theta,\phi)\,\psi_{m_s'}(\sigma)\,r^2\,dr\,\sin\theta\,d\theta\,d\phi\,d\sigma. \tag{42}$$

$$\begin{aligned}
&\int_0^\infty R_{n,l}(r)\,\xi(r)\,R_{n,l}(r)\,r^2\,dr \;\;\times \qquad (43)\\
&\quad \int_0^\pi \int_0^{2\pi} \int_{-1/2}^{1/2} \big(Y_l^{m_l}(\theta,\phi)\,\psi_{m_s}(\sigma)\big)^*\,\hat{\boldsymbol{l}}\boldsymbol{\cdot}\hat{\boldsymbol{s}}\,\big(Y_l^{m_l'}(\theta,\phi)\,\psi_{m_s'}(\sigma)\big)\sin\theta\,d\theta\,d\phi\,d\sigma.
\end{aligned}$$

$$hc\,\zeta_{n,l} = \hbar^2 \int_0^\infty R_{n,l}(r)\,\xi(r)\,R_{n,l}(r)\,r^2\,dr. \tag{44}$$

$\zeta_{n,l}$: one-electron spin-orbit coupling constant
basis in Dirac notation: $\big|\,m_l\,m_s\big\rangle$

$$\big|\,1\,\tfrac{1}{2}\big\rangle \quad \big|\,0\,\tfrac{1}{2}\big\rangle \quad \big|-1\,\tfrac{1}{2}\big\rangle \quad \big|\,1\,-\tfrac{1}{2}\big\rangle \quad \big|\,0\,-\tfrac{1}{2}\big\rangle \quad \big|-1\,-\tfrac{1}{2}\big\rangle. \tag{45}$$

Integral eq. (43) has the short form

$$\frac{hc\zeta_{n,l}}{\hbar^2}\big\langle m_l\,m_s\big|\hat{\boldsymbol{l}}\boldsymbol{\cdot}\hat{\boldsymbol{s}}\big|\,m_l'\,m_s'\big\rangle. \tag{46}$$

To determine the 36 matrix elements of the spin-orbit coupling operator $\hat{\boldsymbol{l}}\boldsymbol{\cdot}\hat{\boldsymbol{s}} = \hat{l}_x\hat{s}_x + \hat{l}_y\hat{s}_y + \hat{l}_z\hat{s}_z$, replace the x and y components by the step operators (see eq. (19,21)):

$$\begin{aligned}
\hat{\boldsymbol{l}}\boldsymbol{\cdot}\hat{\boldsymbol{s}} &= \hat{l}_z\hat{s}_z + \tfrac{1}{2}(\hat{l}_+ + \hat{l}_-)\tfrac{1}{2}(\hat{s}_+ + \hat{s}_-) + \tfrac{1}{2i}(\hat{l}_+ - \hat{l}_-)\tfrac{1}{2i}(\hat{s}_+ - \hat{s}_-) \\
&= \hat{l}_z\hat{s}_z + \tfrac{1}{4}(\hat{l}_+\hat{s}_+ + \hat{l}_-\hat{s}_+ + \hat{l}_+\hat{s}_- + \hat{l}_-\hat{s}_- - \hat{l}_+\hat{s}_+ + \hat{l}_-\hat{s}_+ + \hat{l}_+\hat{s}_- - \hat{l}_-\hat{s}_-) \\
&= \hat{l}_z\hat{s}_z + \tfrac{1}{2}(\hat{l}_+\hat{s}_- + \hat{l}_-\hat{s}_+)
\end{aligned} \tag{47}$$

The general matrix element (46) is

$$\begin{aligned}
\big\langle m_l\,m_s\big|\hat{\boldsymbol{l}}\boldsymbol{\cdot}\hat{\boldsymbol{s}}\big|\,m_l'\,m_s'\big\rangle &= \big\langle m_l\,m_s\big|\hat{l}_z\hat{s}_z + \tfrac{1}{2}(\hat{l}_+\hat{s}_- + \hat{l}_-\hat{s}_+)\big|\,m_l'\,m_s'\big\rangle \\
&= \big\langle m_l\,m_s\big|\hat{l}_z\hat{s}_z\big|\,m_l'\,m_s'\big\rangle \\
&\quad + \tfrac{1}{2}\big\langle m_l\,m_s\big|\hat{l}_+\hat{s}_-\big|\,m_l'\,m_s'\big\rangle \\
&\quad + \tfrac{1}{2}\big\langle m_l\,m_s\big|\hat{l}_-\hat{s}_+\big|\,m_l'\,m_s'\big\rangle.
\end{aligned} \tag{48}$$

General hints to the evaluation of matrix elements $\big\langle m\big|\hat{H}^{(1)}\big|n\big\rangle$:

(i) Evaluate $\hat{H}^{(1)}\big|n\big\rangle$. This will result in a constant a multiplied by a wavefunction which may or may not be the same as the original. For the present let us assume $\hat{H}^{(1)}\big|n\big\rangle = a\big|n\big\rangle$.
(ii) The result of (i) is then premultiplied by $\big\langle m\big|$ giving $\big\langle m\big|an\big\rangle$.
(iii) Since a is a constant we have $\big\langle m\big|an\big\rangle = a\big\langle m\big|n\big\rangle$ and we are thus left with the task of evaluating $\big\langle m\big|n\big\rangle$. Provided $\big|m\big\rangle$ and $\big|n\big\rangle$ are orthonormalised, $\big\langle m\big|n\big\rangle = 1$ when $m = n$ but is zero otherwise.
On account of orthonormalised states

$$\big\langle m_l\, m_s\big|\, m_l'\, m_s'\big\rangle = \delta_{m_l,m_l'}\,\delta_{m_s,m_s'}, \tag{49}$$

the integral is not zero when $m_l = m_l'$ and $m_s = m_s'$. The wavefunctions are eigenfunctions of $\hat{l}_z$ und $\hat{s}_z$, so that the application of the operator products in eq. (48) on the wavefunction on its right-hand side yields:

$$\begin{aligned}
\hat{l}_z\hat{s}_z\,\big|\,m_l\,m_s\big\rangle &= m_l\,m_s\,\hbar^2\,\big|\,m_l\,m_s\big\rangle \\
\hat{l}_+\hat{s}_-\,\big|\,m_l\,m_s\big\rangle &= \\
&\sqrt{l(l+1)-m_l(m_l+1)}\sqrt{s(s+1)-m_s(m_s-1)}\,\hbar^2\,\big|\,m_l+1\,m_s-1\big\rangle \\
\hat{l}_-\hat{s}_+\,\big|\,m_l\,m_s\big\rangle &= \\
&\sqrt{l(l+1)-m_l(m_l-1)}\sqrt{s(s+1)-m_s(m_s+1)}\,\hbar^2\,\big|\,m_l-1\,m_s+1\big\rangle
\end{aligned}$$

where $s = \frac{1}{2}$. For diagonal elements only $\hat{l}_z\hat{s}_z$ may contribute, whereas for off-diagonal elements only the step operators may account:

$$\big\langle m_l\,m_s\big|\hat{l}_+\hat{s}_-\big|\,m_l-1\,m_s+1\big\rangle \qquad \big\langle m_l\,m_s\big|\hat{l}_-\hat{s}_+\big|\,m_l+1\,m_s-1\big\rangle$$

Matrix elements (46) which may contribute are restricted to the condition

$$m_l + m_s = m_l' + m_s' \tag{50}$$

The non-zero matrix elements are:

$$\begin{aligned}
&\big\langle\,1\;-\tfrac{1}{2}\,\big|\hat{l}_+\hat{s}_-\big|\,0\;\tfrac{1}{2}\,\big\rangle \qquad \big\langle\,0\;-\tfrac{1}{2}\,\big|\hat{l}_+\hat{s}_-\big|-1\;\tfrac{1}{2}\,\big\rangle \\
&\big\langle\,0\;\tfrac{1}{2}\big|\hat{l}_-\hat{s}_+\big|\,1\;-\tfrac{1}{2}\,\big\rangle \qquad \big\langle\,-1\,\tfrac{1}{2}\,\big|\hat{l}_-\hat{s}_+\big|\,0\;-\tfrac{1}{2}\big\rangle.
\end{aligned}$$

$$\begin{array}{r||cccccc}
m_l m_s & \big|\,1\;\tfrac{1}{2}\,\big\rangle & \big|\,1\;-\tfrac{1}{2}\,\big\rangle & \big|\,0\;\tfrac{1}{2}\,\big\rangle & \big|\,0-\tfrac{1}{2}\,\big\rangle & \big|-1\,\tfrac{1}{2}\,\big\rangle & \big|-1-\tfrac{1}{2}\,\big\rangle \\
\hline
\big\langle\,1\;\tfrac{1}{2}\,\big| & \tfrac{1}{2}\,\zeta & & & & & \\
\big\langle\,1\;-\tfrac{1}{2}\,\big| & & -\tfrac{1}{2}\,\zeta & \sqrt{\tfrac{1}{2}}\,\zeta & & & \\
\big\langle\,0\;\tfrac{1}{2}\,\big| & & \sqrt{\tfrac{1}{2}}\,\zeta & 0 & & & \\
\big\langle\,0\;-\tfrac{1}{2}\,\big| & & & & 0 & \sqrt{\tfrac{1}{2}}\,\zeta & \\
\big\langle\,-1\,\tfrac{1}{2}\,\big| & & & & \sqrt{\tfrac{1}{2}}\,\zeta & -\tfrac{1}{2}\,\zeta & \\
\big\langle\,-1-\tfrac{1}{2}\,\big| & & & & & & \tfrac{1}{2}\,\zeta
\end{array} \tag{51}$$

$$
\begin{aligned}
H_{11} &= \frac{\zeta}{\hbar^2}\big\langle 1\,\tfrac{1}{2}\,\big|\hat{l}_z\hat{s}_z\big|\,1\,\tfrac{1}{2}\,\big\rangle = \zeta\cdot 1\cdot\tfrac{1}{2}\,\big\langle 1\,\tfrac{1}{2}\,\big|\,1\,\tfrac{1}{2}\,\big\rangle = \tfrac{1}{2}\,\zeta \\
H_{22} &= \frac{\zeta}{\hbar^2}\big\langle 1\,-\tfrac{1}{2}\,\big|\hat{l}_z\hat{s}_z\big|\,1\,-\tfrac{1}{2}\big\rangle = \zeta\cdot 1\cdot(-\tfrac{1}{2}) = -\tfrac{1}{2}\,\zeta \\
H_{33} &= \frac{\zeta}{\hbar^2}\big\langle 0\,\tfrac{1}{2}\,\big|\hat{l}_z\hat{s}_z\big|\,0\,\tfrac{1}{2}\,\big\rangle = \zeta\cdot 0\cdot\tfrac{1}{2} = 0 \\
H_{44} &= \frac{\zeta}{\hbar^2}\big\langle 0\,-\tfrac{1}{2}\big|\hat{l}_z\hat{s}_z\big|\,0\,-\tfrac{1}{2}\big\rangle = \zeta\cdot 0\cdot(-\tfrac{1}{2}) = 0 \\
H_{55} &= \frac{\zeta}{\hbar^2}\big\langle -1\,\tfrac{1}{2}\big|\hat{l}_z\hat{s}_z\big|-1\,\tfrac{1}{2}\,\big\rangle = \zeta\cdot(-1)\cdot\tfrac{1}{2} = -\tfrac{1}{2}\,\zeta \\
H_{66} &= \frac{\zeta}{\hbar^2}\big\langle -1\,-\tfrac{1}{2}\,\big|\hat{l}_z\hat{s}_z\big|-1\,-\tfrac{1}{2}\big\rangle = \zeta\cdot(-1)\cdot(-\tfrac{1}{2}) = \tfrac{1}{2}\,\zeta \\
H_{23} &= \frac{\zeta}{\hbar^2}\big\langle 1\,-\tfrac{1}{2}\,\big|\tfrac{1}{2}\hat{l}_+\hat{s}_-\big|\,0\,\tfrac{1}{2}\,\big\rangle = \tfrac{1}{2}\zeta\cdot\sqrt{2}\cdot 1\,\big\langle\,1\,-\tfrac{1}{2}\,\big|\,1\,-\tfrac{1}{2}\,\big\rangle = \sqrt{\tfrac{1}{2}}\,\zeta = H_{32} \\
H_{45} &= \frac{\zeta}{\hbar^2}\big\langle 0\,-\tfrac{1}{2}\,\big|\tfrac{1}{2}\hat{l}_+\hat{s}_-\,\big|-1\,\tfrac{1}{2}\,\big\rangle = \tfrac{1}{2}\zeta\cdot\sqrt{2}\cdot 1 = \sqrt{\tfrac{1}{2}}\,\zeta = H_{54}
\end{aligned}
$$

Diagonalisation of the 2×2 blocks of the H matrix:

$$
\begin{aligned}
\begin{vmatrix} -\tfrac{1}{2}\,\zeta - E^{(1)} & \sqrt{\tfrac{1}{2}}\,\zeta \\ \sqrt{\tfrac{1}{2}}\zeta & -E^{(1)} \end{vmatrix} &= (-\tfrac{1}{2}\zeta - E^{(1)})(-E^{(1)}) - \tfrac{1}{2}\zeta^2 = 0 \\
E^{(1)}_{(1)} &= \tfrac{1}{2}\,\zeta; \qquad\qquad E^{(1)}_{(2)} = -\zeta.
\end{aligned}
$$

Evaluation of the zeroth-order functions for $E^{(1)}_{(1)} = \frac{1}{2}\,\zeta$:

$$
\begin{aligned}
0 &= \left(-\tfrac{1}{2}\,\zeta - \tfrac{1}{2}\,\zeta\right)u_{2(1)} + \sqrt{\tfrac{1}{2}}\,\zeta\,u_{3(1)} \\
x_{(1)} &= \frac{u_{2(1)}}{u_{3(1)}} = \sqrt{\tfrac{1}{2}}; \qquad u_{2(1)} = \sqrt{\tfrac{1}{3}}; \qquad u_{3(1)} = \sqrt{\tfrac{2}{3}} \\
\psi_2 &= \sqrt{\tfrac{1}{3}}\,\big|\,1\,-\tfrac{1}{2}\,\big\rangle + \sqrt{\tfrac{2}{3}}\,\big|\,0\,\tfrac{1}{2}\,\big\rangle. \qquad (52)
\end{aligned}
$$

For $E^{(1)}_{(2)} = -\zeta$, the result is:

$$
\begin{aligned}
0 &= \left(-\tfrac{1}{2}\,\zeta + \zeta\right)u_{2(2)} + \sqrt{\tfrac{1}{2}}\,\zeta\,u_{3(2)} \\
x_{(2)} &= \frac{u_{2(2)}}{u_{3(2)}} = -\sqrt{2}; \qquad u_{2(2)} = -\sqrt{\tfrac{2}{3}}; \qquad u_{3(2)} = \sqrt{\tfrac{1}{3}} \\
\psi_3 &= -\sqrt{\tfrac{2}{3}}\,\big|\,1\,-\tfrac{1}{2}\,\big\rangle + \sqrt{\tfrac{1}{3}}\,\big|\,0\,\tfrac{1}{2}\,\big\rangle. \qquad (53)
\end{aligned}
$$

Evaluating the second 2×2 block the resulting states are

$$
\begin{aligned}
E^{(1)}_{(1)} = \tfrac{1}{2}\,\zeta: \qquad \psi_4 &= \sqrt{\tfrac{1}{3}}\,\big|-1\,\tfrac{1}{2}\,\big\rangle + \sqrt{\tfrac{2}{3}}\,\big|\,0\,-\tfrac{1}{2}\,\big\rangle \qquad (54) \\
E^{(1)}_{(2)} = -\zeta: \qquad \psi_5 &= \sqrt{\tfrac{2}{3}}\,\big|-1\,\tfrac{1}{2}\,\big\rangle - \sqrt{\tfrac{1}{3}}\,\big|\,0\,-\tfrac{1}{2}\,\big\rangle. \qquad (55)
\end{aligned}
$$

The results are given in Table 6.

The functions are not only eigenfunctions of the operators $\hat{\boldsymbol{l}}\cdot\hat{\boldsymbol{s}}$ and $\hat{\boldsymbol{s}}\cdot\hat{\boldsymbol{l}}$ but also of

$$\hat{\boldsymbol{l}}^{\,2} + \hat{\boldsymbol{l}}\cdot\hat{\boldsymbol{s}} + \hat{\boldsymbol{s}}\cdot\hat{\boldsymbol{l}} + \hat{\boldsymbol{s}}^2 = \big(\hat{\boldsymbol{l}} + \hat{\boldsymbol{s}}\big)^2 = \hat{\boldsymbol{j}}^2. \tag{56}$$

If $\hat{\boldsymbol{j}}^2$ acts on a quartet state function ψ_Q $(\psi_1, \psi_2, \psi_4, \psi_6)$ and on a doublet state function ψ_D (ψ_3, ψ_5), respectively, the result is

$$\begin{aligned}
\hat{\boldsymbol{j}}^2\,\psi_Q &= \big(\hat{\boldsymbol{l}}^{\,2} + 2\,\hat{\boldsymbol{l}}\cdot\hat{\boldsymbol{s}} + \hat{\boldsymbol{s}}^2\big)\,\psi_Q \\
&= \hbar^2\,\big(2 + 2\cdot\tfrac{1}{2} + \tfrac{3}{4}\big)\,\psi_Q = \hbar^2\,\big(\tfrac{15}{4}\big)\,\psi_Q = \hbar^2\,\big(\tfrac{3}{2}\big)\big(\tfrac{5}{2}\big)\,\psi_Q \\
&= \hbar^2\,j_2(j_2+1)\,\psi_Q \qquad \text{where} \quad j_2 = \tfrac{3}{2} \qquad (57)\\
\hat{\boldsymbol{j}}^2\,\psi_D &= \big(\hat{\boldsymbol{l}}^{\,2} + 2\,\hat{\boldsymbol{l}}\cdot\hat{\boldsymbol{s}} + \hat{\boldsymbol{s}}^2\big)\,\psi_D \\
&= \hbar^2\,\big(2 - 2\cdot 1 + \tfrac{3}{4}\big)\,\psi_D = \hbar^2\,\big(\tfrac{3}{4}\big)\,\psi_D = \hbar^2\,\big(\tfrac{1}{2}\big)\big(\tfrac{3}{2}\big)\,\psi_D \\
&= \hbar^2\,j_1(j_1+1)\,\psi_D \qquad \text{where} \quad j_1 = \tfrac{1}{2}. \qquad (58)
\end{aligned}$$

Table 6: Functions and energies of the spin-orbit coupled p^1 system

ψ	$\lvert m_l\, m_s\rangle$	$\lvert j\, m_j\rangle$	$m_j = m_l + m_s$	j	$E^{(1)}$
ψ_1	$\lvert 1\ \frac{1}{2}\rangle$	$\lvert \frac{3}{2}\ \frac{3}{2}\rangle$	$\frac{3}{2}$	$\frac{3}{2}$	$\frac{1}{2}\zeta$
ψ_2	$\sqrt{\frac{1}{3}}\,\lvert 1\ -\frac{1}{2}\rangle + \sqrt{\frac{2}{3}}\,\lvert 0\ \frac{1}{2}\rangle$	$\lvert \frac{3}{2}\ \frac{1}{2}\rangle$	$\frac{1}{2}$		
ψ_4	$\sqrt{\frac{1}{3}}\,\lvert -1\ \frac{1}{2}\rangle + \sqrt{\frac{2}{3}}\,\lvert 0\ -\frac{1}{2}\rangle$	$\lvert \frac{3}{2}\ -\frac{1}{2}\rangle$	$-\frac{1}{2}$		
ψ_6	$\lvert -1\ -\frac{1}{2}\rangle$	$\lvert \frac{3}{2}\ -\frac{3}{2}\rangle$	$-\frac{3}{2}$		
ψ_3	$-\sqrt{\frac{2}{3}}\,\lvert 1\ -\frac{1}{2}\rangle + \sqrt{\frac{1}{3}}\,\lvert 0\ \frac{1}{2}\rangle$	$\lvert \frac{1}{2}\ \frac{1}{2}\rangle$	$\frac{1}{2}$	$\frac{1}{2}$	$-\zeta$
ψ_5	$\sqrt{\frac{2}{3}}\,\lvert -1\ \frac{1}{2}\rangle - \sqrt{\frac{1}{3}}\,\lvert 0\ -\frac{1}{2}\rangle$	$\lvert \frac{1}{2}\ -\frac{1}{2}\rangle$	$-\frac{1}{2}$		

Example 2.3 *Spin-orbit coupling of the f^1 and the f^{13} system*

Energy eigenvalues and eigenfunctions of 4f$^{\,1}$ (Ce^{3+}) and 4f$^{\,13}$ (Yb^{3+})

On account of $j = l \pm s = 3 \pm \frac{1}{2}$ (see Example 2.2) for one-electron and one-hole f systems we have

	energies			
$\mathrm{Ln}^{3+}[4\mathrm{f}^{\,N}]$	ground multiplet	E	excited multiplet	E
$\mathrm{Ce}^{3+}[4\mathrm{f}^{\,1}]$	${}^2F_{5/2}\,(j = 5/2)$	$-2\zeta_{\mathrm{Ce}}$	${}^2F_{7/2}\,(j = 7/2)$	$+\frac{3}{2}\zeta_{\mathrm{Ce}}$
$\mathrm{Yb}^{3+}[4\mathrm{f}^{\,13}]$	${}^2F_{7/2}\,(j = 7/2)$	$-\frac{3}{2}\zeta_{\mathrm{Yb}}$	${}^2F_{5/2}\,(j = 5/2)$	$+2\zeta_{\mathrm{Yb}}$

Eigenfunctions are obtained with the help of *vector coupling coefficients* (Clebsch-Gordan coefficients) (see Table 7).

Table 7: Vector coupling coefficients for systems with $j_2 = 1/2$

$j =$	$m_2 = \frac{1}{2}$	$m_2 = -\frac{1}{2}$
$j_1 + \frac{1}{2}$	$\sqrt{\dfrac{j_1 + m + \frac{1}{2}}{2j_1 + 1}}$	$\sqrt{\dfrac{j_1 - m + \frac{1}{2}}{2j_1 + 1}}$
$j_1 - \frac{1}{2}$	$-\sqrt{\dfrac{j_1 - m + \frac{1}{2}}{2j_1 + 1}}$	$\sqrt{\dfrac{j_1 + m + \frac{1}{2}}{2j_1 + 1}}$

Table 8: Spin-orbit coupled eigenfunctions of Ce^{3+} and Yb^{3+} free ions

$^{a)}$	$\lvert\, j\, m_j \rangle \qquad \lvert\, m_l\, m_s \rangle$	$E_J^{(\mathrm{Ce}^{3+})}$	$E_J^{(\mathrm{Yb}^{3+})}$
$\phi_1; \phi_6$	$\lvert\, \frac{5}{2} \pm\frac{5}{2} \,\rangle = \mp\sqrt{\frac{6}{7}}\,\lvert \pm 3 \mp\frac{1}{2} \,\rangle \pm \sqrt{\frac{1}{7}}\,\lvert \pm 2 \pm\frac{1}{2} \,\rangle$	-2ζ	2ζ
$\phi_2; \phi_5$	$\lvert\, \frac{5}{2} \pm\frac{3}{2} \,\rangle = \mp\sqrt{\frac{5}{7}}\,\lvert \pm 2 \mp\frac{1}{2} \,\rangle \pm \sqrt{\frac{2}{7}}\,\lvert \pm 1 \pm\frac{1}{2} \,\rangle$		
$\phi_3; \phi_4$	$\lvert\, \frac{5}{2} \pm\frac{1}{2} \,\rangle = \mp\sqrt{\frac{4}{7}}\,\lvert \pm 1 \mp\frac{1}{2} \,\rangle \pm \sqrt{\frac{3}{7}}\,\lvert 0 \pm\frac{1}{2} \,\rangle$		
$\phi'_1; \phi'_8$	$\lvert\, \frac{7}{2} \pm\frac{7}{2} \,\rangle = \lvert \pm 3 \pm\frac{1}{2} \,\rangle$	$\frac{3}{2}\zeta$	$-\frac{3}{2}\zeta$
$\phi'_2; \phi'_7$	$\lvert\, \frac{7}{2} \pm\frac{5}{2} \,\rangle = \sqrt{\frac{1}{7}}\,\lvert \pm 3 \mp\frac{1}{2} \,\rangle + \sqrt{\frac{6}{7}}\,\lvert \pm 2 \pm\frac{1}{2} \,\rangle$		
$\phi'_3; \phi'_6$	$\lvert\, \frac{7}{2} \pm\frac{3}{2} \,\rangle = \sqrt{\frac{2}{7}}\,\lvert \pm 2 \mp\frac{1}{2} \,\rangle + \sqrt{\frac{5}{7}}\,\lvert \pm 1 \pm\frac{1}{2} \,\rangle$		
$\phi'_4; \phi'_5$	$\lvert\, \frac{7}{2} \pm\frac{1}{2} \,\rangle = \sqrt{\frac{3}{7}}\,\lvert \pm 1 \mp\frac{1}{2} \,\rangle + \sqrt{\frac{4}{7}}\,\lvert 0 \pm\frac{1}{2} \,\rangle$		

$^{a)}$ Short form of the functions: the first symbol refers to the upper sign, the second to the lower one.

The calculation of the coefficients is demonstrated for $\lvert\, \frac{5}{2}\, \frac{5}{2} \,\rangle$ (first line in Table 8).
Assignments: $j = 5/2$, $m = m_j = 5/2$, $j_1 = l = 3$, and $m_2 = m_s = \pm 1/2$ ($j_2 = s = 1/2$)
The roots of the lower row of Table 7 become

$$m_2 = -\tfrac{1}{2}: \quad \sqrt{\frac{j_1 + m + \frac{1}{2}}{2j_1 + 1}} \;=\; \sqrt{\frac{3 + \frac{5}{2} - \frac{1}{2}}{7}} = \sqrt{\tfrac{6}{7}}$$

$$m_2 = \tfrac{1}{2}: \quad -\sqrt{\frac{j_1 - m + \frac{1}{2}}{2j_1 + 1}} \;=\; -\sqrt{\frac{3 - \frac{5}{2} + \frac{1}{2}}{7}} = -\sqrt{\tfrac{1}{7}}$$

Since the Condon-Shortley standard assignment is $j_1 \to s$ and $j_2 \to l$ the sign of the coefficients has to be changed according to the phase relation $|j_b j_a j m\rangle = (-1)^{j_a + j_b - j} |j_a j_b j m\rangle$.
Finally, we obtain
$\lvert\, \frac{5}{2}\, \frac{5}{2} \,\rangle = -\sqrt{\frac{6}{7}}\; \lvert\, 3 -\frac{1}{2} \,\rangle + \sqrt{\frac{1}{7}}\; \lvert\, 2 + \frac{1}{2} \,\rangle$.

Problems

4. Calculate the matrix elements $\langle l, m_l|\hat{l}_q|l, m_l'\rangle$ (where q stands for $z, +, -$):
   (a) $\langle 0,0|\hat{l}_z|0,0\rangle$, (b) $\langle 2,2|\hat{l}_+|2,1\rangle$, (c) $\langle 2,2|\hat{l}_+^2|2,0\rangle$, (d) $\langle 2,0|\hat{l}_+\hat{l}_-|2,0\rangle$.

5. The 14 microstates $|m_l m_s\rangle$ of a f^1 system ($l = 3$, $s = \frac{1}{2}$) yield under the influence of spin-orbit coupling 14 eigenstates $|jm_j\rangle$ which, apart from the states $|\frac{7}{2}\ \pm\frac{7}{2}\rangle$, are linear combinations of two microstates each. Use Table 7 to evaluate the vector coupling coefficients for the coupled states $|\frac{5}{2}\ \frac{1}{2}\rangle$, $|\frac{5}{2}\ -\frac{1}{2}\rangle$, $|\frac{7}{2}\ \frac{3}{2}\rangle$, and $|\frac{7}{2}\ -\frac{3}{2}\rangle$. Control your results with the entries of Table 8.

6. What levels (multiplets J) may arise from the terms (a) ^1S, (b) ^2P, (c) ^3P, (d) ^3D, (e) ^4D? How many states (distinguished by the quantum number M_J) belong to each level?

2.4.2 Magnetic susceptibility, Van Vleck equation

Fundamental magnetisation equation

$$\boxed{M_\mathrm{m} = -N_\mathrm{A}\frac{\sum\limits_n (\partial E_n/\partial B)\exp(-E_n/k_\mathrm{B}T)}{\sum\limits_n \exp(-E_n/k_\mathrm{B}T)} = N_\mathrm{A}\frac{\sum\limits_n \bar{\mu}_n \exp(-E_n/k_\mathrm{B}T)}{\sum\limits_n \exp(-E_n/k_\mathrm{B}T)}} \tag{59}$$

Van Vleck equation

operator: $\hat{H} = \hat{H}^{(0)} + B_z\hat{H}^{(1)}$ $\qquad E_n = W_n^{(0)} + B_z W_n^{(1)} + B_z^2 W_n^{(2)} + \ldots.$

$W_n^{(1)}$, $W_n^{(2)}$: First- and second-order Zeeman coefficient

$\bar{\mu}_n = -\partial E_n/\partial B = -W_n^{(1)} - 2BW_n^{(2)} - \ldots$

$$\boxed{\chi_\mathrm{m} = \mu_0 N_\mathrm{A}\frac{\sum\limits_n [(W_n^{(1)})^2/k_\mathrm{B}T - 2W_n^{(2)}]\exp(-W_n^{(0)}/k_\mathrm{B}T)}{\sum\limits_n \exp(-W_n^{(0)}/k_\mathrm{B}T)}} \tag{60}$$

Eq. (60) is valid for applied magnetic fields $B \to 0$.

Zeeman operator:

one-electron system $\hat{H}_\mathrm{mag} = -\gamma_\mathrm{e}\left(\hat{\boldsymbol{l}} + 2\hat{\boldsymbol{s}}\right)\cdot\boldsymbol{B}$ where $\gamma_\mathrm{e} = -e/(2m_\mathrm{e})$ (61)

$$\hat{H}_{\mathrm{mag},z} = -\gamma_\mathrm{e}\left(\hat{l}_z + 2\hat{s}_z\right)B_z \tag{62}$$

single term $$\hat{H}_\mathrm{mag} = -\gamma_\mathrm{e}\left(\hat{\boldsymbol{L}} + 2\hat{\boldsymbol{S}}\right)\cdot\boldsymbol{B} \tag{63}$$

$$\hat{H}_{\mathrm{mag,z}} = -\gamma_\mathrm{e}\left(\hat{L}_z + 2\hat{S}_z\right)B_z \tag{64}$$

single multiplet $$\hat{H}_\mathrm{mag} = -\gamma_\mathrm{e}\, g_J\, \hat{\boldsymbol{J}}\cdot\boldsymbol{B} \tag{65}$$

$$\hat{H}_{\mathrm{mag},z} = -\gamma_\mathrm{e}\, g_J\, \hat{J}_z\, B_z \tag{66}$$

Example 2.4 *Magnetic susceptibility of the $4f^1/4f^{13}$ free ion systems*

The 14 spin-coupled eigenfunctions of the $4\mathrm{f}^1/4\mathrm{f}^{13}$ systems are given in Table 8. Applying Zeeman operator (63) the assigned matrix elements in scheme (67) are to be evaluated:

$$\begin{array}{c|cccccc|cccccccc}
 & \phi_1 & \phi_2 & \phi_3 & \phi_4 & \phi_5 & \phi_6 & \phi'_1 & \phi'_2 & \phi'_3 & \phi'_4 & \phi'_5 & \phi'_6 & \phi'_7 & \phi'_8 \\
\hline
\phi_1 & \otimes & & & & & & & \times & & & & & & \\
\phi_2 & & \otimes & & & & & & & \times & & & & & \\
\phi_3 & & & \otimes & & & & & & & \times & & & & \\
\phi_4 & & & & \otimes & & & & & & & \times & & & \\
\phi_5 & & & & & \otimes & & & & & & & \times & & \\
\phi_6 & & & & & & \otimes & & & & & & & \times & \\
\hline
\phi'_1 & & & & & & & \otimes & & & & & & & \\
\phi'_2 & \times & & & & & & & \otimes & & & & & & \\
\phi'_3 & & \times & & & & & & & \otimes & & & & & \\
\phi'_4 & & & \times & & & & & & & \otimes & & & & \\
\phi'_5 & & & & \times & & & & & & & \otimes & & & \\
\phi'_6 & & & & & \times & & & & & & & \otimes & & \\
\phi'_7 & & & & & & \times & & & & & & & \otimes & \\
\phi'_8 & & & & & & & & & & & & & & \otimes
\end{array} \tag{67}$$

Calculation of the off-diagonal element $\left\langle\, \phi'_2 \,\middle|\hat{H}_z^{(1)}\middle|\, \phi_1 \,\right\rangle$

$$\begin{aligned}
\left\langle\, \phi'_2 \,\middle|\hat{H}_z^{(1)}\middle|\, \phi_1 \,\right\rangle &= \left\langle \tfrac{7}{2}\ \tfrac{5}{2} \,\middle|\, -\gamma_e(\hat{l}_z + 2\hat{s}_z) \middle|\, \tfrac{5}{2}\ \tfrac{5}{2} \right\rangle \\
= \quad & -\gamma_e \Big\langle \sqrt{\tfrac{1}{7}}\, \langle 3 - \tfrac{1}{2}| + \sqrt{\tfrac{6}{7}}\, \langle 2 + \tfrac{1}{2}\,| \Big| \hat{l}_z + 2\hat{s}_z \Big| \sqrt{\tfrac{6}{7}} |3 - \tfrac{1}{2}\rangle - \sqrt{\tfrac{1}{7}} |2 + \tfrac{1}{2}\rangle \Big\rangle \\
= \quad & -\frac{\gamma_e}{7}\Big[\sqrt{6}\, \underbrace{\langle 3 - \tfrac{1}{2}|\hat{l}_z + 2\hat{s}_z|3 - \tfrac{1}{2}\rangle}_{(3-1)\hbar} - \underbrace{\langle 3 - \tfrac{1}{2}|\hat{l}_z + 2\hat{s}_z|2 + \tfrac{1}{2}\rangle}_{0} \\
& + 6\, \underbrace{\langle 2 + \tfrac{1}{2}\,|\hat{l}_z + 2\hat{s}_z|3 - \tfrac{1}{2}\rangle}_{0} - \sqrt{6}\, \underbrace{\langle 2 + \tfrac{1}{2}\,|\hat{l}_z + 2\hat{s}_z|2 + \tfrac{1}{2}\rangle}_{(2+1)\hbar} \Big] = -\frac{\sqrt{6}}{7}\mu_B
\end{aligned}$$

We obtain with eq. (32) for $W^{(2)}_{|\frac{5}{2}\,\frac{5}{2}\rangle}$:

$$W^{(2)}_{|\frac{5}{2}\,\frac{5}{2}\rangle} = -\frac{\left|\langle\, \frac{7}{2}\ \frac{5}{2} \,|\, -\gamma_e(\hat{l}_z + 2\hat{s}_z) |\, \frac{5}{2}\ \frac{5}{2}\,\rangle\right|^2}{W^{(0)}_{7/2} - W^{(0)}_{5/2}} = -\frac{(6/49)\,\mu_\mathrm{B}^2}{(7/2)\,\zeta} = -\frac{12\,\mu_\mathrm{B}^2}{343\,\zeta}.$$

Tab. 9: Energies $W_n^{(0)}$ and Zeeman coefficients $W_n^{(1)}$, $W_n^{(2)}$ of a free f^1 system ($g_{J_1} = 6/7$ for ${}^2F_{5/2}$, $g_{J_2} = 8/7$ for ${}^2F_{7/2}$)

$\lvert J\, M_J \rangle$	$W_n^{(0)}$	$W_n^{(1)}/\mu_\mathrm{B}$	$W_n^{(2)}/\mu_\mathrm{B}^2$
$\lvert \frac{5}{2} \pm\frac{5}{2} \rangle$	$-2\,\zeta$	$\pm(5/2)\, g_{J_1}$	$-[12/(343\,\zeta)]$
$\lvert \frac{5}{2} \pm\frac{3}{2} \rangle$		$\pm(3/2)\, g_{J_1}$	$-[20/(343\,\zeta)]$
$\lvert \frac{5}{2} \pm\frac{1}{2} \rangle$		$\pm(1/2)\, g_{J_1}$	$-[24/(343\,\zeta)]$
$\lvert \frac{7}{2} \pm\frac{7}{2} \rangle$	$\frac{3}{2}\,\zeta$	$\pm(7/2)\, g_{J_2}$	
$\lvert \frac{7}{2} \pm\frac{5}{2} \rangle$		$\pm(5/2)\, g_{J_2}$	$+[12/(343\,\zeta)]$
$\lvert \frac{7}{2} \pm\frac{3}{2} \rangle$		$\pm(3/2)\, g_{J_2}$	$+[20/(343\,\zeta)]$
$\lvert \frac{7}{2} \pm\frac{1}{2} \rangle$		$\pm(1/2)\, g_{J_2}$	$+[24/(343\,\zeta)]$

In Table 9 the quantities $W_n^{(0)}$, $W_n^{(1)}$ and $W_n^{(2)}$ are collected. The final susceptibility equation for the $\mathrm{f}^1/\mathrm{f}^{13}$ system is obtained by summing up the contributions of the 14 levels:

$$\chi_\mathrm{m} = \mu_0 \frac{N_\mathrm{A}\mu_\mathrm{B}^2}{3k_\mathrm{B}T}\mu_\mathrm{eff}^2 \quad \text{where} \quad \mu_\mathrm{eff}^2 =$$

$$\frac{\left[3\left(\dfrac{45}{7} + \dfrac{16k_\mathrm{B}T}{49\,\zeta}\right) + 4\left(\dfrac{144}{7} - \dfrac{12k_\mathrm{B}T}{49\,\zeta}\right)\exp\left(-\dfrac{7\zeta}{2k_\mathrm{B}T}\right)\right]}{\left[3 + 4\exp\left(-\dfrac{7\zeta}{2k_\mathrm{B}T}\right)\right]}. \tag{68}$$

For Ce^{3+} the parameter ζ in eq. (68) refers to the single-electron spin-orbit coupling constant while in the case of Yb^{3+} the term spin-orbit coupling constant $\lambda_{LS} = -\zeta$ has to be replaced for ζ. (Notice that $\lambda_{LS} = \pm\zeta/(2S)$.)

The absolute energy separation between ${}^2F_{7/2}$ and ${}^2F_{5/2}$ is $\frac{7}{2} \times \zeta_\mathrm{Yb} = \frac{7}{2} \times 2870\,\mathrm{cm}^{-1} \approx 10\,000\,\mathrm{cm}^{-1}$ for the Yb^{3+} ion and $\frac{7}{2} \times \zeta_\mathrm{Ce} = \frac{7}{2} \times 625\,\mathrm{cm}^{-1} \approx 2\,200\,\mathrm{cm}^{-1}$ for the Ce^{3+}-Ion. In magnetochemical practice the higher lying multiplet is often ignored in eq. (68). There are two possibilities for simplification:

1.) $\zeta \to \infty$ ($4\mathrm{f}^1$) and $\lambda_{LS} \to -\infty$ ($4\mathrm{f}^{13}$) respectively:

$$\chi_\mathrm{m}(4\mathrm{f}^1) = \mu_0 \frac{N_\mathrm{A}\mu_\mathrm{B}^2}{3k_\mathrm{B}T} \underbrace{\frac{45}{7}}_{\mu_\mathrm{eff}^2} \qquad \chi_\mathrm{m}(4\mathrm{f}^{13}) = \mu_0 \frac{N_\mathrm{A}\mu_\mathrm{B}^2}{3k_\mathrm{B}T} \underbrace{\frac{144}{7}}_{\mu_\mathrm{eff}^2} \tag{69}$$

$$\mu_\mathrm{eff}^2(4\mathrm{f}^1) = \frac{45}{7} = \left(\frac{6}{7}\right)^2 \left(\frac{5}{2}\right)\left(\frac{7}{2}\right) \qquad \mu_\mathrm{eff}^2(4\mathrm{f}^{13}) = \frac{144}{7} = \left(\frac{8}{7}\right)^2 \left(\frac{7}{2}\right)\left(\frac{9}{2}\right).$$

In this approximation μ_eff^2 is temperature independent.

2.) In a less drastic approximation the contribution of the excited multiplet is again neglected, but not $W^{(2)}$ of the ground multiplet, so that in the case of the $4\mathrm{f}^1$ system the susceptibility equation reads

$$\chi_\mathrm{m}(4\mathrm{f}^1) = \mu_0 \frac{N_\mathrm{A}\mu_\mathrm{B}^2}{3k_\mathrm{B}T}\left\{\frac{45}{7} + \frac{16k_\mathrm{B}T}{49\,\zeta}\right\}, \quad \text{in general} \quad \chi_\mathrm{m} = \mu_0 \frac{N_\mathrm{A} g_J^2 J(J+1)\mu_\mathrm{B}^2}{3k_\mathrm{B}T} + \chi_0 \tag{70}$$

χ_0 is positive, leading to a weak increase of μ_eff with increasing temperature.

3 Lanthanide ions in cubic and non-cubic ligand fields

The evaluation of LF effects on f systems requires more effort than on d systems:

- On account of the larger angular momentum quantum number l, the number of ligand field parameters is larger, for example two instead of one for cubic symmetry;
- The number of microstates used in complete magnetochemical analyses is larger for f systems (for example 91 microstates for f^2 compared to 45 for d^2).

Ground multiplets of the f^1 to f^{13} ions:

$\mathrm{f}^{\mathrm{N}}/\mathrm{f}^{14-\mathrm{N}}$	$\mathrm{f}^1/\mathrm{f}^{13}$	$\mathrm{f}^2/\mathrm{f}^{12}$	$\mathrm{f}^3/\mathrm{f}^{11}$	$\mathrm{f}^4/\mathrm{f}^{10}$	$\mathrm{f}^5/\mathrm{f}^9$	$\mathrm{f}^6/\mathrm{f}^8$	f^7
ground multiplet	${}^2F_{\frac{5}{2}}/{}^2F_{\frac{7}{2}}$	${}^3H_4/{}^3H_6$	${}^4I_{\frac{9}{2}}/{}^4I_{\frac{15}{2}}$	${}^5I_4/{}^5I_8$	${}^6H_{\frac{5}{2}}/{}^6H_{\frac{15}{2}}$	${}^7F_0/{}^7F_6$	${}^8S_{\frac{7}{2}}$

(71)

3.1 Ligand-field (LF) operators [7]

General form of the LF operator for **one-electron** systems:

$$\hat{H}_{\mathrm{LF}} = \sum_{k=0}^{\infty} \sum_{q=-k}^{+k} A_k^q r^k C_q^k(\theta,\phi), \quad \text{where} \tag{72}$$

$$\underbrace{A_k^q = -e(-1)^q \int \frac{\rho(\boldsymbol{R})}{R^{k+1}}\, C_{-q}^k(\theta,\phi)\, d\tau_{\boldsymbol{R}}}_{\text{geometrical coordination factor}} \qquad \text{and} \qquad \underbrace{C_q^k = \left(\frac{4\pi}{2k+1}\right)^{1/2} Y_q^k(\theta,\phi)}_{\text{Racah tensor}}$$

LF operator for cubic ligand fields:

$$\hat{H}_{\mathrm{LF}}^{\mathrm{cub}} = \overbrace{\underbrace{A_4^0\, r^4 \left[C_0^4 + \sqrt{5/14}\left(C_4^4 + C_{-4}^4\right)\right]}_{\text{for d}^1 \text{ system}} + A_6^0\, r^6 \left[C_0^6 - \sqrt{7/2}\left(C_4^6 + C_{-4}^6\right)\right]}^{\text{for f}^1 \text{ system}}, \quad \text{where} \tag{73}$$

$$\begin{aligned}
C_0^4 &= \tfrac{1}{8}(35\cos^4\theta - 30\cos^2\theta + 3)\\
C_{\pm 4}^4 &= \tfrac{1}{16}\sqrt{70}\sin^4\theta\, e^{\pm i4\phi}\\
C_0^6 &= \tfrac{1}{16}(231\cos^6\theta - 315\cos^4\theta + 105\cos^2\theta - 5)\\
C_{\pm 4}^6 &= \tfrac{3}{32}\sqrt{14}\sin^4\theta(11\cos^2\theta - 1)\, e^{\pm i4\phi}
\end{aligned}$$

General LF matrix element:

$$\int \psi_{n,l,m_l}^*(r,\theta,\phi)\, \hat{H}_{\mathrm{LF}}\, \psi_{n,l,m_l'}(r,\theta,\phi) d\tau \tag{74}$$

Specific LF matrix element with $k = 4$ and $q = 0$:

$$\overbrace{A_4^0 \underbrace{\int_0^\infty R_{n,l}(r)\, r^4\, R_{n,l}(r)\, r^2 dr}_{\text{radial integral } < r^4 >}}^{\text{LF parameter } B_0^4} \int_0^\pi \int_0^{2\pi} Y_{m_l}^{l*}(\theta,\phi)\, [C_0^4 + \sqrt{5/14}(C_4^4 + C_{-4}^4)]\, Y_{m_l'}^l(\theta,\phi) \sin\theta\, d\theta\, d\phi$$

$$\hat{H}^{\mathrm{cub}}_{\mathrm{LF}} = B^4_0 \left[C^4_0 + \sqrt{5/14}\,(C^4_4 + C^4_{-4})\right] + B^6_0 \left[C^6_0 - \sqrt{7/2}\,(C^6_4 + C^6_{-4})\right] \tag{75}$$

With the help of integrals of the type $\langle Y^l_{m_l} | C^k_q | Y^l_{m'_l} \rangle$ [3], listed in Table 10 (p electrons) and Table 13 (f electrons), LF effects can be evaluated. The k values in eq. (72) comprise terms with $k \leq 2l$ and k even. The term with $k = 0$ has spherical symmetry, produces no splitting and is therefore omitted. The relevant k values for LF terms are $k = 2$ (p electrons), $k = 2$ and 4 (d electrons), $k = 2$, 4, and 6 (f electrons). Notice that the operators C^k_q act only on the orbital part of a wave function.

3.2 Introduction: p^1 system

3.2.1 Cylindrical LF: $H^{\mathrm{cyl}}_{\mathrm{LF}} + H_{\mathrm{SO}}$

Example 3.1 *The p^1 ion in a cylindrical LF*

To introduce the use of LF operators and electrostatic matrix elements, the p^1 system in a cylindrical LF ($\mathrm{D}_{\infty\mathrm{h}}$) is discussed[4]. The LF operator consists of a single term with $k = 2$ and $q = 0$:

$$\hat{H}^{\mathrm{cyl}}_{\mathrm{LF}} = B^2_0\, C^2_0, \quad \text{where} \quad B^2_0 = A^0_2 < r^2 > \quad \text{and} \quad C^2_0 = \tfrac{1}{2}(3\cos^2\theta - 1) \tag{76}$$

With the help of the matrix components of the electrostatic interactions, shown in Table 10, the 3×3 matrix (77) is obtained. Notice that only the red numbers corresponding to c^2 are relevant. Since the operator C^2_0 does not change m_l, matrix elements $< m_l \,|\, C^2_0 \,|\, m'_l >$ with $m_l \neq m'_l$ are automatically zero.

Table 10: Matrix components of electrostatic interactions, $c^k(lm_l, l'm'_l)$ for $l = l' = 1$; $c^k(l'm'_l, lm_l) = (-1)^{m_l - m'_l} c^k(lm_l, l'm'_l)$. Red numbers are relevant for Examples 3.1 and 3.3, the blue number for Example 3.3 only.

m_l	m'_l	c^0	$5\,c^{2\ a)}$
± 1	**± 1**	$+1$	**-1**
± 1	0	0	$+\sqrt{3}$
0	**0**	$+1$	**$+2$**
± 1	∓ 1	0	$-\sqrt{6}$

$^{a)}$ The numerical factor '5' is the denominator for all c^k values of the column.

3 × 3 matrix of operator (76):

$$\begin{array}{c|ccc} m_l & |\,1\,\rangle & |\,{-1}\,\rangle & |\,0\,\rangle \\ \hline \langle\,1\,| & -\frac{1}{5}B^2_0 & & \\ \langle\,{-1}\,| & & -\frac{1}{5}B^2_0 & \\ \langle\,0\,| & & & \frac{2}{5}B^2_0 \end{array} \tag{77}$$

Results: (i) All off-diagonal matrix elements are zero; (ii) LF operator eq. (76) splits the threefold degenerate p^1 system (in the absence of spin-orbit coupling) into an orbital doublet $|\pm 1\rangle$ with energy $E_{\mathrm{LF}} = -B^2_0/5$ and a singlet $|\,0\,\rangle$ with energy $E_{\mathrm{LF}} = 2B^2_0/5$.

---

[4] Electronic p states are not split by cubic ligand fields.

Example 3.2 *The p^1 system under the action of spin-orbit coupling and a cylindrical ligand field (cf. spin-orbit matrix (51))*

$$\hat{H}_{\mathrm{SO}} + \hat{H}_{\mathrm{LF}}^{\mathrm{cyl}} = \xi(r)\, \hat{\boldsymbol{l}}\boldsymbol{\cdot}\hat{\boldsymbol{s}} + B_0^2\, C_0^2 \tag{78}$$

$m_l m_s$	$\left\vert 1\ \tfrac{1}{2} \right\rangle$	$\left\vert 1\ -\tfrac{1}{2} \right\rangle$	$\left\vert 0\ \tfrac{1}{2} \right\rangle$	$\left\vert 0\ -\tfrac{1}{2} \right\rangle$	$\left\vert -1\ \tfrac{1}{2} \right\rangle$	$\left\vert -1\ -\tfrac{1}{2} \right\rangle$
$\left\langle 1\ \tfrac{1}{2} \right\vert$	$\tfrac{1}{2}\zeta - B_0^2/5$					
$\left\langle 1\ -\tfrac{1}{2} \right\vert$		$-\tfrac{1}{2}\zeta - B_0^2/5$	$\sqrt{\tfrac{1}{2}}\,\zeta$			
$\left\langle 0\ \tfrac{1}{2} \right\vert$		$\sqrt{\tfrac{1}{2}}\,\zeta$	$2B_0^2/5$			
$\left\langle 0\ -\tfrac{1}{2} \right\vert$				$2B_0^2/5$	$\sqrt{\tfrac{1}{2}}\,\zeta$	
$\left\langle -1\ \tfrac{1}{2} \right\vert$				$\sqrt{\tfrac{1}{2}}\,\zeta$	$-\tfrac{1}{2}\zeta - B_0^2/5$	
$\left\langle -1\ -\tfrac{1}{2} \right\vert$						$\tfrac{1}{2}\zeta - B_0^2/5$

$$\begin{aligned}
H_{11} &= \frac{\zeta}{\hbar^2}\underbrace{\left\langle 1\ \tfrac{1}{2}\middle\vert \hat{l}_z\hat{s}_z\middle\vert 1\ \tfrac{1}{2}\right\rangle}_{\hbar^2/2} + B_0^2\underbrace{\left\langle 1\middle\vert C_0^2\middle\vert 1\right\rangle}_{-1/5}\underbrace{\left\langle \tfrac{1}{2}\ \middle\vert\ \tfrac{1}{2}\right\rangle}_{1} = \tfrac{1}{2}\zeta - B_0^2/5 \\
H_{22} &= \frac{\zeta}{\hbar^2}\underbrace{\left\langle 1\ -\tfrac{1}{2}\middle\vert \hat{l}_z\hat{s}_z\middle\vert 1\ -\tfrac{1}{2}\right\rangle}_{-\hbar^2/2} + B_0^2\underbrace{\left\langle 1\middle\vert C_0^2\middle\vert 1\right\rangle}_{-1/5}\underbrace{\left\langle -\tfrac{1}{2}\ \middle\vert\ -\tfrac{1}{2}\right\rangle}_{1} = -\tfrac{1}{2}\zeta - B_0^2/5 \\
H_{33} &= \frac{\zeta}{\hbar^2}\underbrace{\left\langle 0\ \tfrac{1}{2}\middle\vert \hat{l}_z\hat{s}_z\middle\vert 0\ \tfrac{1}{2}\right\rangle}_{0} + B_0^2\underbrace{\left\langle 0\middle\vert C_0^2\middle\vert 0\right\rangle}_{2/5}\underbrace{\left\langle \tfrac{1}{2}\ \middle\vert\ \tfrac{1}{2}\right\rangle}_{1} = 2B_0^2/5 \\
H_{44} &= \frac{\zeta}{\hbar^2}\underbrace{\left\langle 0\ -\tfrac{1}{2}\middle\vert \hat{l}_z\hat{s}_z\middle\vert 0\ -\tfrac{1}{2}\right\rangle}_{0} + B_0^2\underbrace{\left\langle 0\middle\vert C_0^2\middle\vert 0\right\rangle}_{2/5}\underbrace{\left\langle -\tfrac{1}{2}\ \middle\vert\ -\tfrac{1}{2}\right\rangle}_{1} = 2B_0^2/5 \\
H_{55} &= \frac{\zeta}{\hbar^2}\underbrace{\left\langle -1\ \tfrac{1}{2}\middle\vert \hat{l}_z\hat{s}_z\middle\vert -1\ \tfrac{1}{2}\right\rangle}_{-\hbar^2/2} + B_0^2\underbrace{\left\langle -1\middle\vert C_0^2\middle\vert -1\right\rangle}_{-1/5}\underbrace{\left\langle \tfrac{1}{2}\ \middle\vert\ \tfrac{1}{2}\right\rangle}_{1} = -\tfrac{1}{2}\zeta - B_0^2/5 \\
H_{66} &= \frac{\zeta}{\hbar^2}\underbrace{\left\langle -1\ -\tfrac{1}{2}\middle\vert \hat{l}_z\hat{s}_z\middle\vert -1\ -\tfrac{1}{2}\right\rangle}_{\hbar^2/2} + B_0^2\underbrace{\left\langle -1\middle\vert C_0^2\middle\vert -1\right\rangle}_{-1/5}\underbrace{\left\langle -\tfrac{1}{2}\ \middle\vert\ -\tfrac{1}{2}\right\rangle}_{1} = \tfrac{1}{2}\zeta - B_0^2/5 \\
H_{23} &= \frac{\zeta}{\hbar^2}\underbrace{\left\langle 1\ -\tfrac{1}{2}\middle\vert \tfrac{1}{2}\hat{l}_+\hat{s}_-\middle\vert 0\ \tfrac{1}{2}\right\rangle}_{\sqrt{2}/2} = \sqrt{\tfrac{1}{2}}\,\zeta = H_{32} \\
H_{45} &= \frac{\zeta}{\hbar^2}\underbrace{\left\langle 0\ -\tfrac{1}{2}\middle\vert \tfrac{1}{2}\hat{l}_+\hat{s}_-\middle\vert -1\ \tfrac{1}{2}\right\rangle}_{\sqrt{2}/2} = \sqrt{\tfrac{1}{2}}\,\zeta = H_{54}
\end{aligned}$$

Application of scheme eq. (37) on the 2×2 matrices yields

$$H_{22} = -\zeta/2 - B_0^2/5, \qquad H_{33} = 2B_0^2/5, \qquad H_{23} = H_{32} = -\zeta/\sqrt{2}$$

$$\tan 2\alpha = \frac{2\,H_{23}}{H_{22} - H_{33}} = \frac{\sqrt{2}\,\zeta}{\zeta/2 + 3B_0^2/5} = \frac{\sqrt{2}}{\frac{1}{2} + \frac{3}{5}B_0^2/\zeta} \tag{79}$$

Result: The combined effect of $H_{\rm SO} + H_{\rm LF}^{\rm cyl}$ splits the sixfold degenerate spin orbital states into three doublets. The composition of the wave functions depends on the ratio B_0^2/ζ. No simple closed expressions can be given for the functions.

3.2.2 Orthorhombic LF: $H_{\rm LF}^{\rm or} + H_{\rm SO}$

Example 3.3 *The p^1 system in orthorhombic ligand fields*

$$\hat{H}_{\rm LF}^{\rm or} = B_0^2\,C_0^2 + B_2^2\,\left(C_2^2 + C_{-2}^2\right) \quad \text{where} \quad C_{\pm 2}^2 = \sqrt{\tfrac{3}{8}}\sin^2\theta\,\exp(\pm 2i\phi) \tag{80}$$

Matrix elements of operator eq. (80):

m_l	$\|\,1\,\rangle$	$\|\,-1\,\rangle$	$\|\,0\,\rangle$
$\langle\,1\,\|$	$-\frac{1}{5}B_0^2$	$-\frac{\sqrt{6}}{5}\,B_2^2$	
$\langle\,-1\,\|$	$-\frac{\sqrt{6}}{5}\,B_2^2$	$-\frac{1}{5}B_0^2$	
$\langle\,0\,\|$			$\frac{2}{5}B_0^2$

Determination of the correct zeroth order functions by application of scheme eq. (37):

$$H_{11} = H_{22} = -B_0^2/5, \qquad H_{12} = H_{21} = -\sqrt{6}\,B_2^2/5$$

$$\begin{aligned}
\tan 2\alpha &= \frac{2\,H_{12}}{H_{11} - H_{22}} = \frac{-2\sqrt{6}\,B_2^2/5}{-B_0^2/5 + B_0^2/5} = \frac{-2\sqrt{6}\,B_2^2/5}{0} = \begin{cases} +\infty & \text{for} \quad B_2^2 < 0 \\ -\infty & \text{for} \quad B_2^2 > 0 \end{cases} \\
2\alpha &= \pm 90^\circ \quad \rightarrow \quad \alpha = \pm 45^\circ; \quad \cot 45^\circ = \pm 1 \\
E_{1,2} &= -B_0^2/5 \pm \sqrt{6}\,B_2^2/5, \qquad \Psi_{1,2} = (\sqrt{2})^{-1}\,(|\,1\,\rangle \mp |\,-1\,\rangle) \\
E_3 &= 2\,B_0^2/5, \qquad\qquad\qquad \Psi_3 = |\,0\,\rangle
\end{aligned}$$

Result: Neglecting spin, the orthorhombic ligand field splits the threefold degenerate orbital states into three singlets.

Example 3.4 *The p^1 system under the action of spin-orbit coupling and an orthorhombic ligand field*

$$\hat{H}_{\rm SO} + \hat{H}_{\rm LF}^{\rm or} = \xi(r)\,\hat{\boldsymbol{l}}\boldsymbol{\cdot}\hat{\boldsymbol{s}} + B_0^2\,C_0^2 + B_2^2(C_2^2 + C_{-2}^2) \tag{81}$$

The matrix elements of this operator are stated in scheme (82). The $-E^{(1)}$'s in the diagonal elements are omitted and also the multiplicative factor hc for the spin-orbit coupling matrix elements which are usually given in the energy equivalent cm^{-1}. The empty off-diagonal elements are automatically zero. The diagonalisation of the 3×3

blocks, the energies and the composition of the wave functions must be calculated with the aid of a computer.

$$
\begin{array}{r||ccc|ccc}
m_l m_s & \left|1\,\tfrac{1}{2}\right\rangle & \left|0\,-\tfrac{1}{2}\right\rangle & \left|-1\,\tfrac{1}{2}\right\rangle & \left|1\,-\tfrac{1}{2}\right\rangle & \left|0\,\tfrac{1}{2}\right\rangle & \left|-1\,-\tfrac{1}{2}\right\rangle \\
\hline
\left\langle 1\,\tfrac{1}{2}\right| & \tfrac{1}{2}\zeta - B_0^2/5 & 0 & -\sqrt{6}B_2^2/5 & & & \\
\left\langle 0\,-\tfrac{1}{2}\right| & 0 & 2B_0^2/5 & \sqrt{\tfrac{1}{2}}\,\zeta & & & \\
\left\langle -1\,\tfrac{1}{2}\right| & -\sqrt{6}B_2^2/5 & \sqrt{\tfrac{1}{2}}\,\zeta & -\tfrac{1}{2}\zeta - B_0^2/5 & & & \\
\hline
\left\langle 1\,-\tfrac{1}{2}\right| & & & & -\tfrac{1}{2}\zeta - B_0^2/5 & \sqrt{\tfrac{1}{2}}\,\zeta & -\sqrt{6}B_2^2/5 \\
\left\langle 0\,\tfrac{1}{2}\right| & & & & \sqrt{\tfrac{1}{2}}\,\zeta & 2B_0^2/5 & 0 \\
\left\langle -1\,-\tfrac{1}{2}\right| & & & & -\sqrt{6}B_2^2/5 & 0 & \tfrac{1}{2}\zeta - B_0^2/5
\end{array}
\tag{82}
$$

3.3 Cubic LF

3.3.1 Group theoretical tools I [9, 8]

Character tables of the point groups serve to assign the LF states with respect to symmetry and degeration. For the cubic systems O and T_d Table 11 is relevant. It is applicable to Ln ions with integer J. The degree of degeneration of the LF states is responsible for the orbital contribution of the lanthanides' magnetic moment: The singlet states $A_1(\Gamma_1)$ and $A_2(\Gamma_2)$ as well as the doublet state $E(\Gamma_3)$ are non-magnetic, while the triplet states $T_1(\Gamma_4)$ and $T_2(\Gamma_5)$ are magnetic. For half-integer J all states are on principle magnetic; for cubic LF character tables of the respective *double groups* O′ and T'_d are relevant [8, 10] (*cf.* Table 12). Usually Bethe's nomenclature is used for f systems, see , e. g., the article of Lea, Leask, Wolf (LLW[16]).

Tab. 11: Character table of the symmetry groups O and T_d

O	E	8 C_3	3 C_2	6 C_4	6 C'_2	
T_d	E	8 C_3	3 C_2	6 S_4	6 σ_d	
A_1 [a]	1	1	1	1	1	Γ_1 [b]
A_2	1	1	1	−1	−1	Γ_2
E	2	−1	2	0	0	Γ_3
T_1	3	0	−1	1	−1	Γ_4
T_2	3	0	−1	−1	1	Γ_5

---

[a] Mulliken nomenclature.

[b] Bethe nomenclature.

3.3.2 4f^1 system (Ce^{3+}, ^2F: $H_{SO} + H_{LF}^{cub}$)

Ce^{3+} is a half-integer system. So, O′, T'_d are relevant. Under the action of the LF operator

$$\hat{H}_{\mathrm{LF}}^{\mathrm{cub}}(4\mathrm{f}^1) = B_0^4 \left\{ C_0^4 + \sqrt{\tfrac{5}{14}}\,[C_4^4 + C_{-4}^4] \right\} \quad + \quad \underbrace{B_0^6 \left\{ C_0^6 - \sqrt{\tfrac{7}{2}}\,[C_4^6 + C_{-4}^6] \right\}}_{\text{irrelevant for restricted basis } ^2F_{5/2}},$$

the free ion multiplets split according to $^2F_{5/2} \longrightarrow$ G′ (Γ_8) + E″ (Γ_7) and $^2F_{7/2} \longrightarrow$ G′ (Γ_8) + E″ (Γ_7) + E′ (Γ_6). If H_{SO} is distinctly stronger than H_{LF} it is convenient to consider

Tab. 12: Character table of the double groups O' and T_d'

O'	E	R	$4\,\mathrm{C}_3$	$4\,\mathrm{C}_3^2$	$3\,\mathrm{C}_2$	$3\,\mathrm{C}_4$	$3\,\mathrm{C}_4^3$	$6\,\mathrm{C}_2'$
			$4\,\mathrm{C}_3^2\mathrm{R}$	$4\,\mathrm{C}_3\mathrm{R}$	$3\,\mathrm{C}_2\mathrm{R}$	$3\,\mathrm{C}_4^3\mathrm{R}$	$3\,\mathrm{C}_4\mathrm{R}$	$6\,\mathrm{C}_2'\mathrm{R}$
T_d'	E	R	$4\,\mathrm{C}_3$	$4\,\mathrm{C}_3^2$	$3\,\mathrm{C}_2$	$3\,\mathrm{S}_4$	$3\,\mathrm{S}_4^3$	$6\,\sigma_\mathrm{d}$
			$4\,\mathrm{C}_3^2\mathrm{R}$	$4\,\mathrm{C}_3\mathrm{R}$	$3\,\mathrm{C}_2\mathrm{R}$	$3\,\mathrm{S}_4^3\mathrm{R}$	$3\,\mathrm{S}_4\mathrm{R}$	$6\,\sigma_\mathrm{d}\mathrm{R}$
$\mathrm{A}_1(\Gamma_1)$[a]	1	1	1	1	1	1	1	1
$\mathrm{A}_2(\Gamma_2)$	1	1	1	1	1	-1	-1	-1
$\mathrm{E}(\Gamma_3)$	2	2	-1	-1	2	0	0	0
$\mathrm{T}_1(\Gamma_4)$	3	3	0	0	-1	1	1	-1
$\mathrm{T}_2(\Gamma_5)$	3	3	0	0	-1	-1	-1	1
$\mathrm{E}'(\Gamma_6)$[b]	2	-2	1	-1	0	$\sqrt{2}$	$-\sqrt{2}$	0
$\mathrm{E}''(\Gamma_7)$	2	-2	1	-1	0	$-\sqrt{2}$	$\sqrt{2}$	0
$\mathrm{G}'(\Gamma_8)$	4	-4	-1	1	0	0	0	0

---

[a] $\Gamma_1 - \Gamma_5$: integer J; $\Gamma_1 - \Gamma_3$: non-magnetic.
[b] $\Gamma_6 - \Gamma_8$: half-integer J; magnetic.

H_LF acting only on the ground multiplet ${}^2F_{5/2}$ [$\rightarrow \mathrm{G}'(\Gamma_8) + \mathrm{E}''(\Gamma_7)$]. This approximation has the advantage that $\hat{H}_\mathrm{LF}^\mathrm{cub}$ can be restricted to the fourth degree term ($k = 4$), since the corresponding LF matrix elements of the sixth degree term are zero. Using Table 8 and Table 13 the matrix elements of $\hat{H}_\mathrm{LF}^\mathrm{cub}$ in scheme (83) are obtained.

Normally, the spin-orbit coupled states $|J\ M_J\rangle$ are used as a basis for the multiplet. In the following examples, however, we write them as $|M_L\ M_S\rangle$ basis with the advantage that the action of $\hat{H}_\mathrm{LF}^\mathrm{cub}$ on the orbital function $|M_L\rangle$ becomes obvious.

Table 13: Matrix components of electrostatic interactions, $c^k(lm_l, l'm_l')$ for $l = l' = 3$; $c^k(l'm_l', lm_l) = (-1)^{m_l - m_l'} c^k(lm_l, l'm_l')$ [3]

m_l	m_l'	c^0	$15\,c^2$ [a]	$33\,c^4$ [a]	$\frac{429}{5}\,c^6$ [a]	m_l	m_l'	c^0	$15\,c^2$	$33\,c^4$	$\frac{429}{5}\,c^6$
±3	±3	$+1$	-5	**$+3$**	**-1**	±1	0	0	$+\sqrt{2}$	$+\sqrt{15}$	$+\sqrt{350}$
±3	±2	0	$+5$	$-\sqrt{30}$	$+\sqrt{7}$	0	0	$+1$	$+4$	**$+6$**	$+20$
±3	±1	0	$-\sqrt{10}$	$+\sqrt{54}$	$-\sqrt{28}$	±3	∓3	0	0	0	$-\sqrt{924}$
±3	0	0	0	$-\sqrt{63}$	$+\sqrt{84}$	±3	∓2	0	0	0	$+\sqrt{462}$
±2	±2	$+1$	0	**-7**	**$+6$**	±3	∓1	0	0	**$+\sqrt{42}$**	**$-\sqrt{210}$**
±2	±1	0	$+\sqrt{15}$	$+\sqrt{32}$	$-\sqrt{105}$	±2	∓2	0	0	**$+\sqrt{70}$**	**$+\sqrt{504}$**
±2	0	0	$-\sqrt{20}$	$-\sqrt{3}$	$+\sqrt{224}$	±2	∓1	0	0	$-\sqrt{14}$	$-\sqrt{378}$
±1	±1	$+1$	$+3$	**$+1$**	-15	±1	∓1	0	$-\sqrt{24}$	$-\sqrt{40}$	$-\sqrt{420}$

---

[a] The numerical factor is the denominator for all c^k values of a column. (Notice that only the red terms are relevant in Example 3.5.)

Example 3.5 *Evaluation of the diagonal element* $H_{11} = \langle \tfrac{5}{2}\,|\hat{H}^{\rm cub}_{\rm LF}|\,\tfrac{5}{2}\rangle$ *of matrix (83)*

$$H_{11} = \tfrac{1}{7}\big\langle -\sqrt{6}\,\langle 3,-\tfrac{1}{2}\,| + \langle 2,\tfrac{1}{2}\,|\big|\,\hat{H}^{\rm cub}_{\rm LF}\,\big| -\sqrt{6}\,|\,3,-\tfrac{1}{2}\rangle + |\,2,\tfrac{1}{2}\rangle\big\rangle$$

(i) 'Integration' with respect to the spin, (ii) insert of $c^k(lm_l, l'm_l')$ values[5]:

$$\begin{aligned} H_{11} &= \tfrac{1}{7}\Big(6\,\langle 3\,|\hat{H}^{\rm cub}_{\rm LF}|\,3\rangle + \langle 2\,|\hat{H}^{\rm cub}_{\rm LF}|\,2\rangle\Big) = \\ &\tfrac{1}{7}\Big[B^4_0\,\big(6\,\underbrace{\langle 3\,|C^4_0|\,3\rangle}_{c^4(33,33)=3/33} + \underbrace{\langle 2\,|C^4_0|\,2\rangle}_{c^4(22,22)=-7/33}\big) + B^6_0\,\big(\underbrace{6\,\langle 3\,|C^6_0|\,3\rangle + \langle 2\,|C^6_0|\,2\rangle}_{0}\big)\Big] = \tfrac{1}{21}\,B^4_0. \end{aligned}$$

$$H_{\rm LF} \text{ matrix of } {}^2F_{5/2} \qquad \begin{array}{r|cccccc} 4\mathrm{f}^1(\mathrm{cub}) & |\,\tfrac{5}{2}\rangle & |-\tfrac{3}{2}\rangle & |-\tfrac{5}{2}\rangle & |\,\tfrac{3}{2}\rangle & |\,\tfrac{1}{2}\rangle & |-\tfrac{1}{2}\rangle \\ \hline \langle\,\tfrac{5}{2}\,| & \frac{1}{21} & \frac{\sqrt{5}}{21} & & & & \\ \langle -\tfrac{3}{2}\,| & \frac{\sqrt{5}}{21} & -\frac{3}{21} & & & & \\ \langle -\tfrac{5}{2}\,| & & & \frac{1}{21} & \frac{\sqrt{5}}{21} & & \\ \langle\,\tfrac{3}{2}\,| & & & \frac{\sqrt{5}}{21} & -\frac{3}{21} & & \\ \langle\,\tfrac{1}{2}\,| & & & & & \frac{2}{21} & \\ \langle -\tfrac{1}{2}\,| & & & & & & \frac{2}{21} \end{array} \qquad (83)$$

Example 3.6 *Evaluation of the off-diagonal element* $\langle \tfrac{5}{2}\,|\hat{H}^{\rm cub}_{\rm LF}|-\tfrac{3}{2}\rangle$

$$H_{12} = \tfrac{1}{7}\big\langle -\sqrt{6}\,\langle 3,-\tfrac{1}{2}| + \langle 2,\tfrac{1}{2}|\big|\,\hat{H}^{\rm cub}_{\rm LF}\,\big| -\sqrt{2}\,|-1,-\tfrac{1}{2}\rangle + \sqrt{5}\,|-2,\tfrac{1}{2}\rangle\big\rangle$$

$$\begin{aligned} H_{12} &= \tfrac{1}{7}\Big(\sqrt{12}\,\langle 3\,|\hat{H}^{\rm cub}_{\rm LF}|-1\rangle + \sqrt{5}\,\langle 2\,|\hat{H}^{\rm cub}_{\rm LF}|-2\rangle\Big) = \\ &\qquad \tfrac{1}{7}\,\Big[\,B^4_0\sqrt{\tfrac{5}{14}}\Big(\sqrt{12}\,\underbrace{\langle 3\,|C^4_4|-1\rangle}_{\sqrt{42}/33} + \sqrt{5}\,\underbrace{\langle 2\,|C^4_4|-2\rangle}_{\sqrt{70}/33}\Big)\Big] \\ &\qquad -\sqrt{\tfrac{7}{2}}\,B^6_0\Big[\Big(\underbrace{\sqrt{12}\langle 3\,|C^6_4|-1\rangle + \sqrt{5}\,\langle 2\,|C^6_4|-2\rangle}_{0}\Big)\Big] = \tfrac{\sqrt{5}}{21}\,B^4_0 \end{aligned}$$

The $H_{\rm LF}$ matrix (83) has two identical 1×1 and two identical 2×2 blocks. The former two correspond to the $|M_J\rangle$ states $|\,\tfrac{1}{2}\rangle$ and $|-\tfrac{1}{2}\rangle$ yielding the first-order correction to the energy $E^{(1)} = E_{\rm LF} = (2/21)\,B^4_0$. The energy of the other states is obtained by applying eqn. (36):

$$\begin{vmatrix} \frac{1}{21}\,B^4_0 - E & \frac{\sqrt{5}}{21}\,B^4_0 \\ \frac{\sqrt{5}}{21}\,B^4_0 & -\frac{3}{21}\,B^4_0 - E \end{vmatrix} = 0 \implies \begin{cases} E_1 = \frac{2}{21}\,B^4_0 \\ E_2 = -\frac{4}{21}\,B^4_0. \end{cases}$$

---

[5] Note that the sixth degree term ($k=6$) of $\hat{H}^{\rm cub}_{\rm LF}$, applied to ${}^2F_{5/2}[n\mathrm{f}^1]$, has no influence, that is, the corresponding matrix elements vanish.

The sixfold degenerate multiplet ${}^2F_{5/2}$ is split by a cubic LF in a doublet (E$''$; Γ_7) and a quartet (G$'$; Γ_8) (see Table 14). In octahedral surrounding with negatively charged ligands E'' is the ground state ($A_0^4, B_0^4 > 0$), whereas in tetrahedral symmetry the splitting pattern is reversed. The splitting $\Delta E(\mathrm{G}', \mathrm{E}'') = (6/21)\, B_0^4$ is in the range of a few $100\,\mathrm{cm}^{-1}$, that is, several orders of magnitude smaller than for d ions, caused by smaller radial integrals and larger metal–ligand distances for the 4f ions.

Table 14: Wavefunctions and energies of the ${}^2F_{5/2}$ multiplet perturbed by a cubic LF

$\lvert\Gamma\bar{M}\rangle$ [a)] [b)]	$\lvert M_J\rangle$	E_{LF}
$\lvert\mathrm{G}'\kappa, \mu\rangle$	$\pm\sqrt{\frac{5}{6}}\,\lvert \pm\frac{5}{2}\,\rangle \pm \sqrt{\frac{1}{6}}\,\lvert \mp\frac{3}{2}\,\rangle$	$\frac{2}{21}B_0^4$
$\lvert\mathrm{G}'\lambda, \nu\rangle$	$\pm\lvert \pm\frac{1}{2}\,\rangle$	
$\lvert\mathrm{E}''\alpha''\beta''\rangle$	$\sqrt{\frac{1}{6}}\,\lvert \pm\frac{5}{2}\,\rangle - \sqrt{\frac{5}{6}}\lvert \mp\frac{3}{2}\,\rangle$ [c)]	$-\frac{4}{21}B_0^4$

[a)] $\mathrm{G}' \equiv \Gamma_8; \mathrm{E}'' \equiv \Gamma_7$.

[b)] For the states in short *cf.* ref. [6].

[c)] Phase for Kramers doublets:
$\lvert\xi\rangle = \sum_{J,M} C_{J,M}\lvert JM\rangle$
$\lvert\bar{\xi}\rangle = \sum_{J,M} C^*_{J,M}(-1)^{J-M}\lvert J-M\rangle$.

Magnetic susceptibility
Zeeman operator (eq. (66)):

$$\hat{H}_{\mathrm{mag},z} = -\gamma_{\mathrm{e}} g_J \hat{J}_z B_z \quad \text{where} \quad \gamma_{\mathrm{e}} = -e/(2m_{\mathrm{e}}), \quad g_J = 6/7$$

Application of the z component of the Zeeman operator onto the six symmetry-adapted linear combinations of the ground multiplet ${}^2F_{5/2}$ (Table 14) yields the matrix elements in Table 15 (in units of $g_J\mu_{\mathrm{B}}B_z$ and $\Delta = E_{\mathrm{LF}}(\mathrm{G}') - E_{\mathrm{LF}}(\mathrm{E}'') = (6/21)\, B_0^4$).

Table 15: $W_n^{(0)}$, $W_n^{(1)}$ and $W_n^{(2)}$ of the 4f^1 system perturbed by $H_{\mathrm{LF}}^{\mathrm{cub}}$ ($\Delta \equiv (6/21)B_0^4$)

	$W_n^{(0)}$	$\dfrac{W_n^{(1)}}{g_J\,\mu_{\mathrm{B}}}$	$\dfrac{W_n^{(2)}}{g_J^2\,\mu_{\mathrm{B}}^2}$
$\lvert\mathrm{G}'\kappa, \nu\rangle$	Δ	$\pm 11/6$	$+\dfrac{20}{9\,\Delta}$
$\lvert\mathrm{G}'\lambda, \mu\rangle$		$\pm 1/2$	0
$\lvert\mathrm{E}''\bar{M}''\rangle$	0	$\mp 5/6$	$-\dfrac{20}{9\,\Delta}$

Diagonal element:

$$\begin{aligned} H_{11} &= \langle\mathrm{G}'\kappa\lvert\hat{H}_{\mathrm{mag},z}\rvert\mathrm{G}'\kappa\rangle \\ &= \left[(\tfrac{5}{6})(\tfrac{5}{2}) + (\tfrac{1}{6})(-\tfrac{3}{2})\right] g_J\mu_{\mathrm{B}}B_z = (\tfrac{11}{6})g_J\mu_{\mathrm{B}}B_z \end{aligned}$$

Off-diagonal element:

$$\begin{aligned} H_{15} &= \langle\mathrm{G}'\kappa\lvert\hat{H}_{\mathrm{mag}_z}\rvert\mathrm{E}''\alpha''\rangle \\ &= \left[\sqrt{\tfrac{1}{6}}\sqrt{\tfrac{5}{6}}\,(\tfrac{5}{2}) - \sqrt{\tfrac{1}{6}}\sqrt{\tfrac{5}{6}}\,(-\tfrac{3}{2})\right] g_J\mu_{\mathrm{B}}B_z = (\tfrac{2\sqrt{5}}{3})\, g_J\mu_{\mathrm{B}}B_z. \end{aligned}$$

Substitution of $W_n^{(0)}$, $W_n^{(1)}$, and $W_n^{(2)}$ into the Van Vleck eq. (60) yields the magnetic susceptibility of the $4f^1$ system in cubic ligand fields:

$$\chi_{\mathrm{m}} = \mu_0 \frac{N_A \mu_{\mathrm{B}}^2}{3 k_{\mathrm{B}} T} \mu_{\mathrm{eff}}^2 \quad \text{where} \tag{84}$$

$$\mu_{\mathrm{eff}}^2 = \frac{g_J^2 \left[\frac{25}{12} + \frac{40}{3\Delta} k_{\mathrm{B}} T + \left(\frac{130}{12} - \frac{40}{3\Delta} k_{\mathrm{B}} T \right) \exp\left(-\frac{\Delta}{k_{\mathrm{B}} T} \right) \right]}{\left[1 + 2 \exp\left(-\frac{\Delta}{k_{\mathrm{B}} T} \right) \right]}.$$

Fig. 8 shows the μ_{eff}–T and the χ_{m}^{-1}–T behaviour for $\Delta = +605\,\mathrm{cm}^{-1}$ (LF ground state $\mathrm{E}''(\Gamma_7)$, $B_0^4 = 2\,119\ \mathrm{cm}^{-1}$, oct.) and $\Delta = -605\,\mathrm{cm}^{-1}$ ($\mathrm{G}'(\Gamma_8)$, $B_0^4 = -2\,119\ \mathrm{cm}^{-1}$, tetrah., cube).

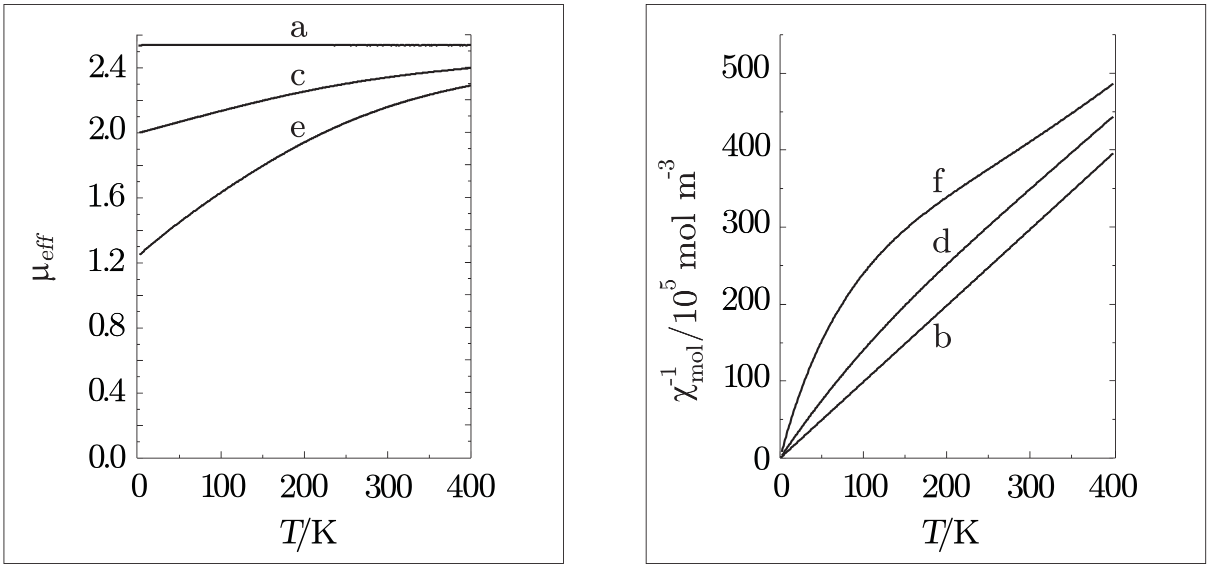

Fig. 8: Ce^{3+} in cubic LF; μ_{eff}–T (a,c,e) and χ_{m}^{-1}–T diagrams (b,d,f); $\Delta = 605\,\mathrm{cm}^{-1}$ oct., (e,f), $\Delta = -605\,\mathrm{cm}^{-1}$ tetrah., cube, (c,d); straight lines (a,b) correspond to the free ion.

Discussion

1. The ligand field effect produces a distinct deviation from free ion magnetic behaviour, except Ln ions with $4f^7$ configuration ($\mathrm{Eu}^{2+}, \mathrm{Gd}^{3+}$).

2. At very low temperature the χ_{m}^{-1} *vs.* T curves for systems with an odd number of 4f electrons (half-integral J) become nearly straight lines running into the origin (Curie-like behaviour, explicable with eq. (84)), provided that cooperative magnetic effects are absent.

3. In the case of integral J the low-temperatur magnetic behaviour is more complicated (see Section 3.3.4).

4. **Warning**: The upper region of the χ_{m}^{-1} versus T curves does not follow the Curie or Curie-Weiss law (except $4f^7$ ions). To compare the magnetic behaviour of Ln ions in a crystal with that of free ions, the μ_{eff} versus T plot is suited.

5. Cooperative effects between magnetically active ions can be described by a so-called molecular-field parameter λ_{MF}:

$$\chi_{\mathrm{m}}^{-1} = \chi_{\mathrm{m}}^{-1}(\mathrm{LF}) - \lambda_{\mathrm{MF}}. \tag{85}$$

6. Susceptibility equations of the type (84) are not only suited for molecular and ionic systems, but also for intermetallics with stable Ln valence. The 6s and 5d valence electrons are delocalised to a high degree and yield normally only a small TIP.

7. Ce, Yb, Eu are candidates for mixed-valence behaviour ($\mathrm{Ce}^{3+/4+}$, $\mathrm{Yb}^{2+/3+}$, $\mathrm{Eu}^{2+/3+}$).

Paramagnetism of $\mathbf{Ce^{3+}, Yb^{3+}, U^{5+}}$ ions in an octahedral LF

Figs. 9 and 10 exhibit the typical paramagnetic behaviour of octahedrally coordinated Ce(III), Yb(III) and U(V) compounds as χ_{m}^{-1}–T and μ_{eff}–T plots calculated with program CONDON [12], using the parameter values (in cm^{-1}):

Ce(III): $B_0^4 = 2\,119$, $B_0^6 = 261$, $\zeta = 623$, see Tab. 16 [13];
Yb(III): $B_0^4 = 1\,471$, $B_0^6 = 0$, $\zeta = 2\,903$ [13];
U(V): $B_0^4 = 23\,100$, $B_0^6 = 3\,750$, $\zeta = 2\,200$ [14].

The $4\mathrm{f}^{13}$ ion with ground multiplet ${}^2F_{7/2}$ is the strongest paramagnet, the $5\mathrm{f}^1$ ion (${}^2F_{5/2}$) the weakest one. The lower μ_{eff} value of the latter compared to μ_{eff} of Ce(III) is the consequence of the much stronger LF effect.

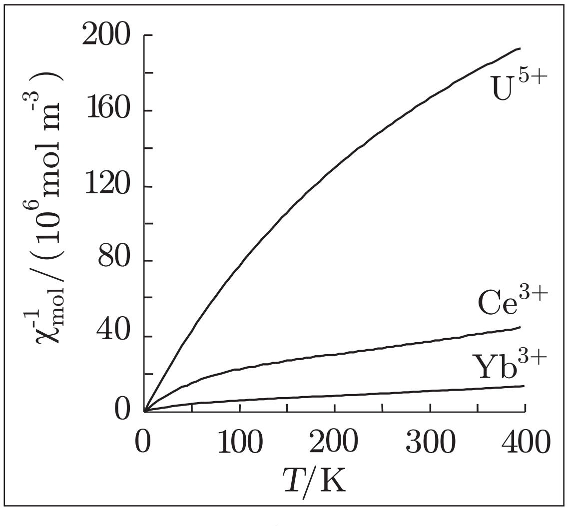

Fig. 9: Typical χ_{m}^{-1}–T diagrams of compounds with Ce(III), Yb(III) and U(V) in an octahedral ligand field.

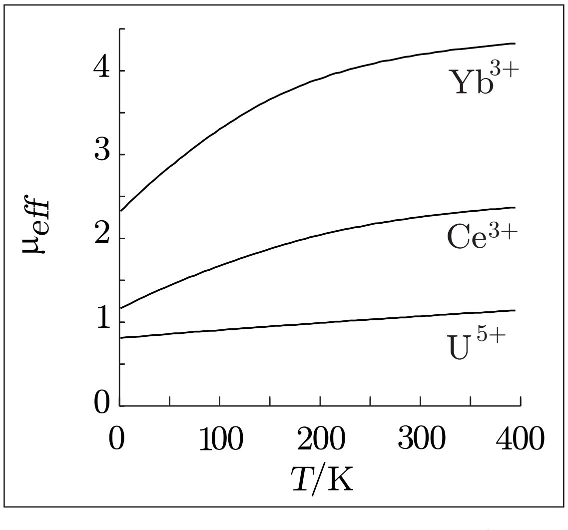

Fig. 10: Typical μ_{eff}–T diagrams of compounds with Ce(III), Yb(III) and U(V) in an octahedral ligand field.

3.3.3 $\mathbf{4f^N}$ systems

For many-electron lanthanide systems $\hat{H}_{\mathrm{LF}}^{\mathrm{cub}}$ reads

$$\hat{H}_{\mathrm{LF}}^{\mathrm{cub}}(4\mathrm{f}^{\mathrm{N}}) = B_0^4 \sum_{i=1}^{\mathrm{N}} \left\{ C_0^4(i) + \sqrt{\tfrac{5}{14}}\,[C_4^4(i) + C_{-4}^4(i)] \right\} + B_0^6 \sum_{i=1}^{\mathrm{N}} \left\{ C_0^6(i) - \sqrt{\tfrac{7}{2}}\,[C_4^6(i) + C_{-4}^6(i)] \right\} \tag{86}$$

Coupling schemes: The 4f states are controlled by H_{ee}, H_{SO} (see Fig. 11) and the ligand field[6] (H_{LF}), where the order of energetic effects is $H_{\mathrm{ee}} > H_{\mathrm{SO}} > H_{\mathrm{LF}}$ (except for the $4f^4, 4f^5, 4f^6$ systems where $H_{\mathrm{SO}} \approx H_{\mathrm{LF}}$)[7]. To describe the electronic situation, three coupling schemes are distinguished, depending on the relative strength of H_{LF} and on the desired accuracy in LF parameter determination [15].

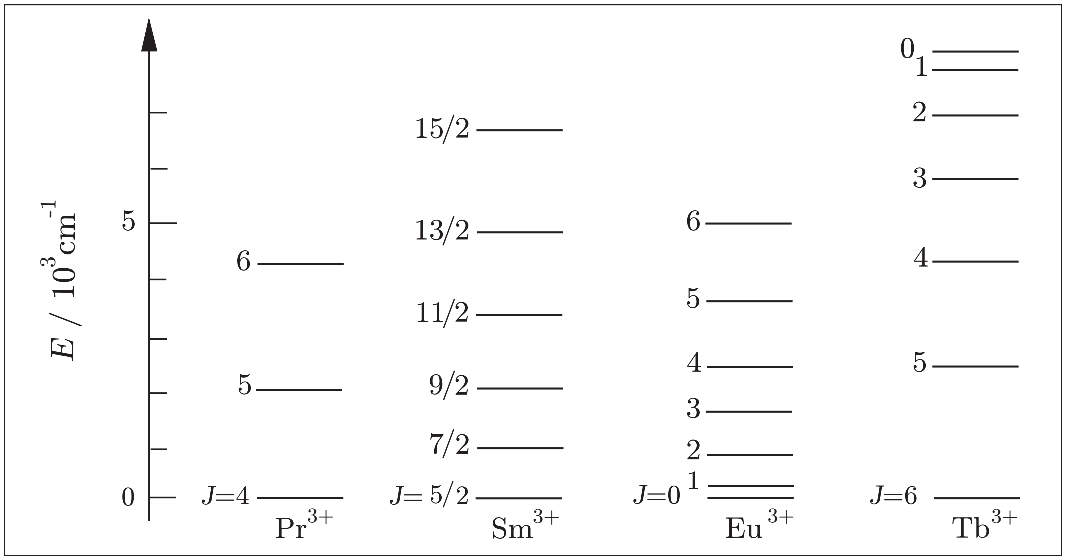

Fig. 11: Energies of ground state multiplets of selected Ln^{3+} ions ($k_{\mathrm{B}}T = 208.6\,\mathrm{cm}^{-1}$ at 300 K)

- Russell-Saunders coupling scheme (LS coupling scheme)
  Including spin-orbit coupling in 1^{st} order, S, L, and J are good quantum numbers in this coupling scheme, i. e., this model requires multiplets ${}^{2S+1}L_J$ that are (i) well separated in energy and (ii) only slightly influenced by H_{LF}. To estimate LF parameters it is sufficient to study the action of H_{LF} solely on the ground multiplet ${}^{2S+1}L_J$ [16] (except the $4f^4, 4f^5, 4f^6$ systems).

- Intermediate coupling scheme
  The intermediate coupling scheme is applicable, if S and L are no longer good quantum numbers on account of the competing perturbations by H_{ee} and H_{SO} while J remains a good quantum number. This model is adequate, if the ligand field splitting is not too strong, i. e., in the case of the *weak-field lanthanide system*[8]. Examples: lanthanide chlorides and bromides (Cl^-, Br^-).

- J-mixing scheme
  The J-mixing coupling scheme is favourable for *strong-field lanthanide systems*. If J-mixing, caused by H_{LF}, is considered, a ${}^{2S+1}L_J$ multiplet may have contributions from terms with other J values, that is, J is no longer a good quantum number. Examples: lanthanide oxides and fluorides (O^{2-}, F^-).

---

[6] For lanthanides the term *crystal field* is often used instead of *ligand field*.

[7] For actinides in high oxidation states there is no energetic order, that is, $H_{\mathrm{ee}} \approx H_{\mathrm{SO}} \approx H_{\mathrm{LF}}$.

[8] The terms 'weak field' and 'strong field' here have another meaning than for transition metal compounds. For a strong-field transition metal system, H_{LF} is a stronger interaction than H_{ee} whereas for lanthanides H_{LF} is always weaker than H_{ee}.

3.3.4 Magnetic behaviour of the series $Cs_2NaLnCl_6$ (overview)

On the basis of spectroscopic data of the series $Cs_2NaLnCl_6$ [9][13] (see Tab. 16) the magnetic behaviour is calculated with program CONDON [10], developed by Schilder and Lueken [12]. The μ_{eff}–T data for the representative metal ions $Pr^{3+}[4f^2]$, $Nd^{3+}[4f^3]$, $Sm^{3+}[4f^5]$ and $Eu^{3+}[4f^6]$ are compared with those of the free ions.

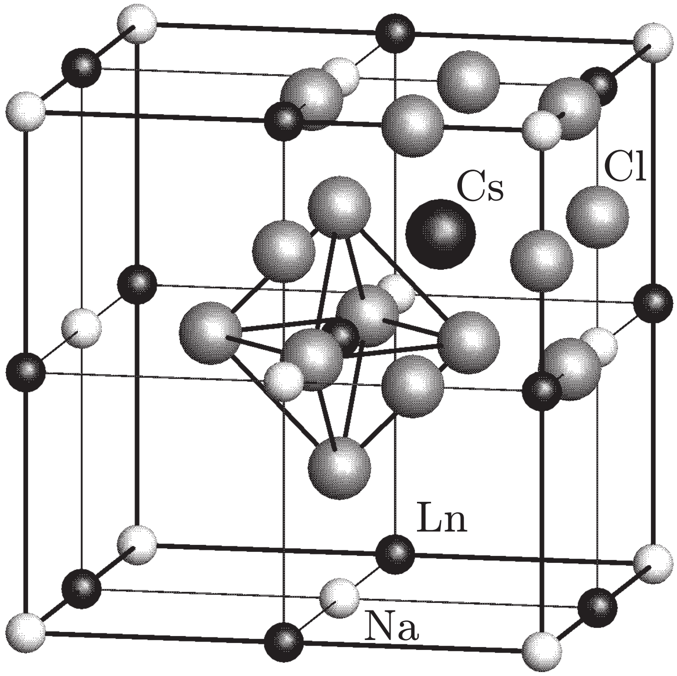

Fig. 12: $Cs_2NaLnCl_6$: unit cell of the elpasolite type

Table 16: LF parameters B_0^4 and B_0^6 of octahedrally coordinated Ln^{3+} ions in $Cs_2NaLnCl_6$

Ln^{3+}	$B_0^{4\,a)}$	$B_0^{6\,a)}$	Ln^{3+}	B_0^4	B_0^6
Ce^{3+}	2119	261	Tb^{3+}	1624	150
Pr^{3+}	1938	290	Dy^{3+}	1614	148
Nd^{3+}	1966	258	Ho^{3+}	1593	171
Sm^{3+}	$(1671)^{b)}$	$(228)^{b)}$	Er^{3+}	1492	163
Eu^{3+}	2055	308	Tm^{3+}	1498	159
Gd^{3+}	1776	136	Yb^{3+}	1471	[0]

[a] Values in cm^{-1}.
[b] Values for $Cs_2NaYCl_6 : Sm^{3+}$.

The chemical environment of the Ln ions, compared to the one of d ions, has only a minor effect on the 4f electrons. The LF effect produces splittings of $H_{\text{LF}} \approx 10^2\,\text{cm}^{-1}$

---

[9] Elpasolite type structure, Ln^{3+} point symmetry O_h.

[10] CONDON considers ligand field effects on the J-mixing level and, beyond this model, the applied field dependence of the magnetic susceptibility as well as intermolecular spin-spin exchange couplings.

leading generally to paramagnetism, described by the temperature dependence of the effective Bohr magneton number μ_{eff}:

$$\chi_{\text{m}} = \mu_0 \frac{N_{\text{A}} \mu_{\text{eff}}^2 \mu_{\text{B}}^2}{3 k_{\text{B}} T} \quad \text{where} \quad \mu_{\text{eff}} = \left(\frac{3 k_{\text{B}} T \chi_{\text{m}}}{\mu_0 N_{\text{A}} \mu_{\text{B}}^2} \right)^{1/2} = 797.7 (T \chi_{\text{m}})^{1/2} \tag{87}$$

As a rule, μ_{eff} approaches the free Ln ion value for $T > 200\,\text{K}$ (see Table 2, Figs. 8, 10, 13, 14).

Pr^{3+}: Applying $B_0^4 = 1938\,\text{cm}^{-1}$ and $B_0^6 = 290\,\text{cm}^{-1}$ the χ_{m}^{-1}–T plot in Fig. 13 (left) is obtained. The octahedral LF effect produces temperature independent paramagnetism below 100 K in agreement with the predicted non-magnetic ground state A_1 (see Table 17).

Nd^{3+}: The magnetic behaviour of $\text{Cs}_2\text{NaNdCl}_6$ exhibits Curie paramagnetism in the temperature range under investigation (see Fig. 13, right). This behaviour is expected for Ln ions with an odd number of 4f electrons in magnetically diluted systems without cooperative interactions.

Sm^{3+}: On account of low lying multiplets, μ_{eff} of the free Sm^{3+} ion is already temperature dependent (see Fig. 14 (left), curve b, and Fig. 11). After switching on the cubic ligand field (curve a), a drastic modification is observed at $T < 200\,\text{K}$.

Eu^{3+}: In the complete temperature range the magnetic properties of Eu^{3+} compounds are determined by the TIP on account of the non-magnetic ground multiplet with $J = 0$ (see Fig. 14, right). The effect of a cubic ligand field is negligible.

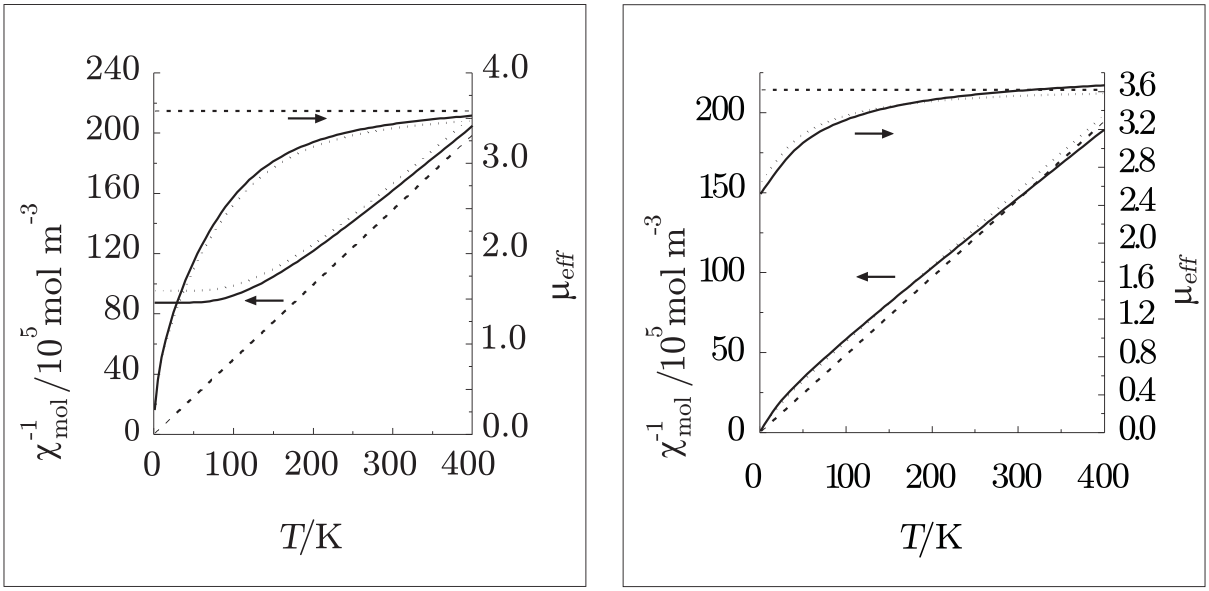

Fig. 13: χ_{m}^{-1}–T and μ_{eff}–T diagrams for Pr^{3+} (left) and Nd^{3+} (right), calculated with the spectroscopically determined data of $\text{Cs}_2\text{NaPrCl}_6$ and $\text{Cs}_2\text{NaNdCl}_6$, respectively (solid lines: full basis; dottet lines: ground multiplet only; dashed lines: free ions)

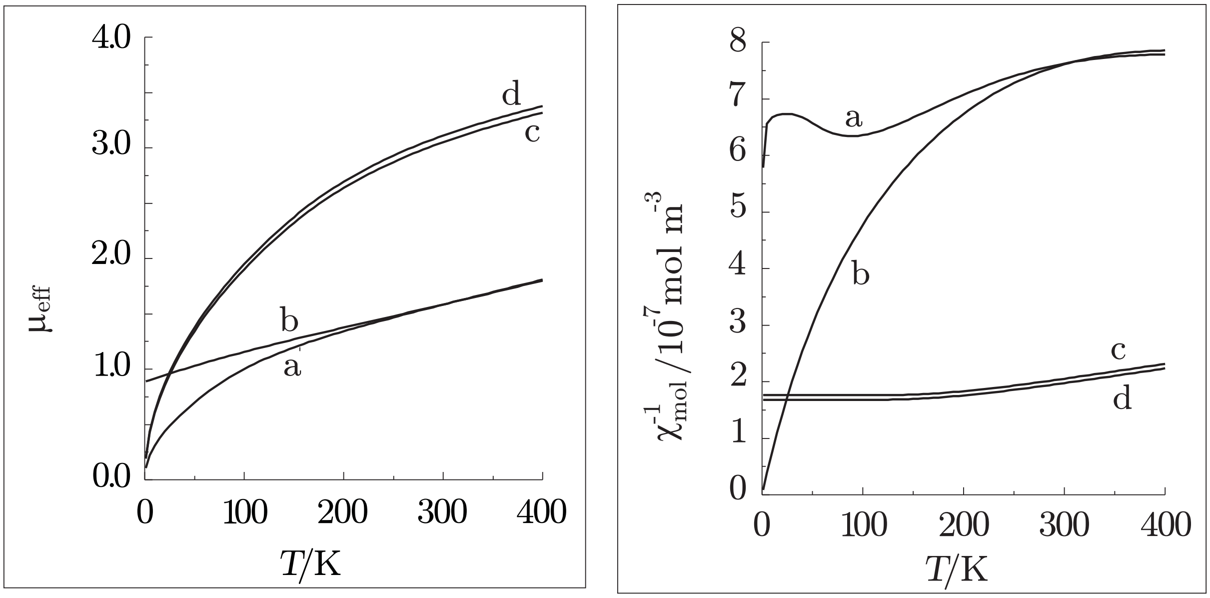

Fig. 14: μ_{eff}–T (left) and χ_{m}^{-1}–T diagrams (right) for Sm^{3+} and Eu^{3+}, calculated with the spectroscopically determined data of $\mathrm{Cs_2NaYCl_6{:}Sm^{3+}}$ (a) and $\mathrm{Cs_2NaEuCl_6}$ (d), respectively; free Sm^{3+} ion (b), free Eu^{3+} ion (c).

3.3.5 4f^2 system (Pr^{3+}, $^3H_4$: $H_{\mathbf{LF}}^{\mathbf{cub}}$)

For a 4f^2 system $\hat{H}_{\text{LF}}^{\text{cub}}$ reads:

$$\hat{H}_{\text{LF}}^{\text{cub}}(4\text{f}^2) = B_0^4 \sum_{i=1}^{2} \left\{ C_0^4(i) + \sqrt{\tfrac{5}{14}}\,[C_4^4(i) + C_{-4}^4(i)] \right\} + B_0^6 \sum_{i=1}^{2} \left\{ C_0^6(i) - \sqrt{\tfrac{7}{2}}\,[C_4^6(i) + C_{-4}^6(i)] \right\} \tag{88}$$

Compared to the two multiplets of the 4f^1 (Ce^{3+}) free ion, the 4f^2 (Pr^{3+}) free ion has 13 multiplets and, in consequence, exhibits a more complicated LF splitting pattern (see Table 17 and ref. [13]).

Table 17: Spectroscopically determined levels of the Pr^{3+} ion (O$_\text{h}$, octahedron) in Cs$_2$NaPrCl$_6$. The energy increases from top to bottom and from left to right.

$^3H_4$	$^3H_5$	$^3H_6$	$^3F_2$	$^3F_3$	$^3F_4$	$^1G_4$	$^1D_2$	$^3P_0$	$^3P_1$	$^1I_6$	$^3P_2$	$^1S_0$
$\mathrm{A_1[\Gamma_1]}(0^{a)})$	$\mathrm{T}_1^{(1)\,b)}$	$\mathrm{E}^{c)}$	E	$\mathrm{T_1}$	E	$\mathrm{A_1}$	$\mathrm{T_2}$	$\mathrm{A_1}$	$\mathrm{T_1}$	$\mathrm{A_1}$	$\mathrm{T_2}$	$\mathrm{A_1}$
$\mathrm{T_1[\Gamma_4]}(236)$	$\mathrm{T_2}$	$\mathrm{T}_2^{(1)}$	$\mathrm{T_2}$	$\mathrm{T_2}$	$\mathrm{T_1}$	E	E			$\mathrm{T_1}$	E	
$\mathrm{E[\Gamma_3]}(422)$	E	$\mathrm{A_1}$		$\mathrm{A_2}$	$\mathrm{A_1}$	$\mathrm{T_1}$				$\mathrm{T}_2^{(1)}$		
$\mathrm{T_2[\Gamma_5]}(701)$	$\mathrm{T}_1^{(2)}$	$\mathrm{A_2[\Gamma_2]}$			$\mathrm{T_2}$	$\mathrm{T_2}$				$\mathrm{A_2}$		
		$\mathrm{T_1}$								$\mathrm{T}_2^{(2)}$		
		$\mathrm{T}_2^{(2)}$								E		

$^{a)}$ Experimental energy data in cm^{-1}; $^{b)}$2300 cm^{-1}; $^{c)}$4392 cm^{-1} [13].

According to the procedure outlined in 3.3.2, only the ground multiplet $^3H_4$ will be considered for the 4f^2 ion, that is, one starts with the $|JM_J\rangle$ basis consisting of the $2J+1 = 9$ states $|4\,4\rangle, |4\,3\rangle, \ldots, |4\,-4\rangle$. The 4f^2 situation is much more complicated than the 4f^1 one for the following reasons: In order to apply the entries of Table 13, the $|JM_J\rangle$ functions have to be decomposed into the microstates of the two electrons (*cf.* ref. [7], page 120). Subsequently, the operator eq. (88) must be applied. Then the respective LF matrix elements have to be summed up and collected in a 9×9 matrix. After diagonalisation of this matrix, the symmetry adapted functions and their energies are obtained as a function of the LF parameters B_0^4 and B_0^6.

These calculations would be time-consuming and must be worked out by a computer, using, for example, the program CONDON [12] which is at our disposal. In general, this program uses the complete set of basis functions, but can be restricted to the ground multiplet[11]. The results, obtained by CONDON with the restricted basis, are presented in Table 18. A splitting in a singlet (A_1), a doublet (E) and two triplets ($\mathrm{T}_1, \mathrm{T}_2$) is obtained and the entries of Table 17 are confirmed.

Tab. 18: Functions and energies after perturbation of the $^3H_4(4\mathrm{f}^2)$ ground multiplet by a cubic ligand field

functions $\vert M_J\rangle$ $(J=4)$	$\vert\Gamma\bar{M}\rangle^{a)})$	$E_{LF}\,^{b)}$
$\sqrt{\frac{1}{24}}\left(\sqrt{14}\,\vert\,0\,\rangle + \sqrt{5}\,\vert\,4\,\rangle + \sqrt{5}\,\vert\,-4\,\rangle\right)$	$\vert \mathrm{A}_1 a_1\rangle$	$28\,b_4 - 80\,b_6$
$\sqrt{\frac{1}{24}}\left(-\sqrt{10}\,\vert\,0\,\rangle + \sqrt{7}\,\vert\,4\,\rangle + \sqrt{7}\,\vert\,-4\,\rangle\right)$	$\vert \mathrm{E}\theta\rangle$	$4\,b_4 + 64\,b_6$
$\sqrt{\frac{1}{2}}\,(\vert\,2\,\rangle + \vert\,-2\,\rangle)$	$\vert \mathrm{E}\epsilon\rangle$	
$-\sqrt{\frac{1}{8}}\,\vert\,-3\,\rangle - \sqrt{\frac{7}{8}}\,\vert\,1\,\rangle$	$\vert \mathrm{T}_1 1\rangle$	$14\,b_4 + 4\,b_6$
$\sqrt{\frac{1}{2}}\,(\vert\,4\,\rangle - \vert\,-4\,\rangle)$	$\vert \mathrm{T}_1 0\rangle$	
$\sqrt{\frac{1}{8}}\,\vert\,3\,\rangle + \sqrt{\frac{7}{8}}\,\vert\,-1\,\rangle$	$\vert \mathrm{T}_1\,-1\rangle$	
$\sqrt{\frac{7}{8}}\,\vert\,3\,\rangle - \sqrt{\frac{1}{8}}\,\vert\,-1\,\rangle$	$\vert \mathrm{T}_2 1\rangle$	$-26\,b_4 - 20\,b_6$
$\sqrt{\frac{1}{2}}\,(\vert\,2\,\rangle - \vert\,-2\,\rangle)$	$\vert \mathrm{T}_2 0\rangle$	
$-\sqrt{\frac{7}{8}}\,\vert\,-3\,\rangle + \sqrt{\frac{1}{8}}\,\vert\,1\,\rangle$	$\vert \mathrm{T}_2\,-1\rangle$	

a) $\mathrm{A}_1 \equiv \Gamma_1, \mathrm{E} \equiv \Gamma_3, \mathrm{T}_1 \equiv \Gamma_4, \mathrm{T}_2 \equiv \Gamma_5$ [6].

b) $b_4 = (15/2)\beta_J B_0^4, \quad b_6 = (315/4)\gamma_J B_0^6; \qquad \beta_J = -\frac{4}{5\,445}, \quad \gamma_J = \frac{272}{4\,459\,455}.$

---

[11] As an alternative, a rather simple method is available to determine LF effects for cubic lanthanide systems, if the description of the LF effect within the ground multiplet is sufficient. In this method an operator is applied that consists of so-called *operator-equivalents* instead of the Racah tensors. We will come back to its practice in 3.3.7 and in Appendix 2.

3.3.6 4f^2 system (Pr^{3+}, $^3H_4$: $H_{\mathrm{LF}}^{\mathrm{cub}} + H_{\mathrm{mag}}$)

Applying the Zeeman operator eq. (66) on the eigenfunctions, the matrix elements (89) are obtained (in units of $g_J \mu_{\mathrm{B}} B_z$; $g_J = 4/5$).

(89)

Γ		A_1	E		T_1			T_2		
	$\bar{M}$	a_1	θ	ϵ	1	0	-1	1	0	-1
A_1	a_1	0	0			$\sqrt{\frac{20}{3}}$				
E	θ	0	0			$\sqrt{\frac{28}{3}}$				
	ϵ			0					2	
T_1	1				$\frac{1}{2}$					$-\frac{\sqrt{7}}{2}$
	0	$\sqrt{\frac{20}{3}}$	$\sqrt{\frac{28}{3}}$			0				
	-1						$-\frac{1}{2}$	$\frac{\sqrt{7}}{2}$		
T_2	1						$-\frac{\sqrt{7}}{2}$	$\frac{5}{2}$		
	0			2					0	
	-1				$\frac{\sqrt{7}}{2}$					$-\frac{5}{2}$

In Table 19 the energies $W_n^{(0)}$ and the Zeeman coefficients $W_n^{(1)}$, $W_n^{(2)}$ are listed.

Tab. 19: Energies $W_n^{(0)}$ and Zeeman coefficients $W_n^{(1)}$, $W_n^{(2)}$ of the 4f^2 system (Pr^{3+}) after perturbation of the $^3H_4$ multiplet by a cubic ligand field.

	$W_n^{(0)\,a)}$	$\dfrac{W_n^{(1)}}{g_J\,\mu_B}$	$\dfrac{W_n^{(2)}}{g_J^2\,\mu_B^2}\,^{b)}$
$\vert \mathrm{A}_1 a_1\rangle$	$28\,b_4 - 80\,b_6$	0	$-\dfrac{(20/3)}{\Delta(\mathrm{T}_1;\mathrm{A}_1)}$
$\vert \mathrm{E}\theta\rangle$	$4\,b_4 + 64\,b_6$	0	$-\dfrac{(28/3)}{\Delta(\mathrm{T}_1;\mathrm{E})}$
$\vert \mathrm{E}\epsilon\rangle$		0	$-\dfrac{4}{\Delta(\mathrm{T}_2;\mathrm{E})}$
$\vert \mathrm{T}_1 \pm 1\rangle$	$14\,b_4 + 4\,b_6$	$\pm 1/2$	$-\dfrac{(7/4)}{\Delta(\mathrm{T}_2;\mathrm{T}_1)}$
$\vert \mathrm{T}_1 0\rangle$		0	$+\dfrac{(20/3)}{\Delta(\mathrm{T}_1;\mathrm{A}_1)} + \dfrac{(28/3)}{\Delta(\mathrm{T}_1;\mathrm{E})}$
$\vert \mathrm{T}_2 \pm 1\rangle$	$-26\,b_4 - 20\,b_6$	$\pm 5/2$	$+\dfrac{(7/4)}{\Delta(\mathrm{T}_2;\mathrm{T}_1)}$
$\vert \mathrm{T}_2 0\rangle$		0	$+\dfrac{4}{\Delta(\mathrm{T}_2;\mathrm{E})}$

---

[a] Further contributions to $W_n^{(0)}$ beside E_{LF} are equal in magnitude for all levels and are reduced; $b_4 = \left(\frac{15}{2}\right)\beta_J B_0^4$, $b_6 = \left(\frac{315}{4}\right)\gamma_J B_0^6$.

[b] $\Delta(\Gamma_m;\Gamma_n) = W_m^{(0)} - W_n^{(0)}$.

Setting $W_n^{(0)}, W_n^{(1)}$ and $W_n^{(2)}$ into the Van Vleck eq. (60), the susceptibility equation for the Pr^{3+} ion in cubic ligand fields is developed (where $X_\Gamma \equiv W_n^{(0)}(\Gamma)/k_\mathrm{B}T$):

$$\chi_\mathrm{m}(\mathrm{Pr}^{3+}) = \mu_0 \frac{N_\mathrm{A}\,\mu_\mathrm{B}^2}{3k_\mathrm{B}T}\,\mu_\mathrm{eff}^2 \quad \text{where} \quad \mu_\mathrm{eff}^2 = g_J^2 \times \tag{90}$$

$$\left\{\left[\frac{40k_\mathrm{B}T}{\Delta(\mathrm{T_1;A_1})}\right]\exp(-X_\mathrm{A_1}) + \left[\frac{56k_\mathrm{B}T}{\Delta(\mathrm{T_1;E})} + \frac{24k_\mathrm{B}T}{\Delta(\mathrm{T_2;E})}\right]\exp(-X_\mathrm{E}) \right.$$
$$+ \left[\frac{3}{2} + \frac{21k_\mathrm{B}T}{\Delta(\mathrm{T_2;T_1})} - \frac{40k_\mathrm{B}T}{\Delta(\mathrm{T_1;A_1})} - \frac{56k_\mathrm{B}T}{\Delta(\mathrm{T_1;E})}\right]\exp(-X_\mathrm{T_1})$$
$$\left. + \left[\frac{75}{2} - \frac{21k_\mathrm{B}T}{\Delta(\mathrm{T_2;T_1})} - \frac{24k_\mathrm{B}T}{\Delta(\mathrm{T_2;E})}\right]\exp(-X_\mathrm{T_2})\right\} \times$$
$$\left\{\exp(-X_\mathrm{A_1}) + 2\exp(-X_\mathrm{E}) + 3\exp(-X_\mathrm{T_1}) + 3\exp(-X_\mathrm{T_2})\right\}^{-1}$$

Fig. 13 (left) exhibits calculated χ_m^{-1}–T and μ_eff–T diagrams for the Pr^{3+} ion in an octahedral ligand field where $B_0^4 = 1938\,\mathrm{cm}^{-1}$ and $B_0^6 = 290\,\mathrm{cm}^{-1}$. Dotted lines refer to calculations with the reduced basis ${}^3H_4$ (eq. (90)), whereas the solid lines correspond to calculations with the complete basis (91 microstates). Differences in χ_m values between the two models amount to 3 %. In addition, the expected magnetic behaviour of the free ion is shown for comparison (dashed lines).

3.3.7 Prediction of LF splittings by means of the operator-equivalent method

The magnetic behaviour of Ln ions depends on position and charge of the ligands, both controlling sign and amount of the LF parameters B_q^k. If one accepts the qualitative validity of the point charge electrostatic model (PCEM) for the geometrical coordination factor A_k^q (defined in eq. (72)), the sign of the corresponding $B_q^k = A_k^q < r^k >$, that is, the sign of B_0^4 and B_0^6 in the case of cubic coordination polyhedra (octahedron, cube, tetrahedron), can be predicted reliably[12]. We consider the point charges $-Qe$[13] at the vertices of regular polyhedra (octahedron, tetrahedron, cube) with the distance R to the centre of the polyhedron, and calculate $A_4^\mathbf{0}$ and $A_6^\mathbf{0}$.

Geometrical coordination factors

$\boxed{A_4^0}$ For the octahedron the integration in eq. (72) reduces to a summation of the six ligands with (Θ_j, Φ_j) coordinates $(0,0)$, $(\pi,0)$, $(\pi/2,0)$, $(\pi/2,\pi/2)$, $(\pi/2,\pi)$, $(\pi/2,3\pi/2)$:

$$A_4^0(\mathrm{oct.}) = \frac{Qe^2}{R^5}\sum_{j=1}^{6} C_0^4(\Theta_j,\Phi_j) = \frac{Qe^2}{R^5}\sum_{j=1}^{6} \tfrac{1}{8}(35\cos^4\Theta_j - 30\cos^2\Theta_j + 3) = \frac{7}{2}\frac{Qe^2}{R^5}, \tag{91}$$

For negatively charged ligands ($Q > 0$) which coordinate the Ln ion octahedrally, $A_4^0(\mathrm{oct.})$ is positive and consequently also $A_4^0 < r^4 > = B_0^4$, whereas the A_4^0's for tetrahedron and cube are negative (angle coordinates for tetrahedron: $(\alpha,\pi/4)$, $(\alpha,5\pi/4)$, $(\pi-\alpha,3\pi/4)$,

---

[12] Notice, that radial integrals $< r^k >$ are positive quantities.

[13] The elementary charge e is positive; the charge of the electron is $-e$. Ligands with the charge $-Qe$ are negatively charged for $Q > 0$.

$(\pi-\alpha, 7\pi/4)$, where $\cos\alpha = 1/\sqrt{3}$; additionally for the cube $(\alpha, 3\pi/4)$, $(\alpha, 7\pi/4)$, $(\pi - \alpha, \pi/4)$, $(\pi-\alpha, 5\pi/4)$):

$$A_4^0(\text{tetr.}) = -\frac{14}{9}\frac{Qe^2}{R^5}; \qquad A_4^0(\text{cube}) = -\frac{28}{9}\frac{Qe^2}{R^5} \tag{92}$$

$\boxed{\boldsymbol{A_6^0}}$

$$\begin{aligned} A_6^0(\text{oct.}) &= \frac{Qe^2}{R^7}\sum_{j=1}^{6} C_0^6(\Theta_j, \Phi_j), \quad \text{where} \quad C_0^6(\Theta_j, \Phi_j) = \left(\frac{4\pi}{13}\right)^{1/2} Y_0^6(\Theta_j, \Phi_j) \\ &= \frac{Qe^2}{R^7}\sum_{j=1}^{6} \tfrac{1}{16}(231\cos^6\Theta_j - 315\cos^4\Theta_j + 105\cos^2\Theta_j - 5) = \frac{3}{4}\frac{Qe^2}{R^7} \end{aligned} \tag{93}$$

$$A_6^0(\text{tetr.}) = \frac{8}{9}\frac{Qe^2}{R^7}; \qquad A_6^0(\text{cube}) = \frac{16}{9}\frac{Qe^2}{R^7} \tag{94}$$

For negatively charged ligands ($Q > 0$), A_6^0 is positive, regardless the polyhedron.

Having fixed the *sign* of the LF parameters B_0^4 and B_0^6, the possible LF ground states of the Ln ion under investigation can be determined. If the program CONDON is at our disposal, we need only the values of B_0^4 and B_0^6 as an input to obtain energy and composition of the LF states. Otherwise, we can benifit from tables of eigenvectors and diagrams of energy eigenvalues, expressed as a function of the ratio between the fourth and sixth degree terms of $\hat{H}_{\text{LF}}^{\text{cub}}$, that are published for all J-manifolds of the lanthanides by Lea, Leask, Wolf [16]. The immediate application of these diagrams and tables is the prediction of spectroscopic energy level schemes and possible g-factors for lanthanide ions in cubic coordination. We start with introductory remarks concerning the operator equivalent technique.

Operator equivalents: To describe the *fundamental* magnetic behaviour of Ln ions in a solid, a model is sufficient that, according to the Russell-Saunders coupling scheme, takes solely the ground multiplet ${}^{2S+1}L_J$ and its perturbation by $\hat{H}_{\text{LF}}$ into consideration (exceptions: Sm^{3+}[4f^5], Eu^{3+}[4f^6]). The restriction of the basis functions allows a simple calculation of the matrix elements $\langle J\,M_J|\hat{H}_{\text{LF}}|J\,M_J'\rangle$ by application of the so-called operator-equivalent technique. Using this technique, the calculation of the integrals $\langle l_i m_{l_1}|C_q^k(i)|l_i m_{l_1}'\rangle$ — entailing a troublesome decoding of the $|J\,M_J\rangle$ basis with regard to the microstates — is unnecessary.

The operator equivalent technique is founded on the fact that the operators $C_q^k = \sqrt{4\pi/(2k+1)}\,Y_q^k$, written in cartesian coordinates, can be replaced by operators $\hat{J}_x$, $\hat{J}_y$, $\hat{J}_z$ of the total angular momentum [17] (14). By this means operator equivalents $\tilde{O}_q^k$ are designed whose matrix elements are proportional to the corresponding matrix elements of $\hat{H}_{\text{LF}}$. The restriction to the ground multiplet has the advantage that the matrix elements $\langle JM_J|\hat{H}_{\text{LF}}^{\text{cub}}|JM_J'\rangle$ are easily evaluated: Given the wave functions in the $|JM_J\rangle$ basis, the action of $\hat{H}_{\text{LF}}^{\text{cub}}$ on the orbital part of the functions is taken into consideration by a simple factor (Stevens factor [18]). If x, y, z in the Racah tensors $C_q^k(x, y, z)$ of $\hat{H}_{\text{LF}}^{\text{cub}}$ (eq. (72)) are replaced by the total angular momentum operators $\hat{J}_x$, $\hat{J}_y$, $\hat{J}_z$ [17], operator equivalents

---

(14) Originally, the operator equivalents are related to the spherical harmonics Y_q^k [18, 21]. Conversion factors are published in ref. [22]. Details are given in the 'Final remarks', p. 49.

$\tilde{O}_q^k$ are obtained, whose matrix elements are proportional to the matrix elements of $\hat{H}_{\mathrm{LF}}^{\mathrm{cub}}$. Simple examples of operator equivalents are:

$$x^2 - y^2 \equiv \theta(\hat{J}_x^2 - \hat{J}_y^2), \qquad 3z^2 - r^2 \equiv \theta[3\hat{J}_z^2 - J(J+1)], \qquad xy \equiv \theta(\tfrac{1}{2})(\hat{J}_x\hat{J}_y + \hat{J}_y\hat{J}_x).$$

The multiplicative (Stevens) factor θ depends on k:

$$\alpha_J \;\; (k=2) \qquad \boxed{\beta_J \;\; (k=4) \qquad \gamma_J \;\; (k=6)} \qquad \text{(see Table 23 and example 3.8)}$$

For cubic symmetry only terms with $k = 4$ and 6 are relevant, so that the multiplet under consideration is generally characterised by the two figures β_J and γ_J[15]. The two following equations show the operator and its operator equivalent:

$$\hat{H}_{\mathrm{LF}}^{\mathrm{cub}}(4\mathrm{f}^{\mathrm{N}}) = B_0^4 \sum_{i=1}^{\mathrm{N}} \left\{ C_0^4(i) + \sqrt{\tfrac{5}{14}}\,[C_4^4(i) + C_{-4}^4(i)] \right\} + B_0^6 \sum_{i=1}^{\mathrm{N}} \left\{ C_0^6(i) - \sqrt{\tfrac{7}{2}}\,[C_4^6(i) + C_{-4}^6(i)] \right\}$$

$$\hat{H}_{\mathrm{LF}}^{\mathrm{cub}} = B_0^4\,\beta_J \left[\tilde{O}_0^4 + \sqrt{\tfrac{5}{14}} \left(\tilde{O}_4^4 + \tilde{O}_{-4}^4 \right) \right] + B_0^6\,\gamma_J \left[\tilde{O}_0^6 - \sqrt{\tfrac{7}{2}} \left(\tilde{O}_4^6 + \tilde{O}_{-4}^6 \right) \right] \tag{95}$$

The operators C_q^4 and $\tilde{O}_q^4$ as well as C_q^6 and $\tilde{O}_q^6$ are related (see ref. [17]) by

$$\begin{aligned}
\sum_{i=1}^{N} C_0^4(i) &= \beta_J\,\tilde{O}_0^4 = \beta_J \left(\tfrac{1}{8}\right) \left\{ 35\hat{J}_z^4 - [30J(J+1) - 25]\hat{J}_z^2 + 3J^2(J+1)^2 - 6J(J+1) \right\} \\
\sum_{i=1}^{N} C_{\pm 4}^4(i) &= \beta_J\,\tilde{O}_{\pm 4}^4 = \beta_J \left(\tfrac{1}{8}\right) \sqrt{70}\, \left(\tfrac{1}{2}\right) \hat{J}_{\pm}^4 && (96) \\
\sum_{i=1}^{N} C_0^6(i) &= \gamma_J\,\tilde{O}_0^6 = \gamma_J \left(\tfrac{1}{16}\right) \left\{ 231\,\hat{J}_z^6 - [315\,J(J+1) - 735]\hat{J}_z^4 + [105\,J^2(J+1)^2 \right. \\
&\qquad \left. -525\,J(J+1) + 294]\hat{J}_z^2 - 5\,J^3(J+1)^3 + 40\,J^2(J+1)^2 - 60\,J(J+1) \right\} \\
\sum_{i=1}^{N} C_{\pm 4}^6(i) &= \gamma_J\,\tilde{O}_{\pm 4}^6 = \gamma_J \sqrt{\tfrac{63}{128}} \left(\tfrac{1}{4}\right) \left\{ [11\,\hat{J}_z^2 - J(J+1) - 38]\hat{J}_{\pm}^4 + \hat{J}_{\pm}^4[\ldots] \right\} && (97)
\end{aligned}$$

The matrix elements $\langle JM_J|\tilde{O}_q^k|JM'_J\rangle$ that are necessary to set up H_{LF} matrices are available and collected in the Tables 35 – 38 on pages 89 – 90. In the following three examples the handling of operator equivalents is shown.

Example 3.7 *Application of the operator-equivalent method to* $^2F_{5/2}$ *of* $\mathrm{Ce}^{3+}[4\mathrm{f}^1]$
The H_{LF} operator equivalent for the cubic 4f^1 system reads

$$\hat{H}_{\mathrm{LF}}^{\mathrm{cub}} = B_0^4\,\beta_J \left[\tilde{O}_0^4 + \sqrt{\tfrac{5}{14}} \left(\tilde{O}_4^4 + \tilde{O}_{-4}^4 \right) \right] \tag{98}$$

Inspecting the Tables 35 and 36 the relevant data for the basis $|\tfrac{5}{2}\,M_J\rangle$ are:

$$\begin{array}{lclclcl}
\langle \pm\frac{1}{2}\,|\tilde{O}_0^4|\pm\frac{1}{2}\,\rangle & = & 15 & \qquad & \langle \pm\frac{5}{2}\,|\tilde{O}_0^4|\pm\frac{5}{2}\,\rangle & = & 15/2 \\
\langle \pm\frac{3}{2}\,|\tilde{O}_0^4|\pm\frac{3}{2}\,\rangle & = & -45/2 & \qquad & \langle \pm\frac{5}{2}\,|\tilde{O}_{\pm 4}^4|\mp\frac{3}{2}\,\rangle & = & 15\sqrt{14}/2.
\end{array} \tag{99}$$

---

[15] Exceptions are the multiplets $^2F_{5/2}$ ($\mathrm{Ce}^{3+}[4\mathrm{f}^1]$) and $^6H_{5/2}$ ($\mathrm{Sm}^{3+}[4\mathrm{f}^5]$) with $J = 5/2$, where only the fourth degree term ($k = 4$) in $\hat{H}_{\mathrm{LF}}$ is relevant.

Verification of $\langle \tfrac{5}{2}\,|\tilde{O}_0^4|\,\tfrac{5}{2}\rangle = \tfrac{15}{2}$, given in eq. (99)

$$\begin{aligned}\langle \tfrac{5}{2}\,|\tilde{O}_0^4|\,\tfrac{5}{2}\rangle &= \left(\tfrac{1}{8}\right)\left\{35\left(\tfrac{5}{2}\right)^4 - \left[30\left(\tfrac{5}{2}\right)\left(\tfrac{7}{2}\right) - 25\right]\left(\tfrac{5}{2}\right)^2 + 3\left(\tfrac{5}{2}\right)^2\left(\tfrac{7}{2}\right)^2 - 6\left(\tfrac{5}{2}\right)\left(\tfrac{7}{2}\right)\right\}\\ &= \left(\tfrac{1}{128}\right)(21\,875 - 23\,750 + 3\,675 - 840) = \tfrac{960}{128} = \tfrac{15}{2}\end{aligned}$$

Notice that, applying operator equivalents, the factor $\hbar$ is always omitted.

To complete the matrix elements they must be multiplied by $\beta_J = \frac{2}{315}$ (see Table 23). Example 3.8 shows the evaluation of the Stevens factor β_J.

Example 3.8 *Evaluation of* β_J *for* ${}^2F_{5/2}\,[4\mathrm{f}^1]$
β_J is derived by comparing $\langle \tfrac{5}{2}\,|C_0^4|\,\tfrac{5}{2}\rangle$ (Example 3.5) with $\langle \tfrac{5}{2}\,|\tilde{O}_0^4|\,\tfrac{5}{2}\rangle$ (Example 3.7):

$$\underbrace{\langle \tfrac{5}{2}\,|C_0^4|\,\tfrac{5}{2}\rangle}_{1/21} \;=\; \beta_J\,\underbrace{\langle \tfrac{5}{2}\,|\tilde{O}_0^4|\,\tfrac{5}{2}\rangle}_{15/2} \quad\longrightarrow\quad \beta_J = \frac{2}{3^2\cdot 5\cdot 7} = \frac{2}{315}$$

On the basis of the operator-equivalent matrix elements (99) and $\beta_J = \frac{2}{315}$ (Example 3.8) the $\hat{H}_{\mathrm{LF}}^{\mathrm{cub}}$ matrix within the basis ${}^2F_{5/2}$ can be set up. It is identical to matrix (83).

Example 3.9 *Application of the operator-equivalent method to* $\mathrm{Pr}^{3+}[4\mathrm{f}^2]$, ${}^3H_4$, $J = 4$
For the $4\mathrm{f}^2$ system both the fourth and the sixth degree terms of the LF operator equivalents eq. (95) have to be applied. According to the 1^{st} column in Table 17, the 9-fold degenerate ground multiplet ${}^3H_4$ decomposes under the action of a cubic LF into the terms A_1, E, T_1, and T_2. In order to verify the splitting by use of the operator-equivalent method, we need the matrix elements $\langle M_J|\tilde{O}_0^k|M_J\rangle$ and $\langle M_J|\tilde{O}_{\pm4}^k|M_J \mp 4\rangle$ for $k = 4$ and $k = 6$ (Table 20 and Tables 35 – 38 in Appendix 2) as well as $\beta_J = -(4/5\,445)$ and $\gamma_J = (272/4\,459\,455)$, given in Table 23. The 9×9 matrix is divided into one 3×3 block and three 2×2 blocks:

$$\begin{array}{c|ccc} & |\,4\,\rangle & |\,0\,\rangle & |\,{-4}\,\rangle \\ \hline \langle\,4\,| & 14\,b_4 + 4\,b_6 & \sqrt{70}\;(b_4 - 6\,b_6) & 0 \\ \langle\,0\,| & \sqrt{70}\;(b_4 - 6\,b_6) & 18\,b_4 - 20\,b_6 & \sqrt{70}\;(b_4 - 6\,b_6) \\ \langle\,{-4}\,| & 0 & \sqrt{70}\;(b_4 - 6\,b_6) & 14\,b_4 + 4\,b_6 \end{array}$$

$$\text{where}\quad b_4 = \left(\tfrac{15}{2}\right)\beta_J\,B_0^4, \qquad \text{and}\quad b_6 = \left(\tfrac{315}{4}\right)\gamma_J\,B_0^6 \tag{100}$$

$$\begin{array}{c|cc|cc} & |\,\pm3\,\rangle & |\,\mp1\,\rangle & |\,2\,\rangle & |\,{-2}\,\rangle \\ \hline \langle\,\pm3\,| & -21\,b_4 - 17\,b_6 & \sqrt{7}\,(5\,b_4 + 3\,b_6) & & \\ \langle\,\mp1\,| & \sqrt{7}\,(5\,b_4 + 3\,b_6) & 9\,b_4 + b_6 & & \\ \hline \langle\,2\,| & & & -11\,b_4 + 22\,b_6 & 15\,b_4 + 42\,b_6 \\ \langle\,{-2}\,| & & & 15\,b_4 + 42\,b_6 & -11\,b_4 + 22\,b_6 \end{array}$$

Evaluation of the $\hat{H}_{\mathrm{LF}}^{\mathrm{cub}}$ matrix yields the energies and eigenfunctions given in Table 21. The splitting in a singlet (A_1), a doublet (E) and two triplets ($\mathrm{T}_1, \mathrm{T}_2$) is confirmed.

Tab. 20: Matrix elements of the operator equivalents $\tilde{O}_q^k$ in the basis $|JM_J\rangle$ ($J = 4$) for 4f^2 and cubic symmetry (see Appendix 2)

$\langle M_J\|\tilde{O}_q^k\|M_J'\rangle$	$k=4$	$k=6$	$\langle M_J\|\tilde{O}_q^k\|M_J'\rangle$	$k=4$	$k=6$
$\langle 0\,\|\tilde{O}_0^k\|\,0\,\rangle$	135	-1575	$\langle \pm4\,\|\tilde{O}_0^k\|\pm4\,\rangle$	105	315
$\langle \pm1\,\|\tilde{O}_0^k\|\pm1\,\rangle$	$\frac{135}{2}$	$\frac{315}{4}$	$\langle \pm2\,\|\tilde{O}_{\pm4}^k\|\mp2\,\rangle$	$\frac{45}{2}\sqrt{70}$	$-\frac{945}{2}\sqrt{14}$
$\langle \pm2\,\|\tilde{O}_0^k\|\pm2\,\rangle$	$-\frac{165}{2}$	$\frac{3465}{2}$	$\langle \pm3\,\|\tilde{O}_{\pm4}^k\|\mp1\,\rangle$	$\frac{105}{2}\sqrt{10}$	$-\frac{945}{4}\sqrt{2}$
$\langle \pm3\,\|\tilde{O}_0^k\|\pm3\,\rangle$	$-\frac{315}{2}$	$-\frac{5355}{4}$	$\langle \pm4\,\|\tilde{O}_{\pm4}^k\|\,0\,\rangle$	105	$945\sqrt{5}$

Tab. 21: Functions and energies after perturbation of the $^3H_4$(4f^2) multiplet by a cubic ligand field

functions $\|M_J\rangle$ ($J=4$)	$\|\Gamma\bar{M}\rangle^{a)}$)	E_{LF} $^{b)}$
$\sqrt{\frac{1}{24}}\left(\sqrt{14}\,\|\,0\,\rangle+\sqrt{5}\,\|\,4\,\rangle+\sqrt{5}\,\|\,-4\,\rangle\right)$	$\|\mathrm{A}_1a_1\rangle$	$28\,b_4-80\,b_6$
$\sqrt{\frac{1}{24}}\left(-\sqrt{10}\,\|\,0\,\rangle+\sqrt{7}\,\|\,4\,\rangle+\sqrt{7}\,\|\,-4\,\rangle\right)$	$\|\mathrm{E}\theta\rangle$	$4\,b_4+64\,b_6$
$\sqrt{\frac{1}{2}}\,(\|\,2\,\rangle+\|\,-2\,\rangle)$	$\|\mathrm{E}\epsilon\rangle$	
$-\sqrt{\frac{1}{8}}\,\|\,-3\,\rangle-\sqrt{\frac{7}{8}}\,\|\,1\,\rangle$	$\|\mathrm{T}_1 1\rangle$	$14\,b_4+4\,b_6$
$\sqrt{\frac{1}{2}}\,(\|\,4\,\rangle-\|\,-4\,\rangle)$	$\|\mathrm{T}_1 0\rangle$	
$\sqrt{\frac{1}{8}}\,\|\,3\,\rangle+\sqrt{\frac{7}{8}}\,\|\,-1\,\rangle$	$\|\mathrm{T}_1\,-1\rangle$	
$\sqrt{\frac{7}{8}}\,\|\,3\,\rangle-\sqrt{\frac{1}{8}}\,\|\,-1\,\rangle$	$\|\mathrm{T}_2 1\rangle$	$-26\,b_4-20\,b_6$
$\sqrt{\frac{1}{2}}\,(\|\,2\,\rangle-\|\,-2\,\rangle)$	$\|\mathrm{T}_2 0\rangle$	
$-\sqrt{\frac{7}{8}}\,\|\,-3\,\rangle+\sqrt{\frac{1}{8}}\,\|\,1\,\rangle$	$\|\mathrm{T}_2\,-1\rangle$	

---

a) Assignment of the states see ref. [6]; $\mathrm{A}_1\equiv\Gamma_1, \mathrm{E}\equiv\Gamma_3, \mathrm{T}_1\equiv\Gamma_4, \mathrm{T}_2\equiv\Gamma_5$.

b) $b_4=(15/2)\beta_J B_0^4$; $b_6=(315/4)\gamma_J B_0^6$.

Level tuning [16]: The ground state of an Ln ion in a cubic LF depends on $\beta_J B_0^4$ and $\gamma_J B_0^6$. We want to obtain information about the succession of E_{LF} of the LF states as a function of the ratio $\beta_J B_0^4/\gamma_J B_0^6$. Using the operator equivalent matrix elements in Tables 35 – 38, the $(2J+1)\times(2J+1)$ matrix can in principle be drawn up. The tables contain factors common to all the matrix elements, $\tilde{F}(4)$ and $\tilde{F}(6)$. These factors are separated out in order to keep the energy values in the same numerical range for all ratios of the fourth and sixth degree terms. We start out from eq. (95)

$$\hat{H}_{\mathrm{LF}}^{\mathrm{cub}} = \beta_J\,B_0^4\underbrace{\left[\tilde{O}_0^4+\sqrt{\tfrac{5}{14}}\left(\tilde{O}_4^4+\tilde{O}_{-4}^4\right)\right]}_{\widehat{\mathcal{O}}^{\,4}}+\gamma_J\,B_0^6\underbrace{\left[\tilde{O}_0^6-\sqrt{\tfrac{7}{2}}\left(\tilde{O}_4^6+\tilde{O}_{-4}^6\right)\right]}_{\widehat{\mathcal{O}}^{\,6}}$$

$$= \beta_J B_0^4 \,\widehat{\mathcal{O}}^{\,4} + \gamma_J B_0^6 \,\widehat{\mathcal{O}}^{\,6}$$

$$= \beta_J B_0^4 \tilde{F}(4) \frac{\widehat{\mathcal{O}}^{\,4}}{\tilde{F}(4)} + \gamma_J B_0^6 \tilde{F}(6) \frac{\widehat{\mathcal{O}}^{\,6}}{\tilde{F}(6)}. \tag{101}$$

In order to cover all possible values of the ratio between the fourth and sixth degree terms a mixing parameter x has been introduced which is governed by the relative magnitude of B_0^4 and B_0^6. Furthermore, a factor W has been defined that scales E_{LF}:

$$\underbrace{\beta_J B_0^4 \,\tilde{F}(4)}_{b_4} = Wx, \qquad \underbrace{\gamma_J B_0^6 \,\tilde{F}(6)}_{b_6} = W(1-|x|) \qquad \text{where} \quad -1 < x < +1 \tag{102}$$

Solving both eqs. (102) for W, an equation is obtained that covers all possible values of the ratio between B_0^4 and B_0^6. It follows that

$$\frac{\beta_J \, B_0^4}{\gamma_J \, B_0^6} = \frac{x}{1-|x|} \, \frac{\tilde{F}(6)}{\tilde{F}(4)}, \tag{103}$$

so that $(\beta_J B_0^4/\gamma_J B_0^6) = 0$ for $x = 0$, while $(\beta_J B_0^4/\gamma_J B_0^6) = \pm\infty$ for $x = \pm 1$. In consequence, eq. (101) can be rewritten as

$$\hat{H}_{\mathrm{LF}}^{\mathrm{cub}} = W \left[x \left(\frac{\widehat{\mathcal{O}}^{\,4}}{\tilde{F}(4)} \right) + (1-|x|) \left(\frac{\widehat{\mathcal{O}}^{\,6}}{\tilde{F}(6)} \right) \right] \tag{104}$$

For each J-manifold x is allowed to take the values in the range $0 \rightarrow \pm 1$. The energy expressions for the LF states as a function of $\beta B_0^4 \tilde{F}(4) = b_4$ and $\gamma B_0^6 \tilde{F}(4) = b_6$ are replaced by Wx and $W(1-|x|)$, respecticely. Table 22 exhibits the results for the $4\mathrm{f}^2$ system and Fig. 15 displays the corresponding diagram E_{LF}/W *versus* x.

Tab. 22: Energies E_{LF} of the $4\mathrm{f}^2$ system in cubic ligand fields as a function of W and x as well as b_4 and b_6, see eqs. (102)

	E_{LF}		E_{LF}/W	
			$x = 0$	$x = \pm 1$
A_1	$28\,b_4 - 80\,b_6$	$W[28x - 80(1-\|x\|)]$	-80	± 28
E	$4\,b_4 + 64\,b_6$	$W[4x + 64(1-\|x\|)]$	64	± 4
T_1	$14\,b_4 + 4\,b_6$	$W[14x + 4(1-\|x\|)]$	4	± 14
T_2	$-26\,b_4 - 20\,b_6$	$W[-26x - 20(1-\|x\|)]$	-20	∓ 26

Diagrams like Figs. 15 and 16, displaying LF energy eigenvalues E_{LF}/W as a function of the LF parameters, are available for all J-manifolds of the lanthanides' ground multiplets [16]. In examples 3.10 and 3.11 the diagrams are used to determine the LF ground state for $\mathrm{Pr}^{3+}[4\mathrm{f}^{\,2}]$ and $\mathrm{Nd}^{3+}[4\mathrm{f}^{\,3}]$ in cubic LF. In example 3.12 the construction of the $x - E_{\mathrm{LF}}/W$ diagram for Pr^{3+} is demonstrated.

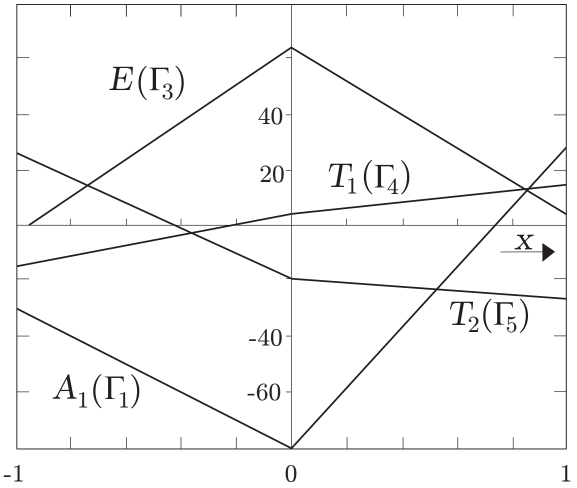

Fig. 15: x–(E_{LF}/W) plot of $\mathrm{Pr}^{3+}[4\mathrm{f}^2]$ ($J = 4$) in cubic ligand fields [16]

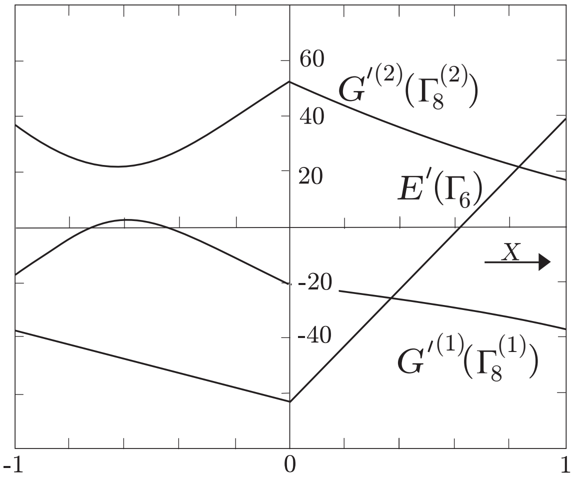

Fig. 16: x–(E_{LF}/W) plot of $\mathrm{Nd}^{3+}[4\mathrm{f}^3]$ ($J = 9/2$) in cubic ligand fields [16]

Example 3.10 *Ground state of* Pr^{3+} *in cubic LF*

Pr^{3+}: The signs of W and x for an octahedral LF:
(i) The PCEM predicts that for an octahedral LF both geometrical parameters, A_4^0 and A_6^0, are positive (see eqs. (91) and (93)) and, consequently, also B_0^4 and B_0^6 [16].
(ii) Since both $\tilde{F}(4)$ and $\tilde{F}(6)$ are positive (for all J's), it is obvious from the right eq. (102) that the sign of W is determined by the sign of $\gamma_J B_0^6$, since $(1 - |x|)$ is always positive for $-1 < x < +1$.
(iii) From eq. (103) we see that the sign of x is determined by the sign of $(\beta_J B_0^4/\gamma_J B_0^6)$. For the Pr^{3+} system under investigation, γ_J, B_0^4, and B_0^6 are positive, while β_J is negative (see Table 23). So, the sign of x is negative.
The x–(E_{LF}/W) diagram in Fig. 15 shows that for the situation $x < 0$ and $W > 0$ the singlet A_1 is the ground state. Thus, an octahedrally coordinated Pr^{3+} ion should exhibit temperature-independent paramagnetism at low temperature. Fig. 13 (left) confirms this magnetic behaviour.

Pr^{3+}: The signs of W and x for a tetrahedral/cubical LF:
Since A_4^0 (B_0^4) is negative, x is positive; the sign of W doesn't change compared to the octahedral case. Consequently, both W and x are positive and the LF ground state may be a singlet (A_1) or a triplet (T_2), depending on the magnitude of x (see the region $x > 0$ in Fig. 15).

Example 3.11 *Ground state of* $\mathrm{Nd}^{3+}[4\mathrm{f}^3]$ *in cubic LF*

Nd^{3+}: The signs of W and x for an octahedral LF:
(i) Applying the PCEM, the situation is identical to the Pr^{3+} case: $B_0^4, B_0^6 > 0$ [17].
(ii) Since γ_J is negative, it is obvious from the right eq. (102) that $W < 0$.
(iii) From eq. (103) we see that the sign of x is determined by the sign of $(\beta_J B_0^4/\gamma_J B_0^6)$. For the Nd^{3+} system under investigation both β_J and γ_J are negative (see Table 23). So, the sign of x is positive.

---

[16] The result of the PCEM calculation is supported by spectroscopic investigations, showing that $B_0^4 = 1\,938\,\mathrm{cm}^{-1}$ and $B_0^6 = 290\,\mathrm{cm}^{-1}$ (see Table 16).

[17] $B_0^4 = 1\,966\,\mathrm{cm}^{-1}$, $B_0^6 = 258\,\mathrm{cm}^{-1}$ (see Table 16).

The x–(E_{LF}/W) diagram in Fig. 16 shows that for the situation $x > 0$ and $W < 0$[18] either the quartet G$'$ or the doublet E$'$ is the ground state. Thus, ignoring interionic spin-spin couplings, an octahedrally coordinated Nd^{3+} ion should exhibit Curie paramagnetism regardless T. Fig. 13 (right) exhibits the magnetic behaviour.

Note, that the diagrams in Figs. 15 and 16 differ distinctly: While for the Pr^{3+} ion exclusively *straight lines* result, one straight line and two *curves* are observed for the Nd^{3+} ion (see 'Remarks' on page 49 for further details).

Nd^{3+}: The signs of W and x for a tetrahedral/cubical LF:

Since both W and x are negative (according to $\beta_J, \gamma_J, B_0^4 < 0$ and $B_0^6 > 0$, eq. (103)) the ground state is the quartet G$'$.

Final remarks

- According to today's standard practice, we use the operator equivalents that are related to the Racah tensors C_q^k [17] while Stevens' definition relates to the spherical harmonics Y_q^k [18, 19]. Since the article of Lea, Leask, Wolf [16] is based on Stevens' definition Y_q^k, some hints to the conversion factors between both derivations is informative with respect to the application of the LLW diagrams:
  - (i) The LLW diagrams can be applied directly, since the conversion factor for both W and x is 1. In other words, the values $O_4/F(4)$ (based on Y_q^k) in equation (5) of ref. [16] and $\widehat{\mathcal{O}}^4/\tilde{F}(4)$ (based on C_q^k) in eq. (104) are identical and the same is true for the sixth degree terms ($k = 6$).
  - (ii) Conversion factors for operator equivalents (see eq. (96) and (97)):
    $\tilde{O}_0^4 = \left(\frac{1}{8}\right) O_0^4, \quad \tilde{O}_4^4 = \left(\sqrt{70}/8\right) O_4^4; \qquad \tilde{O}_0^6 = \left(\frac{1}{16}\right) O_0^6, \quad \tilde{O}_4^6 = \sqrt{63/128}\, O_4^6$
    Consequence of the conversion factors:
    Conversion of $F(4)$ and $F(6)$ [21] into $\tilde{F}(4)$ and $\tilde{F}(6)$ (Table 23), respectively:
    $\tilde{F}(4) = \left(\frac{1}{8}\right) F(4), \qquad \tilde{F}(6) = \left(\frac{1}{16}\right) F(6)$
  - (iii) The LF parameters, used by LLW, $B_0^{4(\mathrm{LLW})}$ and $B_0^{6(\mathrm{LLW})}$ [16], include the Stevens factors β_J and γ_J, while in today's standard practice, used by us, both are separated:
    $B_0^{4(\mathrm{LLW})} = \beta_J\, B_0^4, \qquad B_0^{6(\mathrm{LLW})} = \gamma_J\, B_0^6$
- Within the x–(E_{LF}/W) diagrams there are two types of Γ_i curves to be considered: (i) curves that are straight lines and (ii) curves that deviate more or less from straight lines.
  - (i) A state Γ_i whose energy eigenvalue is a linear function of x, occurs once only in the decomposition of the J-manifold. For example, in the cubic Pr^{3+} systems with ground multiplet $J = 4$ each split term $\mathrm{A}_1(\Gamma_1)$, $\mathrm{E}(\Gamma_3)$, $\mathrm{T}_1(\Gamma_4)$, $\mathrm{T}_2(\Gamma_5)$ occurs once only. So, the diagram exhibits only straight lines. The state functions have fixed compositions (see Table 21) independent of B_0^4 and B_0^6. Other examples are ions in cubic LF's with $J = \frac{5}{2}$ (E$''$ (Γ_7), G$'$ (Γ_8)) and $\frac{7}{2}$ (E$'$ (Γ_6), E$''$ (Γ_7), G$'$ (Γ_8)).

---

[18] According to the negative sign of W, one has to mirror the x–(E_{LF}/W) diagram at the x axis with the consequence that the E_{LF}/W axis shows downwards for $W < 0$.

Tab. 23: Ground states of Ln^{3+} ions in cubic ligand fields [16]

$\mathrm{Ln}^{3+}[4\mathrm{f}^{N}]$ $^{2S+1}L_J$	$\mathrm{Ce}^{3+}[4\mathrm{f}^{1}]$ $^{2}F_{5/2}$	$\mathrm{Pr}^{3+}[4\mathrm{f}^{2}]$ $^{3}H_{4}$	$\mathrm{Nd}^{3+}[4\mathrm{f}^{3}]$ $^{4}I_{9/2}$	$\mathrm{Sm}^{3+}[4\mathrm{f}^{5}]$ $^{6}H_{5/2}$	$\mathrm{Tb}^{3+}[4\mathrm{f}^{8}]$ $^{7}F_{6}$
α_J	$\frac{-2}{35}$	$\frac{-52}{2\,475}$	$\frac{-7}{1\,089}$	$\frac{13}{315}$	$\frac{-1}{99}$
β_J	$\frac{2}{315}$	$\frac{-4}{5\,445}$	$\frac{-136}{467\,181}$	$\frac{26}{10\,395}$	$\frac{2}{16\,335}$
γ_J	0	$\frac{272}{4\,459\,455}$	$\frac{-1\,615}{42\,513\,471}$	0	$\frac{-1}{891\,891}$
$\tilde{F}(4)$ a)	$\frac{15}{2}$	$\frac{15}{2}$	$\frac{21}{2}$	$\frac{15}{2}$	$\frac{15}{2}$
$\tilde{F}(6)$	0	$\frac{315}{4}$ b)	315	0	$\frac{945}{2}$
$\Gamma^{[O]}$ c)	$\mathrm{E}''\left[\frac{\pm}{+1}\right]$ d)	$\mathrm{A}_1\left[\frac{\pm}{-}\right]$	$\mathrm{G}', \mathrm{E}'\left[\frac{-}{+}\right]$	$\mathrm{E}''\left[\frac{\pm}{+1}\right]$	$\mathrm{A}_2, \mathrm{A}_1\left[\frac{-}{-}\right]$
$\Gamma^{[T]}$	$\mathrm{G}'\left[\frac{-}{+1}\right]$	$\mathrm{A}_1, \mathrm{T}_2\left[\frac{\pm}{+}\right]$	$\mathrm{G}'\left[\frac{-}{-}\right]$	$\mathrm{G}'\left[\frac{-}{+1}\right]$	$\mathrm{A}_2, \mathrm{E}\left[\frac{-}{+}\right]$

$\mathrm{Ln}^{3+}[4\mathrm{f}^{N}]$ $^{2S+1}L_J$	$\mathrm{Dy}^{3+}[4\mathrm{f}^{9}]$ $^{6}H_{15/2}$	$\mathrm{Ho}^{3+}[4\mathrm{f}^{10}]$ $^{5}I_{8}$	$\mathrm{Er}^{3+}[4\mathrm{f}^{11}]$ $^{4}I_{15/2}$	$\mathrm{Tm}^{3+}[4\mathrm{f}^{12}]$ $^{3}H_{6}$	$\mathrm{Yb}^{3+}[4\mathrm{f}^{13}]$ $^{2}F_{7/2}$
α_J	$\frac{-2}{315}$	$\frac{-1}{450}$	$\frac{4}{1\,575}$	$\frac{1}{99}$	$\frac{2}{63}$
β_J	$\frac{-8}{135\,135}$	$\frac{-1}{30\,030}$	$\frac{2}{45\,045}$	$\frac{8}{49\,005}$	$\frac{-2}{1\,155}$
γ_J	$\frac{4}{3\,864\,861}$	$\frac{-5}{3\,864\,861}$	$\frac{8}{3\,864\,861}$	$\frac{-5}{891\,891}$	$\frac{4}{27\,027}$
$\tilde{F}(4)$	$\frac{15}{2}$	$\frac{105}{2}$	$\frac{15}{2}$	$\frac{15}{2}$	$\frac{15}{2}$
$\tilde{F}(6)$	$\frac{3\,465}{4}$	$\frac{3\,465}{4}$	$\frac{3\,465}{4}$	$\frac{945}{2}$	$\frac{315}{4}$ b)
$\Gamma^{[O]}$	$\mathrm{E}'', \mathrm{E}'\left[\frac{\pm}{-}\right]$	$\mathrm{E}, \mathrm{A}_1\left[\frac{-}{+}\right]$	$\mathrm{E}'', \mathrm{G}'\left[\frac{\pm}{+}\right]$	$\mathrm{A}_2, \mathrm{A}_1\left[\frac{-}{-}\right]$	$\mathrm{E}'\left[\frac{\pm}{-}\right]$
$\Gamma^{[T]}$	$\mathrm{E}'', \mathrm{G}'\left[\frac{\pm}{+}\right]$	$\mathrm{E}, \mathrm{T}_2\left[\frac{-}{-}\right]$	$\mathrm{E}'', \mathrm{E}'\left[\frac{\pm}{-}\right]$	$\mathrm{A}_2, \mathrm{E}\left[\frac{-}{+}\right]$	$\mathrm{E}', \mathrm{E}''\left[\frac{\pm}{+}\right]$

a) $\tilde{F}(4)$ and $\tilde{F}(6)$ are equivalent to $F(4)$ and $F(6)$ [16] and consider the different definitions of the operator equivalents $\tilde{O}_q^k$ and O_q^k.

b) Note that there is a misprint in the corresponding Table 4.39 of ref. [7].

c) Indices O and T identify the expected LF ground state for octahedral and tetrahedral (cubal) symmetry and negatively charged ligands ($A_1 \equiv \Gamma_1; \mathrm{A}_2 \equiv \Gamma_2; \mathrm{E} \equiv \Gamma_3; \mathrm{T}_1 \equiv \Gamma_4; \mathrm{T}_2 \equiv \Gamma_5; \mathrm{E}' \equiv \Gamma_6; \mathrm{E}'' \equiv \Gamma_7; \mathrm{G}' \equiv \Gamma_8$).

d) Combination of signs for the W and x parameter $\left[\frac{W}{x}\right]$.

(ii) Systems with $J > 4$ decompose as well into states which occur more than once and deviate from straight lines. Taking $J = \frac{9}{2}$ (Nd^{3+}) as an example, decomposition by $H_{\mathrm{LF}}^{\mathrm{cub}}$ takes place into the states $\mathrm{E}'(\Gamma_6)$, $\mathrm{G}'(\Gamma_8^{(1)})$, $\mathrm{G}''(\Gamma_8^{(2)})$. Here the energy of the states $\mathrm{G}'(\Gamma_8^{(1)})$ and $\mathrm{G}''(\Gamma_8^{(2)})$ depends in a more complicated way on the ratio B_0^4/B_0^6 and consequently on x (see Fig. 16)[19]. This is the consequence of the fact that the functions of both states transform according to the same irreducible representation of the cubic group. The state $\mathrm{E}'(\Gamma_6)$, however, occurs once only. So, its energy is a linear function of x.

- The multiplets of Ln^{3+} ions with the same J, e. g., the two pairs $\mathrm{Tb}^{3+}, \mathrm{Tm}^{3+}$ ($J = 6$) and $\mathrm{Dy}^{3+}, \mathrm{Er}^{3+}$ ($J = 15/2$), respectively, are each reduced in cubic ligand fields into the same irreducible representations.

- Exact values for LF parameters cannot be calculated reliably. However, the sign of B_q^k values can often be predicted. Consequently, the signs of x and W can be deduced, leading to the determination of the ground state.

- Systems with non-integer J have exclusively magnetic states (showing Curie paramagnetism [20]), while in the systems with integer J ligand field ground states may be produced which are nonmagnetic, for example $\mathrm{A}_1(\Gamma_1)$, $\mathrm{A}_2(\Gamma_2)$ and $\mathrm{E}(\Gamma_3)$, yielding temperature independent paramagnetism (TIP).

- The x–(E_{LF}/W) diagrams are helpful not only for cubic systems but also for coordination polyhedra that don't deviate greatly from cubic symmetry, that is, have cubic *pseudo symmetry*.

Example 3.12 : Energy of the LF states of $\mathbf{Pr^{3+}}$ in $\mathbf{Cs_2NaPrCl_6}$

To verify Fig. 15 we use Pr^{3+} in $\mathrm{Cs_2NaPrCl_6}$ as an example with $B_0^4 = 1\,938\,\mathrm{cm}^{-1}$ and $B_0^6 = 290\,\mathrm{cm}^{-1}$ (Table 16). With the help of the entries in Table 23 as well as eqs. (102) and (103), the following data result:

$$\begin{aligned} b_4 &= \beta_J \tilde{F}(4) B_0^4 = Wx = -\left(\frac{4}{5\,445}\right)\left(\frac{15}{2}\right) \times 1938\,\mathrm{cm}^{-1} = -10.68\,\mathrm{cm}^{-1} \\ b_6 &= \gamma_J \tilde{F}(6) B_0^6 = W(1-|x|) = \left(\frac{272}{4\,459\,455}\right)\left(\frac{315}{4}\right) \times 290\,\mathrm{cm}^{-1} = 1.393\,\mathrm{cm}^{-1} \\ \frac{b_4}{b_6} &= \frac{x}{1-|x|} = -7.665 \qquad \Longrightarrow \qquad x = -0.8845, \quad W = \frac{b_4}{x} = 12.07 \end{aligned}$$

Table 24 exhibits the LF energies corresponding with $x = -0.8845$ and $W = 12.07$. Note that the calculated energy values, appearing in the last column of Table 24, are not identical with the observed ones (see Table 17). One reason for the discrepancy is caused by the fact that in our model only the ground multiplet $^3H_4$ has been considered instead of the full basis.

The energy difference between the LF term of highest energy (T_2) and lowest energy (A_1) of the ground multiplet, usually called *crystal field overall splitting* (CFOS for short), amounts to $660\,\mathrm{cm}^{-1}$ (calc.) and $701\,\mathrm{cm}^{-1}$ (obs.).

---

[19] The states are listed as a function of x in ref. [16].

[20] *Curie paramagnetism* means that χ_{m} increases with decreasing T.

Tab. 24: Calculated energies E_{LF} of the LF states of Pr^{3+} in $\mathrm{Cs_2NaPrCl_6}$ on the basis of spectroscopically determined values $B_0^4 = 1938$ and $B_0^6 = 290\ \mathrm{cm}^{-1}$ [13].

	$E_{\mathrm{LF,calc.}}/\mathrm{cm}^{-1}$ [a]				$E_{\mathrm{LF,obs.}}$ [b]
$\mathrm{A}_1(\Gamma_1)$	$28\,b_4 - 80\,b_6$	$W[28x - 80(1-\|x\|)]$	-410	0	0
$\mathrm{T}_1(\Gamma_4)$	$14\,b_4 + 4\,b_6$	$W[14x + 4(1-\|x\|)]$	-144	266	236
$\mathrm{E}(\Gamma_3)$	$4\,b_4 + 64\,b_6$	$W[4x + 64(1-\|x\|)]$	46	456	422
$\mathrm{T}_2(\Gamma_5)$	$-26\,b_4 - 20\,b_6$	$W[-26x - 20(1-\|x\|)]$	250	660 [c]	701

---

[a] $W = 12.07$; $x = -0.8845$; see Example 3.12.

[b] Ref. [13].

[c] Crystal field overall splitting (CFOS).

Problems

7. Determine the crystal field overall splitting (CFOS) for the Dy^{3+} ion in $\mathrm{Cs_2NaDyCl_6}$ on the basis of Fig. 35. Apply eqs. (102) and (103) as well as the entries in Table 23 and take the B_0^4 and B_0^6 values for Dy from Table 16. (Solutions are specified in section 5.)

3.4 Non-cubic LF

3.4.1 Ligand field operators (single electron systems)

Lowering the symmetry results in LF operators with an increasing number of terms[21]:

- cylindrical ($\mathrm{D}_{\infty\mathrm{h}}$, $\mathrm{C}_{\infty\mathrm{v}}$ [22])

$$\hat{H}_{\mathrm{LF}}^{\mathrm{cyl}} = B_0^2\, C_0^2 + B_0^4\, C_0^4 + B_0^6\, C_0^6 \tag{105}$$

- hexagonal ($\mathrm{D}_{6\mathrm{h}}$, $\mathrm{D}_{3\mathrm{h}}$, D_6, $\mathrm{C}_{6\mathrm{v}}$)

$$\hat{H}_{\mathrm{LF}}^{\mathrm{hex}} = B_0^2\, C_0^2 + B_0^4\, C_0^4 + B_0^6\, C_0^6 + B_6^6\left(C_{-6}^6 + C_6^6\right) \tag{106}$$

- tetragonal ($\mathrm{D}_{4\mathrm{h}}$, D_4, $\mathrm{C}_{4\mathrm{v}}$, $\mathrm{D}_{2\mathrm{d}}$)

$$\hat{H}_{\mathrm{LF}}^{\mathrm{tet}} = B_0^2\, C_0^2 + B_0^4\, C_0^4 + B_4^4\left(C_{-4}^4 + C_4^4\right) + B_0^6\, C_0^6 + B_4^6\left(C_{-4}^6 + C_4^6\right) \tag{107}$$

- trigonal ($\mathrm{D}_{3\mathrm{d}}$, D_3, $\mathrm{C}_{3\mathrm{v}}$)

$$\hat{H}_{\mathrm{LF}}^{\mathrm{tri}} = B_0^2\, C_0^2 + B_0^4\, C_0^4 + B_3^4\left(C_{-3}^4 - C_3^4\right) + B_0^6\, C_0^6 + B_3^6\left(C_{-3}^6 - C_3^6\right) + B_6^6\left(C_{-6}^6 + C_6^6\right) \tag{108}$$

For d electron systems only terms with $k \leq 4$ are relevant. The number of terms for f(d) systems with cylindrical, hexagonal, tetragonal, trigonal symmetry is 3(2), 4(2), 5(3), 6(3), respectively. A complete list of $\hat{H}_{\mathrm{LF}}$ operators (including the symmetry I_h) is given in ref. [15].

3.4.2 4f^1 system (Ce^{3+}, $^2F_{5/2}$: $H_{\mathrm{LF}}^{\mathrm{cyl}}$)

In the following calculations the basis functions are restricted to the multiplet $^2F_{5/2}$ [23].

Ligand field operator: $\hat{H}_{\mathrm{LF}}^{\mathrm{cyl}}\,(^2F_{5/2}) = B_0^2\, C_0^2 + B_0^4\, C_0^4$ (109)

Operator (109), acting on $^2F_{5/2}$, produces solely diagonal elements ($q = 0$). The matrix elements $\langle M_J | C_0^k | M_J \rangle$ for $k = 4$ are known from matrix (83). The data for $k = 2$ are obtained with the help of Table 8 and Table 13:

$\langle \pm\frac{1}{2} | C_0^2 | \pm\frac{1}{2} \rangle = \frac{8}{35}$; $\quad \langle \pm\frac{3}{2} | C_0^2 | \pm\frac{3}{2} \rangle = \frac{2}{35}$; $\quad \langle \pm\frac{5}{2} | C_0^2 | \pm\frac{5}{2} \rangle = -\frac{10}{35}$.

In Table 25 the results are given.

---

[21] $C_0^2 = \frac{1}{2}\left(3\cos^2\theta - 1\right)$; $\quad C_{\pm 3}^4 = \mp\frac{1}{4}\sqrt{35}\sin^3\theta\cos\theta e^{\pm i3\phi}$; $C_{\pm 3}^6 = \mp\frac{1}{16}\sqrt{105}\sin^3\theta\cos\theta\left(11\cos^2\theta - 3\right)e^{\pm i3\phi}$; $\quad C_{\pm 6}^6 = \frac{1}{32}\sqrt{231}\sin^6\theta e^{\pm i6\phi}$.

[22] $\hat{H}_{\mathrm{LF}}^{\mathrm{cyl}}$ applies also for $\mathrm{D}_{4\mathrm{d}}$.

[23] Note that under this restriction the effects of $\hat{H}_{\mathrm{LF}}^{\mathrm{cyl}}$ and $\hat{H}_{\mathrm{LF}}^{\mathrm{hex}}$ are identical.

Table 25: Splitting of the ${}^2F_{5/2}[4\mathrm{f}^1]$ multiplet by $\hat{H}_{\mathrm{LF}}^{\mathrm{cyl}}$

$\vert M_J\rangle$	$E_{n,\mathrm{LF}} \equiv W_n^{(0)}$
$\vert\pm\frac{1}{2}\rangle^{a)}$	$\frac{8}{35}B_0^2 + \frac{2}{21}B_0^4$
$\vert\pm\frac{3}{2}\rangle$	$\frac{2}{35}B_0^2 - \frac{3}{21}B_0^4$
$\vert\pm\frac{5}{2}\rangle$	$-\frac{10}{35}B_0^2 + \frac{1}{21}B_0^4$

---

[a] Wavefunctions adapted to the magnetic field in x-direction: $|\psi_\pm\rangle = \frac{1}{\sqrt{2}}\left(\pm|\tfrac{1}{2}\rangle + |-\tfrac{1}{2}\rangle\right)$.

In a cylindrical /hexagonal LF ${}^2F_{5/2}$ is split in three doublets whose energy separations are given by B_0^2 and B_0^4.

3.4.3 4f^1 system (Ce^{3+}, ${}^2F_{5/2}$: $H_{\mathrm{LF}}^{\mathrm{cyl}} + H_{\mathrm{mag}}$)

In a cylindrical/hexagonal LF the multiplet ${}^2F_{5/2}$ is split in three doublets depending on B_0^2 and B_0^4 (see section 3.4.2). To gain the susceptibility equation the influence of the magnetic field must be considered parallel to the unique axis z and in a second direction perpendicular to z, that is, x.

Magnetic field parallel to the unique axis: $\boldsymbol{\hat{H}_{\mathrm{mag,z}} = -\gamma_e g_J \hat{J}_z B_z \quad (g_J = \frac{6}{7})}$

The results are available in the third column of Table 26. Applying Van Vleck's equation (60) the susceptibility equation for $\chi_{\mathrm{m}\|}$ is

$$\chi_{\mathrm{m}\|} = \mu_0 \frac{N_A \mu_{\mathrm{B}}^2}{3k_{\mathrm{B}}T}\,\mu_{\mathrm{eff}\|}^2 \quad \text{where} \tag{110}$$

$$\mu_{\mathrm{eff}\|}^2 = g_J^2 \frac{3\left[\frac{1}{4}\exp\left(-\frac{\Delta_1}{k_{\mathrm{B}}T}\right) + \frac{9}{4} + \frac{25}{4}\exp\left(-\frac{\Delta_2}{k_{\mathrm{B}}T}\right)\right]}{\exp\left(-\frac{\Delta_1}{k_{\mathrm{B}}T}\right) + 1 + \exp\left(-\frac{\Delta_2}{k_{\mathrm{B}}T}\right)}, \qquad g_J = \frac{6}{7}$$

and

$$\Delta_1 = W_{1/2}^{(0)} - W_{3/2}^{(0)} = \tfrac{6}{35}B_0^2 + \tfrac{5}{21}B_0^4$$

$$\Delta_2 = W_{5/2}^{(0)} - W_{3/2}^{(0)} = -\tfrac{12}{35}B_0^2 + \tfrac{4}{21}B_0^4.$$

Table 26: Splitting of the ${}^2F_{5/2}[4\mathrm{f}^1]$ multiplet by $\hat{H}_{\mathrm{LF}}^{\mathrm{cyl}}$, $\hat{H}_{\mathrm{mag}\|}$ (z) and $\hat{H}_{\mathrm{mag}\perp}$ (x); energies $E_{\mathrm{LF}} \equiv W_n^{(0)}$, Zeeman coefficients $W_{n,z}^{(1)}$ and $W_{n,x}^{(1)}$, $W_{n,x}^{(2)}$

$\vert M_J\rangle$	$E_{n,\mathrm{LF}} \equiv W_n^{(0)}$	$W_{n,z}^{(1)}/g_J\mu_{\mathrm{B}}$	$W_{n,x}^{(1)}/g_J\mu_{\mathrm{B}}$	$W_{n,x}^{(2)}/g_J^2\mu_{\mathrm{B}}^2$ $^{a)}$
$\vert\pm\frac{1}{2}\rangle^{b)}$	$\frac{8}{35}B_0^2 + \frac{2}{21}B_0^4$	$\pm\frac{1}{2}$	$\pm\frac{3}{2}$	$2/\Delta_1$
$\vert\pm\frac{3}{2}\rangle$	$\frac{2}{35}B_0^2 - \frac{3}{21}B_0^4$	$\pm\frac{3}{2}$	0	$-5/(4\Delta_2) - 2/\Delta_1$
$\vert\pm\frac{5}{2}\rangle$	$-\frac{10}{35}B_0^2 + \frac{1}{21}B_0^4$	$\pm\frac{5}{2}$	0	$5/(4\Delta_2)$

---

[a] $\Delta_1 = W_{1/2}^{(0)} - W_{3/2}^{(0)} = \frac{6}{35}B_0^2 + \frac{5}{21}B_0^4$; $\qquad \Delta_2 = W_{5/2}^{(0)} - W_{3/2}^{(0)} = -\frac{12}{35}B_0^2 + \frac{4}{21}B_0^4$

[b] Wave functions adapted to $\hat{H}_{\mathrm{mag}\perp}$: $|\psi_\pm\rangle = \frac{1}{\sqrt{2}}\left(\pm|\tfrac{1}{2}\rangle + |-\tfrac{1}{2}\rangle\right)$.

Magnetic field perpendicular to the unique axis:

$$\boldsymbol{\hat{H}_{\mathrm{mag,x}} = -\gamma_e g_J \hat{J}_x B_x = -\gamma_e g_J \left(\tfrac{1}{2}\right)\left(\hat{J}_+ + \hat{J}_-\right) B_x}$$

$\langle\, \tfrac{5}{2}\,|\hat{H}_{\mathrm{mag}_x}|-\tfrac{5}{2}\,\rangle$

The matrix elements $\langle\, \tfrac{5}{2}\,|\hat{H}_{\mathrm{mag}_x}|-\tfrac{5}{2}\,\rangle$ and $\langle\, \tfrac{3}{2}\,|\hat{H}_{\mathrm{mag}_x}|-\tfrac{3}{2}\,\rangle$ are zero. On account of the off-diagonal element $\langle\pm\tfrac{1}{2}|\hat{H}_{\mathrm{mag}_x}|\mp\tfrac{1}{2}\rangle = \tfrac{3}{2}g_J\mu_\mathrm{B}B_x$, the correct zeroth-order functions have to be determined:

$$\begin{vmatrix} -W_n^{(1)} & \tfrac{3}{2}\,g_J\mu_\mathrm{B} \\ \tfrac{3}{2}\,g_J\mu_\mathrm{B} & -W_n^{(1)} \end{vmatrix} = 0; \quad W_{n(1,2)}^{(1)} = \pm\tfrac{3}{2}g_J\mu_B; \quad |\psi_\pm\rangle = \tfrac{1}{\sqrt{2}}\left(\pm|\,\tfrac{1}{2}\,\rangle + |-\tfrac{1}{2}\,\rangle\right).$$

The H matrix reads (in units of $g_J\mu_B B_x$):

	$\lvert\,\tfrac{5}{2}\,\rangle$	$\lvert-\tfrac{5}{2}\,\rangle$	$\lvert\,\tfrac{3}{2}\,\rangle$	$\lvert-\tfrac{3}{2}\,\rangle$	$\lvert\,\psi_+\,\rangle$	$\lvert\,\psi_-\,\rangle$
$\langle\,\tfrac{5}{2}\,\rvert$	0		$\tfrac{\sqrt{5}}{2}$			
$\langle-\tfrac{5}{2}\,\rvert$		0		$\tfrac{\sqrt{5}}{2}$		
$\langle\,\tfrac{3}{2}\,\rvert$	$\tfrac{\sqrt{5}}{2}$		0		1	-1
$\langle-\tfrac{3}{2}\,\rvert$		$\tfrac{\sqrt{5}}{2}$		0	1	1
$\langle\,\psi_+\,\rvert$			1	1	$\tfrac{3}{2}$	
$\langle\,\psi_-\,\rvert$			-1	1		$-\tfrac{3}{2}$

In Table 26, column 4 and 5 the results are collected. Substituting $W_n^{(0)}$, $W_{n,x}^{(1)}$ and $W_{n,x}^{(2)}$ in eqn. (60) yields the expression for $\chi_{\mathrm{m}\perp}$:

$$\begin{aligned} \chi_{\mathrm{m}\perp} &= \mu_0\,\frac{N_A\mu_\mathrm{B}^2}{3k_\mathrm{B}T}\,\mu_{\mathrm{eff}\perp}^2 \quad \text{where} \qquad (111) \\ \mu_{\mathrm{eff}\perp}^2 &= g_J^2\,3\left[\left(\frac{9}{4}-\frac{4k_\mathrm{B}T}{\Delta_1}\right)\exp\left(-\frac{\Delta_1}{k_\mathrm{B}T}\right)+\left(\frac{4}{\Delta_1}+\frac{5}{2\Delta_2}\right)k_\mathrm{B}T-\frac{5k_\mathrm{B}T}{2\Delta_2}\exp\left(-\frac{\Delta_2}{k_\mathrm{B}T}\right)\right] \\ &\quad \times\left[\exp\left(-\frac{\Delta_1}{k_\mathrm{B}T}\right)+1+\exp\left(-\frac{\Delta_2}{k_\mathrm{B}T}\right)\right]^{-1} \\ \text{and} \quad & \Delta_1 = W_{1/2}^{(0)} - W_{3/2}^{(0)} = \tfrac{6}{35}B_0^2 + \tfrac{5}{21}B_0^4 \\ & \Delta_2 = W_{5/2}^{(0)} - W_{3/2}^{(0)} = -\tfrac{12}{35}B_0^2 + \tfrac{4}{21}B_0^4. \end{aligned}$$

For a polycrystalline sample the average susceptibility is

$$\overline{\chi}_\mathrm{m} = \tfrac{1}{3}\left(\chi_{\mathrm{m}\parallel} + 2\,\chi_{\mathrm{m}\perp}\right). \qquad (112)$$

This model, extended by a molecular field parameter λ_MF and a temperature-independent parameter χ_0

$$\left(\chi_\mathrm{m} - \chi_0\right)^{-1} = \overline{\chi}_\mathrm{m}^{-1} - \lambda_\mathrm{MF}$$

has been applied to the intermetallic CePt$_5$ (CaCu$_5$-type: Ce^{3+}[4f^1], D$_{6\mathrm{h}}$). A good adaptation to the experimental data was obtained with the parameter values $B_0^2 = -1108\,\mathrm{cm}^{-1}$, $B_0^4 = -104\,\mathrm{cm}^{-1}$, $\lambda_\mathrm{MF} = -0.43 \times 10^5\,\mathrm{mol\,m^{-3}}$, and $\chi_0 = 63 \times 10^{-11}\,\mathrm{m^3\,mol^{-1}}$ [24, 25].

Problems

8. In which respect does the magnetic susceptibility of a mononuclear lanthanide systems with Ln point symmetry (i) O_h, (ii) $D_{\infty h}$, (iii) D_{2h} differ?I

4 Isotropic spin-spin exchange couplings in dinuclear compounds

4.1 Parametrization of exchange interactions

- Heitler-London model of H_2

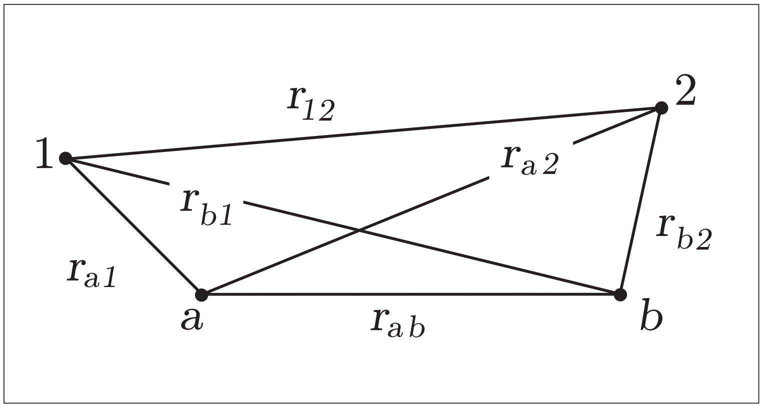

Fig. 17: H_2 model; a and b assign the nuclei, 1 and 2 the electrons

Valence bond ansatz: construction of products with orbital configuration $\phi_a\phi_b$ using the four spin orbitals

$$\phi_a\alpha \qquad \phi_a\beta \qquad \phi_b\alpha \qquad \phi_b\beta$$

Product states in consideration of the Pauli principle:

$$D_1 = \phi_a(1)\alpha(1)\,\phi_b(2)\beta(2) - \phi_a(2)\alpha(2)\,\phi_b(1)\beta(1) \tag{113}$$
$$D_2 = \phi_a(1)\beta(1)\,\phi_b(2)\alpha(2) - \phi_a(2)\beta(2)\,\phi_b(1)\alpha(1) \tag{114}$$
$$D_3 = \phi_a(1)\alpha(1)\,\phi_b(2)\alpha(2) - \phi_a(2)\alpha(2)\,\phi_b(1)\alpha(1) \tag{115}$$
$$D_4 = \phi_a(1)\beta(1)\,\phi_b(2)\beta(2) - \phi_a(2)\beta(2)\,\phi_b(1)\beta(1) \tag{116}$$

- *Construction of eigenfunctions of the total spin*

$\hat{\boldsymbol{S}}' = \hat{\boldsymbol{S}}_1 + \hat{\boldsymbol{S}}_2 \quad (S_1 = S_2 = 1/2)$

D_3 and D_4 are eigenfunctions $|\,S'\,M'_S\,\rangle$ of $\hat{\boldsymbol{S}}'^2 = (\hat{\boldsymbol{S}}_1 + \hat{\boldsymbol{S}}_2)^2$ and $\hat{S}'_z = \hat{S}_{z1} + \hat{S}_{z2}$ with $S' = 1$ and $M_{S'} = 1$ and -1 (Spin triplet functions $|\,1\,1\,\rangle$ and $|\,1\,-1\,\rangle$), respectively, while linear combinations of D_1 and D_2 yield functions with $M_{S'} = 0$:

$D_1 + D_2 \Longrightarrow |\,1\,0\,\rangle$ (spin triplet function); $\qquad D_1 - D_2 \Longrightarrow |\,0\,0\,\rangle$ (spin singlet function)

$$\begin{array}{cccc} \Phi_1 = D_1 - D_2 & \Phi_2 = D_3 & \Phi_3 = D_1 + D_2 & \Phi_4 = D_4 \\ |\,0\,0\,\rangle & |\,1\,1\,\rangle & |\,1\,0\,\rangle & |\,1\,-1\,\rangle \end{array}$$

ϕ_a and ϕ_b are normalised:

$$\int \phi_\mathrm{a}(1)^*\phi_\mathrm{a}(1)d\tau_1 = \int \phi_\mathrm{b}^*(2)\phi_\mathrm{b}(2)d\tau_2 = 1,$$

but not orthogonal:

$$\textit{overlap integral} \quad S_\mathrm{ab} = \int \phi_\mathrm{a}(1)^*\phi_\mathrm{b}(1)d\tau_1 = \int \phi_\mathrm{a}(2)^*\phi_\mathrm{b}(2)d\tau_2 \neq 0$$

Normalised functions of the dinuclear unit:

$$\Phi_1 = N_\mathrm{g}\underbrace{[\phi_\mathrm{a}(1)\phi_\mathrm{b}(2)+\phi_\mathrm{a}(2)\phi_\mathrm{b}(1)]}_{\text{sym}}\underbrace{\sqrt{\tfrac{1}{2}}\,[\alpha(1)\beta(2)-\alpha(2)\beta(1)]}_{\text{anti}}$$

$$\left.\begin{array}{l}\Phi_2\\ \Phi_3\\ \Phi_4\end{array}\right\} = N_\mathrm{u}\underbrace{[\phi_\mathrm{a}(1)\phi_\mathrm{b}(2)-\phi_\mathrm{a}(2)\phi_\mathrm{b}(1)]}_{\text{anti}}\underbrace{\left\{\begin{array}{l}\alpha(1)\alpha(2)\\ \sqrt{\tfrac{1}{2}}\,[\alpha(1)\beta(2)+\alpha(2)\beta(1)]\\ \beta(1)\beta(2)\end{array}\right.}_{\text{sym}}$$

where $N_\mathrm{g} = (2+2S_\mathrm{ab}^2)^{-1/2}$ and $N_\mathrm{u} = (2-2S_\mathrm{ab}^2)^{-1/2}$.

- *Symmetry of the functions with regard to exchange of electrons*

total function:	anti $\quad \Phi_i(1,2) = -\Phi_i(2,1)$
singlet function:	orbital sym (g), spin function anti
triplet functions:	orbital anti (u), spin function sym

$\Longrightarrow$ Symmetry of the orbital forces a distinct multiplicity of the spin function on account of the Pauli principle

- *Evaluation of the energy $E(S)$ and $E(T)$ of the singlet and triplet states*

$$\hat{H} = \underbrace{-\frac{\hbar^2}{2m_\mathrm{e}}\nabla^2(1)-\frac{e^2}{r_\mathrm{a1}}-\frac{e^2}{r_\mathrm{b1}}}_{\hat{h}(1)}\underbrace{-\frac{\hbar^2}{2m_\mathrm{e}}\nabla^2(2)-\frac{e^2}{r_\mathrm{a2}}-\frac{e^2}{r_\mathrm{b2}}}_{\hat{h}(2)}+\frac{e^2}{r_{12}}$$

$$E(S) = \langle {}^1\Phi_1^\mathrm{g}|\hat{H}|{}^1\Phi_1^\mathrm{g}\rangle = \frac{2(h+h_\mathrm{ab}S_\mathrm{ab})+J_\mathrm{ab}+K_\mathrm{ab}}{1+S_\mathrm{ab}^2} \qquad (117)$$

$$E(T) = \langle {}^3\Phi_2^\mathrm{u}|\hat{H}|{}^3\Phi_2^\mathrm{u}\rangle = \frac{2(h-h_\mathrm{ab}S_\mathrm{ab})+J_\mathrm{ab}-K_\mathrm{ab}}{1-S_\mathrm{ab}^2} \qquad (118)$$

where

$$
\begin{aligned}
h &= \left\langle \phi_\mathrm{a}(i) \left| \hat{h}(i) \right| \phi_\mathrm{a}(i) \right\rangle \quad \text{(one-centre} \\
&= \left\langle \phi_\mathrm{b}(i) \left| \hat{h}(i) \right| \phi_\mathrm{b}(i) \right\rangle \quad \text{one-electron integral)} \\
h_\mathrm{ab} &= \left\langle \phi_\mathrm{a}(i) \left| \hat{h}(i) \right| \phi_\mathrm{b}(i) \right\rangle \quad \text{(transfer or hopping integral)} \\
J_\mathrm{ab} &= \left\langle \phi_\mathrm{a}(1)\phi_\mathrm{b}(2) \left| e^2/r_{12} \right| \phi_\mathrm{a}(1)\phi_\mathrm{b}(2) \right\rangle \quad \text{(Coulomb integral)} \\
K_\mathrm{ab} &= \left\langle \phi_\mathrm{a}(1)\phi_\mathrm{b}(2) \left| e^2/r_{12} \right| \phi_\mathrm{a}(2)\phi_\mathrm{b}(1) \right\rangle \quad \text{(Exchange integral).}
\end{aligned}
$$

Example: Evaluation of $E(S) = \left\langle {}^1\Phi_1^\mathrm{g} \left| \hat{H} \right| {}^1\Phi_1^\mathrm{g} \right\rangle$

1. Integration over the spin:

$$
\begin{aligned}
&\tfrac{1}{2} \langle \alpha(1)\beta(2) - \beta(1)\alpha(2) | \alpha(1)\beta(2) - \beta(1)\alpha(2) \rangle = \\
&\quad \tfrac{1}{2} \big[\underbrace{\langle \alpha(1)\beta(2) | \alpha(1)\beta(2) \rangle}_{1} + \underbrace{\langle \alpha(2)\beta(1) | \alpha(2)\beta(1) \rangle}_{1} - \\
&\quad \underbrace{\langle \alpha(2)\beta(1) | \alpha(1)\beta(2) \rangle}_{0} - \underbrace{\langle \alpha(1)\beta(2) | \alpha(2)\beta(1) \rangle}_{0} \big] = 1.
\end{aligned}
$$

2. Integration over the space:

$$
\begin{aligned}
&E(S) = \\
&N_\mathrm{g}^2 \left\langle \phi_\mathrm{a}(1)\phi_\mathrm{b}(2) + \phi_\mathrm{b}(1)\phi_\mathrm{a}(2) \left| \hat{h}(1) + \hat{h}(2) + e^2/r_{12} \right| \phi_\mathrm{a}(1)\phi_\mathrm{b}(2) + \right. \\
&\quad \left. \phi_\mathrm{b}(1)\phi_\mathrm{a}(2) \right\rangle = 2N_\mathrm{g}^2 \left[2(h + h_\mathrm{ab}S_\mathrm{ab}) + J_\mathrm{ab} + K_\mathrm{ab} \right].
\end{aligned} \tag{119}
$$

Singlet-triplet splitting:

$$
\begin{aligned}
\Delta E(T,S) &= E(T) - E(S) \\
&\approx -2K_\mathrm{ab} - 4h_\mathrm{ab}S_\mathrm{ab} + 2S_\mathrm{ab}^2(2h + J_\mathrm{ab})
\end{aligned}
$$

- *Application of the Heitler-London model to dinuclear complexes having* $S_1 = S_2 = \frac{1}{2}$ *centres*

Example: $\mathrm{L}'_\mathrm{n}\mathrm{Cu}_\mathrm{a}\text{–L–}\mathrm{Cu}_\mathrm{b}\mathrm{L}'_\mathrm{n}$

As distinguished from the strong covalent bond in H_2 the interactions between both magnetically active electrons is weak.

$\Longrightarrow$ small $\Delta E(T,S)$.

The highest singly occupied antibonding orbitals ϕ_a and ϕ_b of the fragments $\mathrm{L}'_\mathrm{n}\mathrm{Cu}_\mathrm{a}\mathrm{L}$ and $\mathrm{LCu}_\mathrm{b}\mathrm{L}'_\mathrm{n}$, respectively take over the role of the 1s orbitals of the H atoms. ϕ_a and ϕ_b have mainly d character. They are centered at the metal ions and partially delocalised in the direction of the ligands.

4.2 Heisenberg operator

The interaction between the unpaired electrons of centre 1 with the ones of centre 2 are phenomenologically described by an *apparent spin-spin coupling*, whose magnitude and sign are given by the spin-spin coupling parameter (exchange parameter) J_{ex}:

$$\boxed{\hat{H}_{\mathrm{ex}} = -2J_{\mathrm{ex}}\hat{\boldsymbol{S}}_1\cdot\hat{\boldsymbol{S}}_2 \quad \text{where} \quad -2J_{\mathrm{ex}} = \Delta E(T,S)} \tag{120}$$

$\hat{H}_{\mathrm{ex}}$ is an *effective* operator, describing but not explaining the spin-spin coupling.

Application of $\hat{H}_{\mathrm{ex}}$ to ${}^1\Phi_1^{\mathrm{g}}$ ($S' = 0$) and ${}^3\Phi_i^{\mathrm{u}}$ ($S' = 1, i = 2,3,4$):

$$-2J_{\mathrm{ex}}\hat{\boldsymbol{S}}_1\cdot\hat{\boldsymbol{S}}_2\,{}^1\Phi_1^{\mathrm{g}} = \underbrace{\left(\tfrac{3}{2}\right)J_{\mathrm{ex}}}_{E(S)}\,{}^1\Phi_1^{\mathrm{g}}, \qquad -2J_{\mathrm{ex}}\hat{\boldsymbol{S}}_1\cdot\hat{\boldsymbol{S}}_2\,{}^3\Phi_i^{\mathrm{u}} = \underbrace{-\left(\tfrac{1}{2}\right)J_{\mathrm{ex}}}_{E(T)}\,{}^3\Phi_i^{\mathrm{u}}$$

$$\Longrightarrow \quad \Delta E(T,S) = E(T) - E(S) = -2J_{\mathrm{ex}} \tag{121}$$

$J_{\mathrm{ex}} < 0$: singlet ground state (intramolecular antiferromagnetic interaction)
$J_{\mathrm{ex}} > 0$: triplet ground state (intramolecular ferromagnetic interaction)

Hints to the evaluation of $E(T)$ and $E(S)$:

$$\begin{aligned} \hat{\boldsymbol{S}}'^2 &= \left(\hat{\boldsymbol{S}}_1 + \hat{\boldsymbol{S}}_2\right)^2 = \hat{\boldsymbol{S}}_1^2 + \hat{\boldsymbol{S}}_2^2 + 2\hat{\boldsymbol{S}}_1\cdot\hat{\boldsymbol{S}}_2 \\ 2\hat{\boldsymbol{S}}_1\cdot\hat{\boldsymbol{S}}_2 &= \hat{\boldsymbol{S}}'^2 - \hat{\boldsymbol{S}}_1^2 - \hat{\boldsymbol{S}}_2^2 = \hbar^2\left[\underbrace{S'(S'+1)}_{0 \ \text{or} \ 2} - \underbrace{S_1(S_1+1)}_{\frac{3}{4}} - \underbrace{S_2(S_2+1)}_{\frac{3}{4}}\right] \end{aligned}$$

Heisenberg operator for more than two centres:

$$\hat{H}_{\mathrm{ex}} = -2\sum_{i<j} J_{\mathrm{ex,ij}}\hat{\boldsymbol{S}}_i\cdot\hat{\boldsymbol{S}}_j \tag{122}$$

$$\hat{H}_{\mathrm{ex}} = -2J_{\mathrm{ex}}\sum_{i<j}\hat{\boldsymbol{S}}_i\cdot\hat{\boldsymbol{S}}_j \tag{123}$$

4.3 Exchange-coupled species in a magnetic field

$$\begin{aligned} \hat{H}_{\mathrm{ex}} &= -2J_{\mathrm{ex}}\hat{\boldsymbol{S}}_1\cdot\hat{\boldsymbol{S}}_2 = -2J_{\mathrm{ex}}\left(\hat{S}_{z1}\hat{S}_{z2} + \hat{S}_{x1}\hat{S}_{x2} + \hat{S}_{y1}\hat{S}_{y2}\right) \\ &= -2J_{\mathrm{ex}}\left[\hat{S}_{z1}\hat{S}_{z2} + \tfrac{1}{2}\left(\hat{S}_{+1}\hat{S}_{-2} + \hat{S}_{-1}\hat{S}_{+2}\right)\right] \end{aligned} \tag{124}$$

Basis: spin functions in the form $|\,M_S\,M_S\,\rangle$ where the first M_S refers to electron 1 and the second to electron 2

H-Matrix:

(125)

$M_{S_1}M_{S_2}$	$\lvert\,\frac{1}{2}\,\frac{1}{2}\,\rangle$	$\lvert\,-\frac{1}{2}\,\frac{1}{2}\,\rangle$	$\lvert\,\frac{1}{2}\,-\frac{1}{2}\,\rangle$	$\lvert\,-\frac{1}{2}\,-\frac{1}{2}\,\rangle$
$\langle\,\frac{1}{2}\,\frac{1}{2}\,\rvert$	$-J_{\mathrm{ex}}/2$			
$\langle\,-\frac{1}{2}\,\frac{1}{2}\,\rvert$		$J_{\mathrm{ex}}/2$	$-J_{\mathrm{ex}}$	
$\langle\,\frac{1}{2}\,-\frac{1}{2}\,\rvert$		$-J_{\mathrm{ex}}$	$J_{\mathrm{ex}}/2$	
$\langle\,-\frac{1}{2}\,-\frac{1}{2}\,\rvert$				$-J_{\mathrm{ex}}/2$

Evaluation of the diagonal element H_{11}:

$-2J_{\text{ex}}\left\langle \tfrac{1}{2}\,\tfrac{1}{2} \,\middle|\, \hat{S}_{z1}\hat{S}_{z2} \,\middle|\, \tfrac{1}{2}\,\tfrac{1}{2} \right\rangle = -2J_{\text{ex}}\left(\tfrac{1}{2}\right)\left(\tfrac{1}{2}\right) = -J_{\text{ex}}/2$

Evaluation of the off-diagonal element H_{23}:

$-2J_{\text{ex}}\left\langle -\tfrac{1}{2}\,\tfrac{1}{2} \,\middle|\, \tfrac{1}{2}\hat{S}_{-1}\hat{S}_{+2} \,\middle|\, \tfrac{1}{2}\,-\tfrac{1}{2} \right\rangle = -J_{\text{ex}}(1)(1) = -J_{\text{ex}}$

Results:

Tab. 27: Spin functions and exchange energies of the $S_1 = S_2 = \frac{1}{2}$ system

Spin function	$M_{S'}$	S'	E
$\frac{1}{\sqrt{2}}\left(\left\|\, \frac{1}{2}\, -\frac{1}{2} \right\rangle - \left\|\, -\frac{1}{2}\, \frac{1}{2} \right\rangle\right)$	0	0	$\frac{3}{2}J_{\text{ex}}$
$\left\|\, \frac{1}{2}\, \frac{1}{2} \right\rangle$	1	1	$-\frac{1}{2}J_{\text{ex}}$
$\frac{1}{\sqrt{2}}\left(\left\|\, \frac{1}{2}\, -\frac{1}{2} \right\rangle + \left\|\, -\frac{1}{2}\, \frac{1}{2} \right\rangle\right)$	0		
$\left\|\, -\frac{1}{2}\, -\frac{1}{2} \right\rangle$	-1		

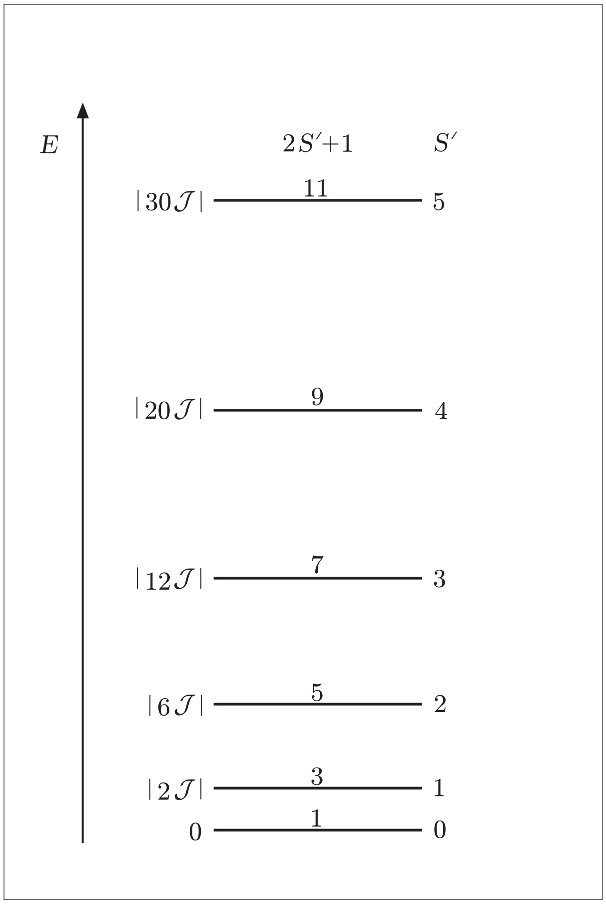

Fig. 18: Relative energies and multiplicities of the spin states of a dinuclear Fe^{3+} complex ($S = \frac{5}{2}$); for Cu^{2+} ($S = \frac{1}{2}$) only the two lowest levels are relevant, while for Gd^{3+} ($S = \frac{7}{2}$) the two levels with $S' = 6$ ($E = |42J_{\text{ex}}|$) and $S' = 7$ ($E = |56J_{\text{ex}}|$) have to be added.

- *Magnetic susceptibility of a spin-spin-coupled system with* $S_1 = S_2 = \frac{1}{2}$

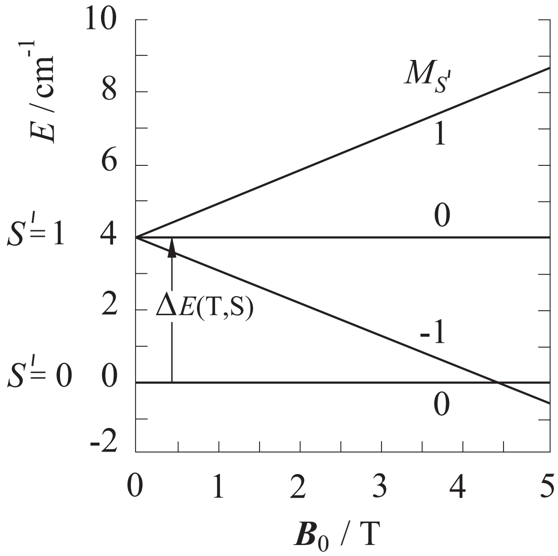

Fig. 19: Correlation diagram of a $S_1 = S_2 = \frac{1}{2}$ system under the influence of isotropic intramolecular spin-spin coupling ($J_{\mathrm{ex}} = -2\,\mathrm{cm}^{-1}$) and applied field

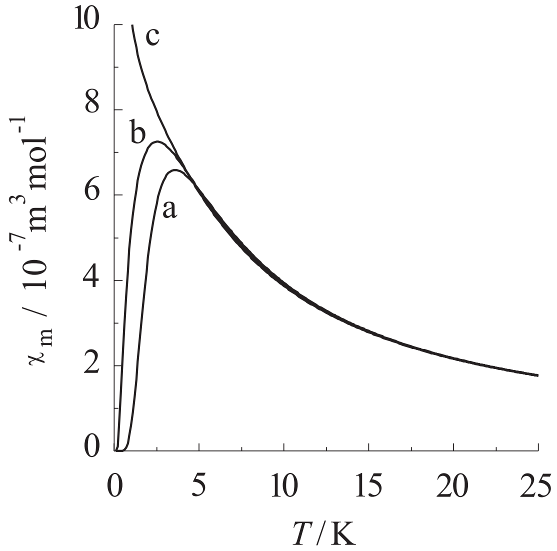

Fig. 20: χ_{m} *versus* T diagram of a $S_1 = S_2 = \frac{1}{2}$ exchange-coupled system with $J_{\mathrm{ex}} = -2\,\mathrm{cm}^{-1}$ at applied fields of $B_0 = 0.01$ T (a), 3.5 T (b), and 5 T (c)

Application of the Van Vleck equation (60) to a dinuclear system with $S_1 = S_2 = \frac{1}{2}$ Zeeman operator:

$$\hat{H}_{M_z} = \underbrace{-\gamma_e\, g(\hat{S}_{z1} + \hat{S}_{z2})}_{\hat{H}^{(1)}} B_z = -\gamma_e\, g\, \hat{S}'_z\, B_z$$

(126)

$S' M_{S'}$	$\lvert 1\,1\rangle$	$\lvert 1\,0\rangle$	$\lvert 1\,-1\rangle$	$\lvert 0\,0\rangle$
$\langle 1\,1\rvert$	$g\mu_B B_z$			
$\langle 1\,0\rvert$		0		
$\langle 1\,-1\rvert$			$-g\mu_B B_z$	
$\langle 0\,0\rvert$				0

Matrix elements:

$$\begin{aligned} \langle 11|\hat{H}_{M_z}|11\rangle &= g\mu_{\mathrm{B}} B_z \longrightarrow W^{(1)}_{|11\rangle} = g\mu_{\mathrm{B}} \\ \langle 1\,{-1}|\hat{H}_{M_z}|1\,{-1}\rangle &= -g\mu_{\mathrm{B}} B_z \longrightarrow W^{(1)}_{|1-1\rangle} = -g\mu_{\mathrm{B}} \end{aligned}$$

The remaining matrix elements (Zeeman coefficients) are zero. $W^{(1)}_{|11\rangle}$, $W^{(1)}_{|1-1\rangle}$, $W^{(0)}_S = E(S)$, and $W^{(0)}_T = E(T)$ are substituted into the Van Vleck equation. After dividing by 2, the Bleaney-Bowers expression (χ_{m} per centre) is obtained, here extended by χ_0.

$$\chi_{\mathrm{m}} = \mu_0 \frac{N_{\mathrm{A}} \mu_{\mathrm{B}}^2 g^2}{3 k_{\mathrm{B}} T} \left[1 + \frac{1}{3} \exp\left(\frac{-2J_{\mathrm{ex}}}{k_{\mathrm{B}} T}\right)\right]^{-1} + \chi_0, \quad \text{only applicable to a (Fig. 20)} \tag{127}$$

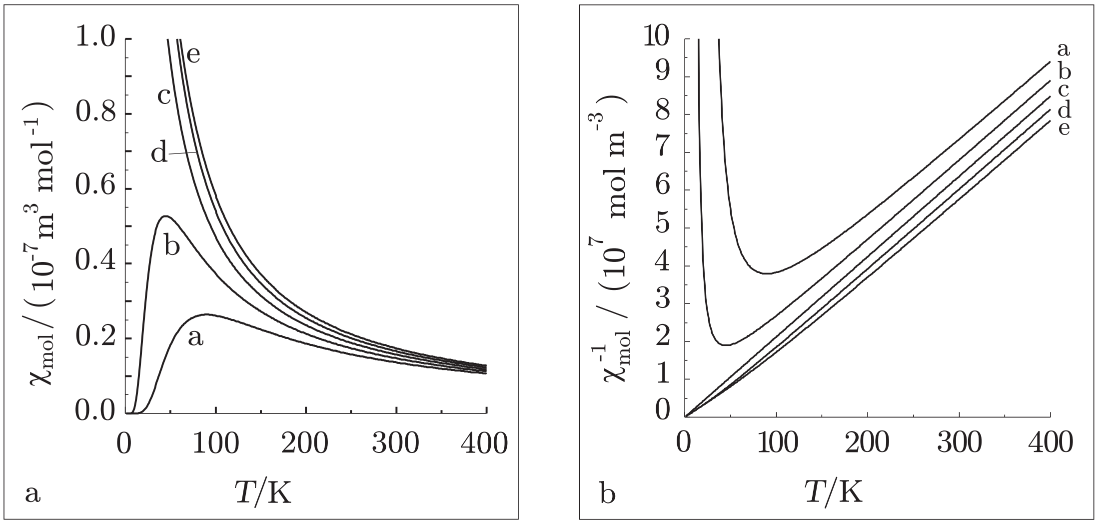

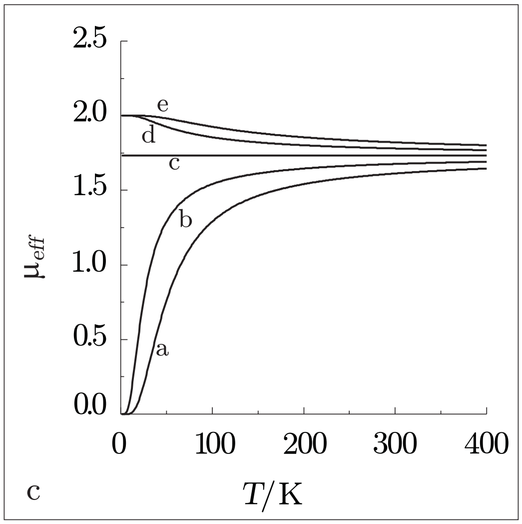

Model calculations concerning the system $S_1 = S_2 = \frac{1}{2}$ with positive and negative J_{ex};

J_{ex} values [cm^{-1}]:
curve a: -50
curve b: -25
curve c: 0
curve d: $+25$
curve e: $+50$

Fig. 21 a: χ_{m}–T diagram
Fig. 21 b: χ_{m}^{-1}–T diagram
Fig. 21 c: μ_{eff}–T diagram

Polynuclear unit of n equivalent centres:

$$\boxed{\chi_{\mathrm{m}} = \frac{\mu_0}{n}\,\frac{N_{\mathrm{A}}\mu_{\mathrm{B}}^2 g^2}{3k_{\mathrm{B}}T}\,\frac{\sum_{S'} S'(S'+1)(2S'+1)\Omega(S')\exp\left(-\frac{E(S')}{k_{\mathrm{B}}T}\right)}{\sum_{S'}(2S'+1)\Omega(S')\exp\left(-\frac{E(S')}{k_{\mathrm{B}}T}\right)}} \qquad (128)$$

Evaluation of S', $E(S')$ and $\Omega(S')$:

S' of the coupled states:
$S' = nS, nS-1, \ldots, 0$ (nS integer) or $\frac{1}{2}$ (nS half integer)

Relative energies $E(S')$:

$$E(S') = -\frac{zJ_{\mathrm{ex}}}{n-1}\left[S'(S'+1) - nS(S+1)\right]$$

z: number of nearest neighbours of a centre
n: number of interacting centres

Frequency $\Omega(S')$ of the states S': $\quad \Omega(S') = \omega(S') - \omega(S'+1)$
$\omega(S')$ is the coefficient of $X^{S'}$ in the expansion $(X^S + X^{S-1} + \ldots + X^{-S})^n$

- **Scope of validity of the Heisenberg model**

1. The magnetic moments are localised (no band magnetism)
2. S of the metal ions is a *good* quantum number
3. the ground term of the metal ion has no first order orbital moment

Examples:

$3d^5$ high spin	$\longrightarrow$	${}^6A_1$	$3d^3(O_h)$, $3d^7(T_d)$	$\longrightarrow$	${}^4A_2$
$3d^8(O_h)$, $3d^2(T_d)$	$\longrightarrow$	${}^3A_2$	$3d^9(O_h)$	$\longrightarrow$	${}^2E$
$4f^7$	$\longrightarrow$	${}^8S_{7/2}$			

4.4 Setup of computational procedures

Application of the computer program CONDON to

- $4f^N$-$4f^N$ (homodinuclear complexes)
- $4f^N$-S where $S = \frac{1}{2}\,[\mathrm{Cu}^{2+}]$, 1, $\frac{3}{2}\,[\mathrm{Cr}^{3+}]$, $\frac{7}{2}\,[\mathrm{Gd}^{3+}]$ (heterodinuclear compl.)

$$\begin{aligned}\hat{H} \;=\; & \underbrace{\sum_{i=1}^{N}\left[-\frac{\hbar^2}{2m_e}\nabla_i^2 + V(r_i)\right]}_{\hat{H}^{(0)}} + \underbrace{\sum_{i>j}^{N}\frac{e^2}{r_{ij}}}_{\hat{H}_{\mathrm{ee}}} + \underbrace{\sum_{i=1}^{N}\xi(r_i)\kappa\hat{\boldsymbol{l}}_i\cdot\hat{\boldsymbol{s}}_i}_{\hat{H}_{\mathrm{SO}}} \\ & + \underbrace{\sum_{i=1}^{N}\sum_{k=0}^{\infty}\left\{B_0^k\,C_0^k(i) + \sum_{q=1}^{k}\left[B_q^k\left(C_{-q}^k(i) + (-1)^q C_q^k(i)\right)\right]\right\}}_{\hat{H}_{\mathrm{LF}}} + \underbrace{\sum_{i=1}^{N}\mu_B(\kappa\hat{\boldsymbol{l}}_i + 2\hat{\boldsymbol{s}}_i)\cdot\boldsymbol{B_0}}_{\hat{H}_{\mathrm{mag}}}\end{aligned}$$

$$\hat{H}_{\mathrm{ex}} = -2J_{\mathrm{ex}}\sum_{k=1}^{N}\sum_{l=1}^{N}\hat{\boldsymbol{s}}_k\cdot\hat{\boldsymbol{s}}_l \qquad\qquad \boldsymbol{B_0} = 0.001\,\mathrm{T}\quad\text{(in general)}$$

With regard to the LF symmetry of the lanthanide our choice is cubic and cylindrical for two reasons: (i) the former is isotropic and the latter anisotropic, (ii) the number of LF parameters is low [15] (*cf.* scheme (129)) [24].

	cubic	**cylindrical**	hexagonal	tetragonal	trigonal
point group	$\mathbf{O_h}$ T_d	$\mathbf{D_{\infty h}}$ $C_{\infty v}$	D_{6h}, D_{3h} D_6, C_{6v}	D_{4h}, D_4 C_{4v}, D_{2d}	D_{3d}, D_3 C_{3v}
no. of B_q^k's	2	3	4	5	6
B_q^k	$\boldsymbol{B_0^4}$ $(+\boldsymbol{B_4^4})$ B_0^6 $(+B_4^6)$	$\boldsymbol{B_0^2}, \boldsymbol{B_0^4}$ B_0^6	B_0^2, B_0^4 B_0^6, B_6^6	B_0^2, B_0^4, B_4^4 B_0^6, B_4^6	B_0^2, B_0^4, B_3^4 B_0^6, B_3^6, B_6^6

(129)

---

[24] For the calculations we use only B_0^4 as LF parameter, except for Ce^{3+}(cyl) where B_0^2 is considered.

Cubic ($\mathrm{O_h}$, $\mathrm{T_d}$)

$$\hat{H}_{\mathrm{LF}}^{\mathrm{cub}} = \sum_{i=1}^{N} B_0^4 \left\{ C_0^4(i) + \sqrt{5/14} \left[C_{-4}^4(i) + C_4^4(i) \right] \right\} + B_0^6 \left\{ C_0^6(i) - \sqrt{7/2} \left[C_{-4}^6(i) + C_4^6(i) \right] \right\}$$

fixed relations: $B_4^4 = \sqrt{5/14}\, B_0^4$, $B_4^6 = -\sqrt{7/2} B_0^6$

Cylindrical ($\mathrm{D_{\infty h}}$)

$$\hat{H}_{\mathrm{LF}}^{\mathrm{cyl}} = \sum_{i=1}^{\mathrm{N}} B_0^2 C_0^2(i) + B_0^4 C_0^4(i) + B_0^6 C_0^6(i)$$

Symmetry options

symmetry	cub	cyl
B_q^k	B_0^4 ($+B_4^4$)	B_0^2 (Ce^{3+}) or B_0^4
coordination polyhedron		
$B_0^k > 0$	octahedron	linear
$B_0^k < 0$	cube, tetrahedron	square antiprism

B_q^k and J_{ex} data (cm^{-1})

Ln	B_q^k	J_{ex} [a]
Ce (cub)	±1 100	±5
Ce (cyl)	±600	
Nd,Sm,Tb,Dy (cub, cyl)	±2 000	±1

4.5 Homodinuclear lanthanide complexes

4.5.1 Gd^{3+}–Gd^{3+}

Application of eq. (128) with $S' = |S_1 - S_2|, |S_1 - S_2 + 1|, \ldots S_1 + S_2$; $S_1, S_2 = \frac{7}{2}$, $n = 2$:

$$\chi_{\mathrm{m}} = \frac{\mu_0 N_{\mathrm{A}} \mu_{\mathrm{B}}^2 g^2}{k_{\mathrm{B}} T} \frac{e^{2x} + 5e^{6x} + 14e^{12x} + 30e^{20x} + 55e^{30x} + 91e^{42x} + 140e^{56x}}{1 + 3e^{2x} + 5e^{6x} + 7e^{12x} + 9e^{20x} + 11e^{30x} + 13e^{42x} + 15e^{56x}}$$
$$\text{where} \quad x = J_{\mathrm{ex}}/(k_{\mathrm{B}} T) \qquad (130)$$

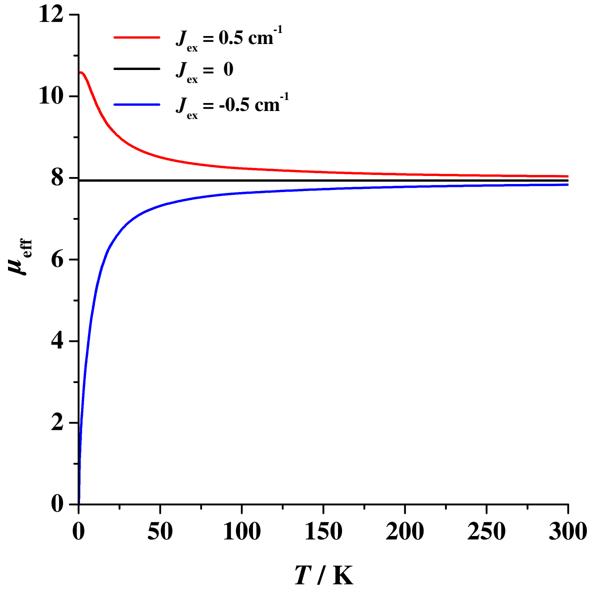

Fig. 22: Homodinuclear complex of Gd^{3+}: μ_{eff} *vs.* T plot, $J_{\mathrm{ex}} = 0, \pm 0.5$ cm^{-1} ($B_0 = 0.001$ T).

---

[a] Occasionally, the selected $|J_{\mathrm{ex}}|$ values are larger than realistic values in order to inspect more distinctly the H_{ex} effect (*cf.* Tab. 1).

4.5.2 Group theoretical tools II

We saw in 3.3.1 that on the basis of group theory it is possible to assign the LF split terms of Ln ions. Symmetry aspects are also useful to assign the splitting produced by the combined effect of $\hat{H}_{\mathrm{LF}}^{\mathrm{cub}}$ (eq. (86)) + $\hat{H}_{\mathrm{ex}}^{\mathrm{iso}}$ (eq. (120)) on the product functions of the two interacting metal ions. The following examination is restricted to the simple case of homodinuclear Ln systems equipped with orbital contributions of the magnetic moments.

The product states split under the action of $\hat{H}_{\mathrm{ex}}^{\mathrm{iso}}$ in singlets, doublets and triplets. The split pattern is obtained in two steps:

- application of $\boxed{\chi_{\mathrm{ab}}(R) = \chi_{\mathrm{a}}(R)\chi_{\mathrm{b}}(R)}$, where χ_i is the character and R is a symmetry operation, given in the headlines of Table 28.

Tab. 28: Character table of the symmetry groups O and $\mathrm{T_d}$

O $\mathrm{T_d}$	E E	8 $\mathrm{C_3}$ 8 $\mathrm{C_3}$	3 $\mathrm{C_2}$ 3 $\mathrm{C_2}$	6 $\mathrm{C_4}$ 6 $\mathrm{S_4}$	6 $\mathrm{C_2'}$ 6 σ_d	irred. reps. of the coupled states
$\Gamma_1(\mathrm{A_1})^{a)}$	1	1	1	1	1	
$\Gamma_2(\mathrm{A_2})$	1	1	1	−1	−1	
$\Gamma_3(\mathrm{E})$	2	−1	2	0	0	
$\Gamma_4(\mathrm{T_1})$	3	0	−1	1	−1	
$\Gamma_5(\mathrm{T_2})$	3	0	−1	−1	1	
$\Gamma_1 \otimes \Gamma_1{}^{b)}$	1	1	1	1	1	$\rightarrow \Gamma_1$
$\Gamma_2 \otimes \Gamma_2$	1	1	1	1	1	$\rightarrow \Gamma_1$
$\Gamma_3 \otimes \Gamma_3$	4	1	4	0	0	$\rightarrow \Gamma_1 \oplus \Gamma_2 \oplus \Gamma_3$
$\Gamma_4 \otimes \Gamma_4$	9	0	1	1	1	$\rightarrow \Gamma_1 \oplus \Gamma_3 \oplus \Gamma_4 \oplus \Gamma_5$
$\Gamma_5 \otimes \Gamma_5$	9	0	1	1	1	$\rightarrow \Gamma_1 \oplus \Gamma_3 \oplus \Gamma_4 \oplus \Gamma_5$
$\Gamma_1 \otimes \Gamma_2$	1	1	1	−1	−1	$\rightarrow \Gamma_2$

---

a) Bethe (Mulliken) nomenclature.

b) Selection of direct products for dinuclear systems with integer J.

$\chi_{\mathrm{a}}(R)$ and $\chi_{\mathrm{b}}(R)$ are the characters of the irreducible representations Γ_{a} and Γ_{b}, while $\chi_{\mathrm{ab}}(R)$ is the character of the (in general reducible) product state.
Example: The character system of the product functions Γ_3^{ab} resulting from the single-ion states Γ_3^{a} and Γ_3^{b}, $\Gamma_3 \otimes \Gamma_3$, is given in line 8 of Table 28.

- application of $\boxed{a_{\Gamma_i} = \frac{1}{h}\sum_R \chi_{\Gamma_i}^*(R)\,\chi_\Gamma(R)}$ to determine the irreducible parts of Γ_3^{ab};
a_{Γ_i}: frequency of Γ_i in Γ; h: order of the group;
$\chi_{\Gamma_i}(R)$: character of the ith irreducible representation Γ_i for the group element R;
$\chi_\Gamma(R)$: character of Γ of the group element R; $\sum_R$: sum over all group elements.

$$\begin{aligned}
a_{\Gamma_1} &= \tfrac{1}{24}(1\cdot 1\cdot 4 + 8\cdot 1\cdot 1 + 3\cdot 1\cdot 4 + 6\cdot 1\cdot 0 + 6\cdot 1\cdot 0) = 1\\
a_{\Gamma_2} &= \tfrac{1}{24}(1\cdot 1\cdot 4 + 8\cdot 1\cdot 1 + 3\cdot 1\cdot 4 - 6\cdot 1\cdot 0 - 6\cdot 1\cdot 0) = 1\\
a_{\Gamma_3} &= \tfrac{1}{24}(1\cdot 2\cdot 4 + 8\cdot(-1)\cdot 1 + 3\cdot 2\cdot 4 + 6\cdot 0\cdot 0 + 6\cdot 0\cdot 0) = 1\\
a_{\Gamma_4} &= a_{\Gamma_5} = 0; \quad \Longrightarrow \quad \Gamma_3\otimes\Gamma_3 \rightarrow \Gamma_1 \oplus \Gamma_2 \oplus \Gamma_3
\end{aligned}$$

Result: $\Gamma_3 \otimes \Gamma_3$ is reducible to two singlets (Γ_1, Γ_2) and a doublet (Γ_3). The energies of the states depend on sign and size of J_{ex}.

For metal ions with half-integer J three types of cubic states exists: the doublets $\Gamma_6(E')$, $\Gamma_7(E'')$, and the quartet $\Gamma_8(G')$ (*cf.* Tab. 29).

Tab. 29: Character table of the double groups O' and T'_d

O' T'_d	E E	R R	$4C_3$ $4C_3^2R$ $4C_3$ $4C_3^2R$	$4C_3^2$ $4C_3R$ $4C_3^2$ $4C_3R$	$3C_2$ $3C_2R$ $3C_2$ $3C_2R$	$3C_4$ $3C_4^3R$ $3S_4$ $3S_4^3R$	$3C_4^3$ $3C_4R$ $3S_4^3$ $3S_4R$	$6C'_2$ $6C'_2R$ $6\sigma_d$ $6\sigma_dR$	irreducible representations of the coupled states
$\Gamma_1(A_1)$[a]	1	1	1	1	1	1	1	1	
$\Gamma_2(A_2)$	1	1	1	1	1	-1	-1	-1	
$\Gamma_3(E)$	2	2	-1	-1	2	0	0	0	
$\Gamma_4(T_1)$	3	3	0	0	-1	1	1	-1	
$\Gamma_5(T_2)$	3	3	0	0	-1	-1	-1	1	
$\Gamma_6(E')$[b]	2	-2	1	-1	0	$\sqrt{2}$	$-\sqrt{2}$	0	
$\Gamma_7(E'')$	2	-2	1	-1	0	$-\sqrt{2}$	$\sqrt{2}$	0	
$\Gamma_8(G')$	4	-4	-1	1	0	0	0	0	
$\Gamma_6 \otimes \Gamma_6$[c]	4	4	1	1	0	2	2	0	$\rightarrow \Gamma_1 \oplus \Gamma_4$
$\Gamma_7 \otimes \Gamma_7$	4	4	1	1	0	2	2	0	$\rightarrow \Gamma_1 \oplus \Gamma_4$
$\Gamma_8 \otimes \Gamma_8$	16	16	1	1	0	0	0	0	$\rightarrow \Gamma_1 \oplus \Gamma_2 \oplus \Gamma_3 \oplus 2\Gamma_4 \oplus 2\Gamma_5$
$\Gamma_6 \otimes \Gamma_7$	4	4	1	1	0	-2	-2	0	$\rightarrow \Gamma_2 \oplus \Gamma_5$
$\Gamma_6 \otimes \Gamma_8$	8	8	-1	-1	0	0	0	0	$\rightarrow \Gamma_3 \oplus \Gamma_4 \oplus \Gamma_5$
$\Gamma_7 \otimes \Gamma_8$	8	8	-1	-1	0	0	0	0	$\rightarrow \Gamma_3 \oplus \Gamma_4 \oplus \Gamma_5$
$\Gamma_4 \otimes \Gamma_6$[d]	6	-6	0	0	0	$\sqrt{2}$	$-\sqrt{2}$	0	$\rightarrow \Gamma_6 \oplus \Gamma_8$
$\Gamma_5 \otimes \Gamma_6$	6	-6	0	0	0	$-\sqrt{2}$	$\sqrt{2}$	0	$\rightarrow \Gamma_7 \oplus \Gamma_8$
$\Gamma_2 \otimes \Gamma_6$	2	-2	1	-1	0	$-\sqrt{2}$	$\sqrt{2}$	0	$\rightarrow \Gamma_7$
$\Gamma_3 \otimes \Gamma_6$	4	-4	-1	1	0	0	0	0	$\rightarrow \Gamma_8$
$\Gamma_4 \otimes \Gamma_7$	6	-6	0	0	0	$-\sqrt{2}$	$\sqrt{2}$	0	$\rightarrow \Gamma_7 \oplus \Gamma_8$
$\Gamma_5 \otimes \Gamma_7$	6	-6	0	0	0	$\sqrt{2}$	$-\sqrt{2}$	0	$\rightarrow \Gamma_6 \oplus \Gamma_8$
$\Gamma_2 \otimes \Gamma_7$	2	-2	1	-1	0	$\sqrt{2}$	$-\sqrt{2}$	0	$\rightarrow \Gamma_6$
$\Gamma_3 \otimes \Gamma_7$	4	-4	-1	1	0	0	0	0	$\rightarrow \Gamma_8$
$\Gamma_2 \otimes \Gamma_8$	4	-4	-1	1	0	0	0	0	$\rightarrow \Gamma_8$
$\Gamma_3 \otimes \Gamma_8$	8	-8	1	-1	0	0	0	0	$\rightarrow \Gamma_6 \oplus \Gamma_7 \oplus \Gamma_8$
$\Gamma_4 \otimes \Gamma_8$	12	-12	0	0	0	0	0	0	$\rightarrow \Gamma_6 \oplus \Gamma_7 \oplus 2\,\Gamma_8$
$\Gamma_5 \otimes \Gamma_8$	12	-12	0	0	0	0	0	0	$\rightarrow \Gamma_6 \oplus \Gamma_7 \oplus 2\,\Gamma_8$

---

[a] $\Gamma_1 - \Gamma_5$: integer J; $\Gamma_1 - \Gamma_3$: non-magnetic.

[b] $\Gamma_6 - \Gamma_8$: half-integer J; magnetic.

[c] Direct products where both metal ions have half-integer J or S.

[d] Direct products where one metal has integer J and the other has half-integer J or S.

4.5.3 Ce^{3+}–Ce^{3+} (cub)

Fig. 23 exhibits the $4\mathrm{f}^1$ ion's cubic LF splitting of ground and excited multiplet $^2F_{5/2}$ and $^2F_{7/2}$, respectively ($^2F_{5/2} \rightarrow \Gamma_7 + \Gamma_8$; $^2F_{7/2} \rightarrow \Gamma_7 + \Gamma_8 + \Gamma_6$). The LF ground state in octahedral coordination is the doublet Γ_7 and in tetrahedral/cubical coordination the quartet Γ_8.

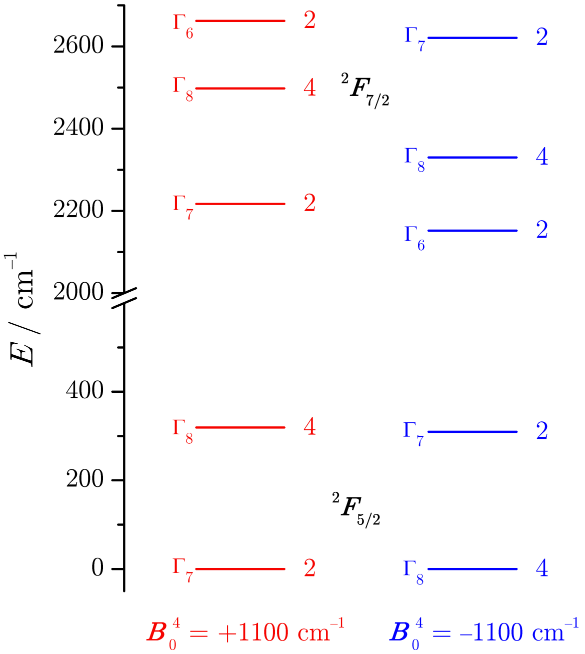

Fig. 23: $\mathrm{Ce}^{3+}[4\mathrm{f}^1]$: Cubic LF splitting of the multiplets $^2F_{5/2}$ and $^2F_{7/2}$; left: octahedral LF; right: tetrahedral/cubical LF.

Switching on $H_{\mathrm{ex}}^{\mathrm{iso}}$ with $J_{\mathrm{ex}} = \pm 5\,\mathrm{cm}^{-1}$ between the two Ce^{3+} ions — each in *octahedral* LF — the four product states $\Gamma_7 \otimes \Gamma_7$ split into $\Gamma_1 \oplus \Gamma_4$ (see Fig. 24) with ground state Γ_1 for $J_{\mathrm{ex}} < 0$ and Γ_4 for $J_{\mathrm{ex}} > 0$. The splitting of the excited 16 product functions $\Gamma_8 \otimes \Gamma_8$ by $H_{\mathrm{ex}}^{\mathrm{iso}}$ is more complicated (see caption of Fig. 24). Figs. 25 and 26 display the variations μ_{eff} *vs.* T for octahedral and tetrahedral/cubical LF and positive and negative J_{ex}. Note that μ_{eff} for the Γ_8 LF ground state is distinctly larger than for the doublet Γ_7 (maximum at 2.2 and 1.3, respectively, at $T = 1\,\mathrm{K}$).

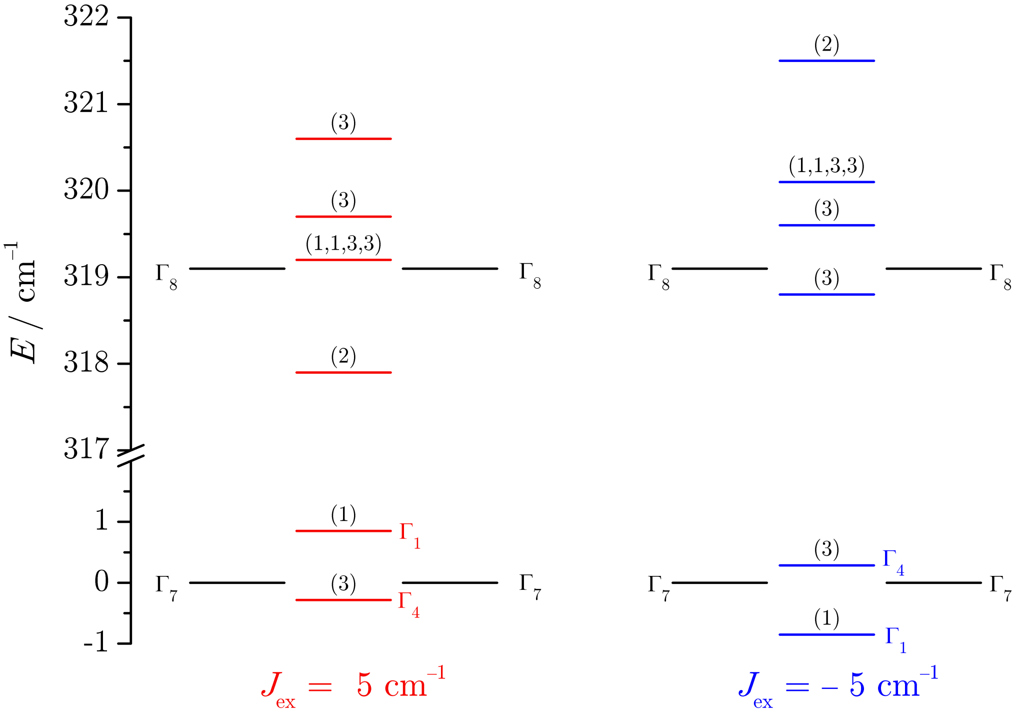

Fig. 24: Splitting of the states of an exchange-coupled Ce–Ce unit in an octahedral LF ($B_0^4 = 1100\,\mathrm{cm}^{-1}$); $\Gamma_7 \otimes \Gamma_7 \rightarrow \Gamma_1 \oplus \Gamma_4$: $J_{\mathrm{ex}} > 0$, triplet ground state (Γ_4); $J_{\mathrm{ex}} < 0$, singlet ground state (Γ_1); $\Gamma_8 \otimes \Gamma_8 \rightarrow \Gamma_1 \oplus \Gamma_2 \oplus \Gamma_3 \oplus 2\,\Gamma_4 \oplus 2\,\Gamma_5$.

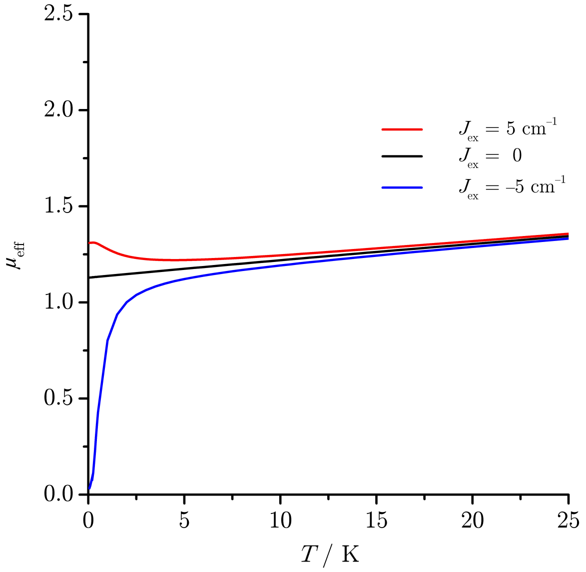

Fig. 25: μ_{eff} *vs.* T plot of an exchange-coupled Ce-Ce unit in an oct. LF ($B_0^4 = 1\,100\,\text{cm}^{-1}$); $J_{\text{ex}} > 0$, triplet ground state (Γ_4); $J_{\text{ex}} < 0$, singlet ground state (Γ_1).

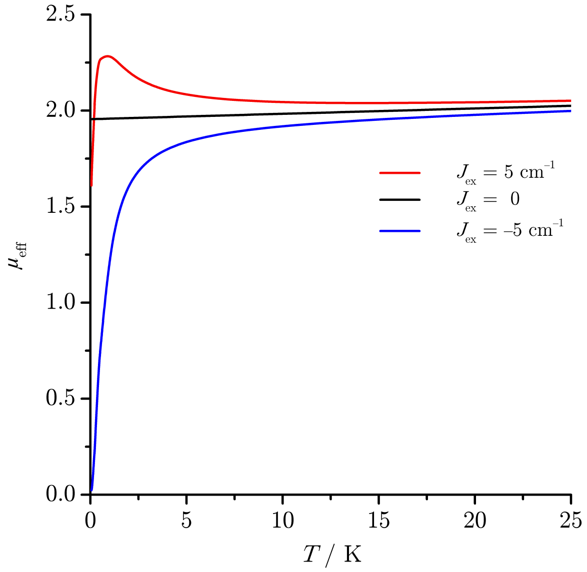

Fig. 26: μ_{eff} *vs.* T plot of an exchange-coupled Ce-Ce unit in a cubical/tet. LF ($B_0^4 = -1\,100$ cm^{-1}); $J_{\text{ex}} > 0$, triplet ground state; $J_{\text{ex}} < 0$, singlet ground state.

Remark to Fig. 26: The product states $\Gamma_8 \otimes \Gamma_8$ are split by H_{ex} into Γ_1(singlet (1)) $\oplus$ Γ_2(singlet (1)) $\oplus$ Γ_3(doublet (2)) $\oplus$ $2\,\Gamma_4$(triplets (3)) $\oplus$ $2\,\Gamma_5$(triplets (3)). For $J_{\text{ex}} > 0$, the sequence of split terms is given with increasing energy by (3) – (3) – (3) – (1) – (3) – (2) – (1); for $J_{\text{ex}} < 0$, this order is reversed. (Remember that only the triplets are magnetic.)

Ce^{3+}–Ce^{3+}(cyl)

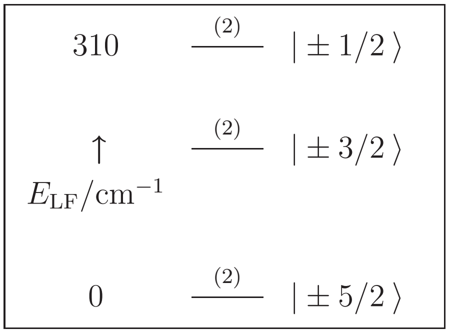

Scheme: Cylindrical LF splitting of the multiplet $^2F_{5/2}$ ($B_0^2 = 600\,\text{cm}^{-1}$; ground state: $|\frac{5}{2}\ \pm\frac{5}{2}\rangle$). Figure 27 exhibits that for $J_{\text{ex}} > 0$ and $T \to 0$ $\mu_{\text{eff}}^{\parallel} = 5.2$ while $\mu_{\text{eff}}^{\perp} \to 0$ (not shown in the figure), that is, strong magnetic anisotropy is observed; —— $\overline{\mu}_{\text{eff}}$ and —— $\overline{\mu}_{\text{eff}}$ represent the temperature dependence of the average μ_{eff} values for positive and negative J_{ex}, respectively.

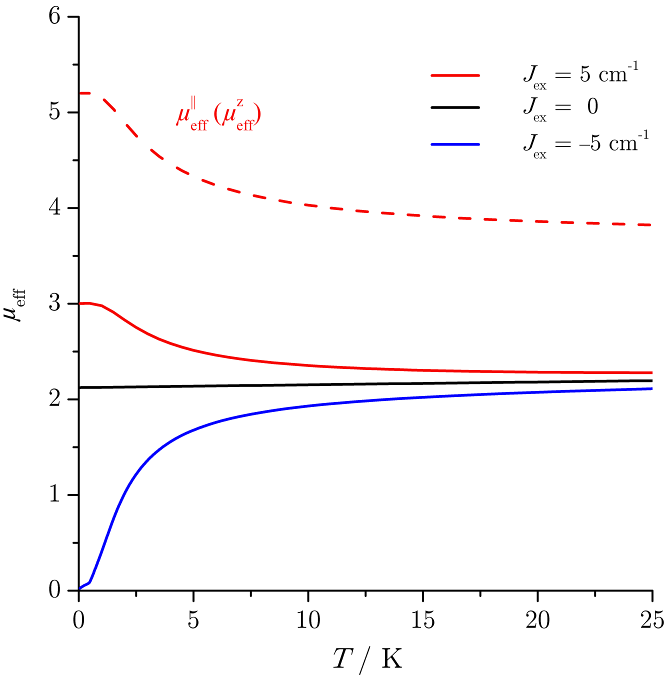

Fig. 27: μ_{eff} *vs.* T plot of an exchange-coupled Ce–Ce unit in a cylindrical LF ($B_0^2 = 600\,\text{cm}^{-1}$).

4.5.4 Nd^{3+}–Nd^{3+} (cub)

For $B_0^4 > 0$ (oct. LF; $W < 0$, $x > 0$; *cf.* Ex. 3.11) the LF ground state is Γ_6 while for $B_0^4 < 0$ (cub/tet) $\Gamma_8^{(2)}$ is lowest in energy (see Fig. 28).

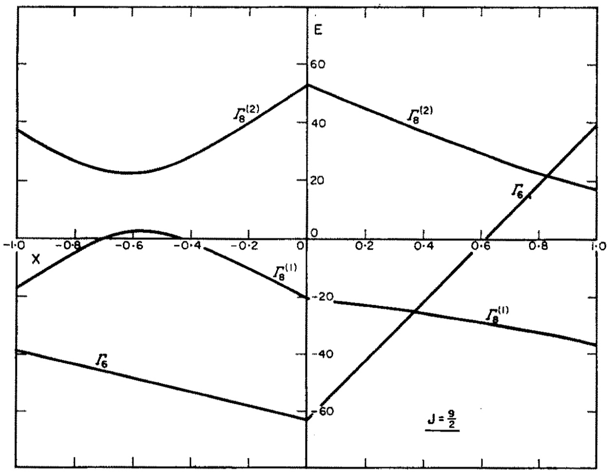

FIG. 8

⇓ $B_0^4 < 0$ $B_0^4 > 0$ ⇓

Fig. 28: Splitting of the Nd ground multiplet by cubic LF's ($^4I_{9/2} \rightarrow \Gamma_6 \oplus \Gamma_8^{(1)} \oplus \Gamma_8^{(2)}$) [16].

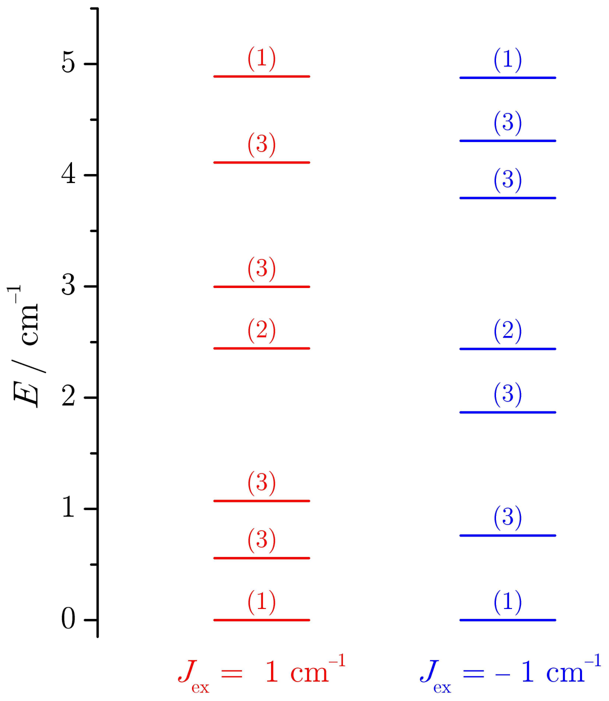

Fig. 29: Splitting of the $\Gamma_8 \otimes \Gamma_8$ product states of Nd–Nd by H_{ex} ($\rightarrow \Gamma_1 \oplus \Gamma_2 \oplus \Gamma_3 \oplus 2\,\Gamma_4 \oplus 2\,\Gamma_5$).

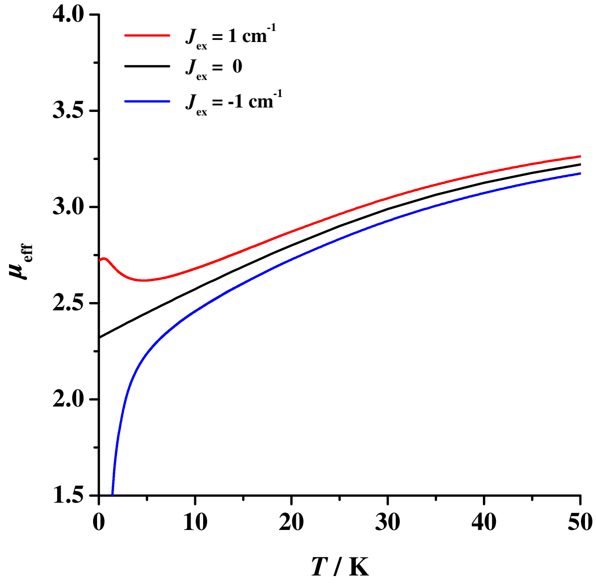

Fig. 30: μ_{eff} *vs.* T plot of an exchange-coupled Nd–Nd unit in an octahedral LF (LF ground state Γ_6). For $J_{\text{ex}} > 0$, the ground state is magnetic (triplet Γ_4), while for $J_{\text{ex}} < 0$, the ground state is nonmagnetic (singlet Γ_1), that is, $\mu_{\text{eff}} \rightarrow 0$ at $T \rightarrow 0$.

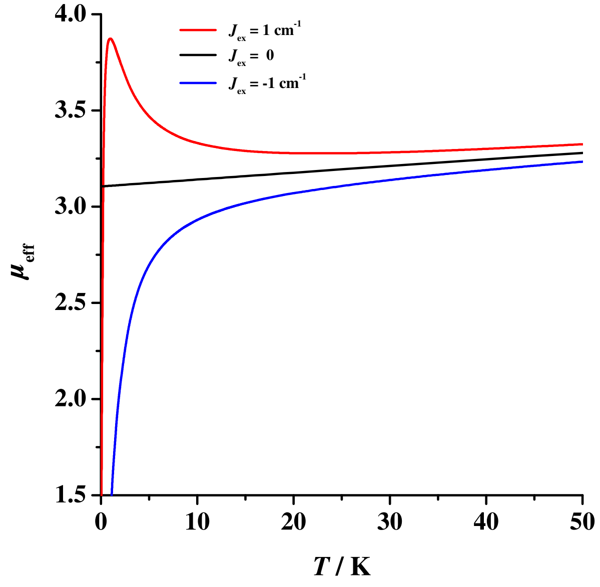

Fig. 31: μ_{eff} *vs.* T plot of an exchange-coupled Nd–Nd unit in a cubical/tetrahedral LF (LF ground state Γ_8). For both situations, $J_{\text{ex}} < 0$ and $J_{\text{ex}} > 0$, the ground state is a singlet, that is, $\mu_{\text{eff}} \rightarrow 0$ as well as $\mu_{\text{eff}} \rightarrow 0$ at $T \rightarrow 0$ (*cf.* Fig. 29).

Results: Fig. 30: Only a little increase of μ_{eff} is observed after switching on H_{ex};
Fig. 31: For the ferromagnetically coupled Nd-Nd the peak of μ_{eff} at 1 K is remarkable.

4.5.5 Sm^{3+}–Sm^{3+} (cub)

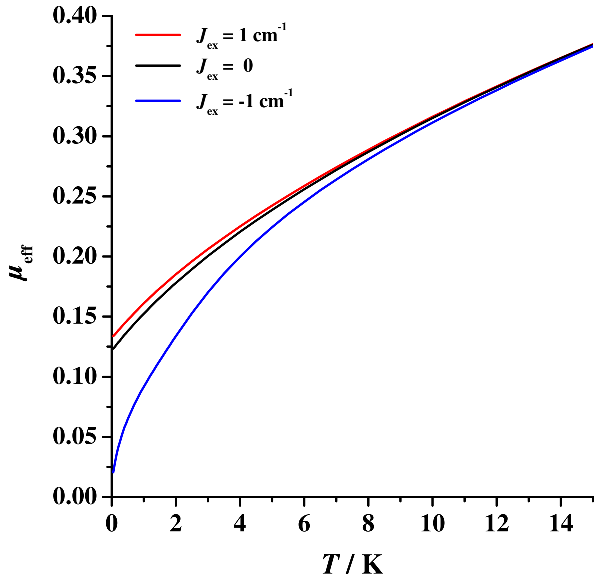

$$\boxed{\Gamma_7 \otimes \Gamma_7 \quad \longrightarrow \quad \Gamma_1 \oplus \Gamma_4}$$

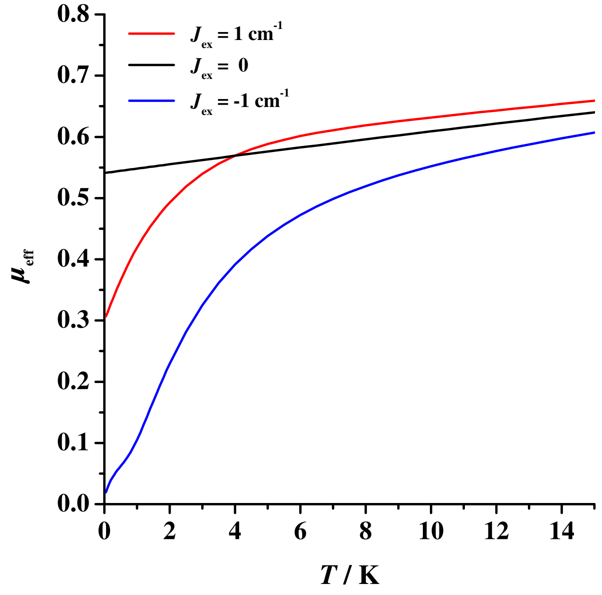

$$\boxed{\Gamma_8 \otimes \Gamma_8 \quad \longrightarrow \quad \Gamma_1 \oplus \Gamma_2 \oplus \Gamma_3 \oplus 2\Gamma_4 \oplus 2\Gamma_5}$$

Fig. 32: $\mu_{\rm eff}$ *vs.* T plot of an exchange-coupled Sm–Sm unit in oct. LF (LF ground state Γ_7). For $J_{\rm ex} > 0$ the $\mu_{\rm eff}$ values are only little enhanced; $\mu_{\rm eff} \to 0$ for $J_{\rm ex} < 0$.

Fig. 33: $\mu_{\rm eff}$ *vs.* T plot of an exchange-coupled Sm–Sm unit in cub/tet. LF (LF ground state Γ_8). Although $J_{\rm ex} > 0$ the $\mu_{\rm eff}$ values fall below the curve of the uncoupled system. (Obviously the magnetic contribution of the uncoupled Sm^{3+} ion with LF ground state Γ_8 is larger than the contribution of the $H_{\rm ex}$ triplet ground state of the Sm-Sm pair.)

4.5.6 Tb^{3+}–Tb^{3+} (cub)

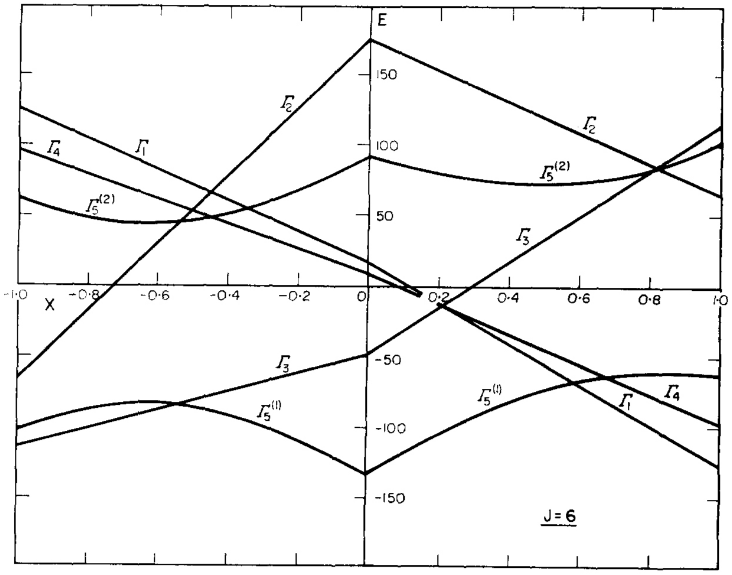

FIG. 5

⇓ $B_0^4 > 0$ TIP at $T \leq 10$ K $B_0^4 < 0$ ⇓

Fig. 34: Splitting of the Tb ground multiplet by a cubic LF ($^7F_6 \longrightarrow \Gamma_1 \oplus \Gamma_2 \oplus \Gamma_3 \oplus \Gamma_4 \oplus \Gamma_5^{(1)} \oplus \Gamma_5^{(2)}$) [16].

Taking into consideration that in the case of $Tb^{3+}[4f^8]$ the parameter W is negative for both octahedral and cubical/tetrahedral coordination polyhedra (see Table 23) [a], the inspection of Fig. 34 shows that apart from the point of intersection of Γ_2, Γ_3 and $\Gamma_5^{(2)}$ at $E \approx 85$, $x = 0.8$, exlusively non-magnetic LF states are ground states. In consequence, the Tb^{3+} ion in cubic LF is not a good candidate for the investigation of spin-spin couplings between each other.

---

[a] Both Examples 3.10 and 3.11 show how to read the x–$E_{\rm LF}/W$ diagrams.

4.5.7 Dy^{3+}–Dy^{3+} (cub)

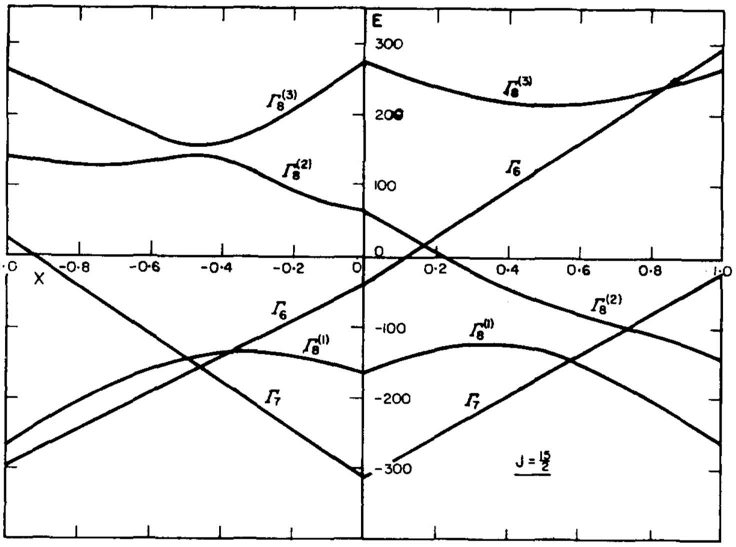

FIG. 2

$\Uparrow$ $B_0^4 > 0$ $B_0^4 < 0$ $\Uparrow$

Fig. 35: Splitting of the Dy^{3+} ground multiplet by a cubic LF ($^6H_{15/2} \longrightarrow \Gamma_6 \oplus \Gamma_7 \oplus \Gamma_8^{(1)} \oplus \Gamma_8^{(2)} \oplus \Gamma_8^{(3)}$) [16]. The sequence of LF states for octahedral coordination is given at $x = -1$ ($B_0^4 = 2000\,\text{cm}^{-1}$, LF ground state Γ_6) and for cubical/tetrahedral coordination at $x = 1$ ($B_0^4 = -2000\,\text{cm}^{-1}$, LF ground state $\Gamma_8^{(1)}$).

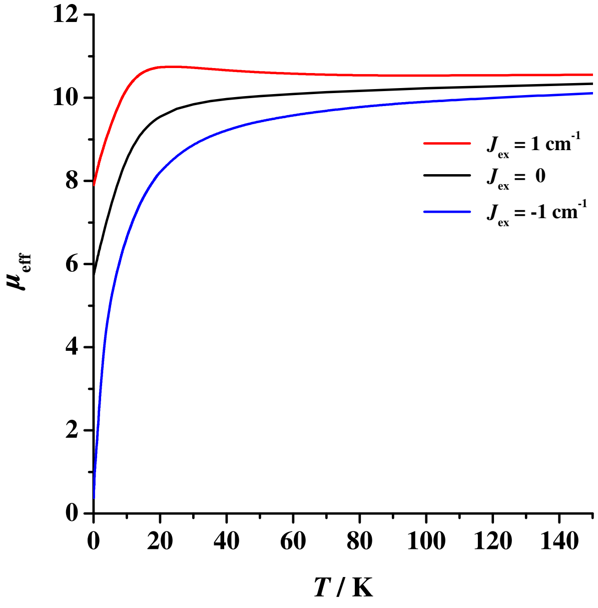

Fig. 36: μ_{eff} *versus* T plot of an exchange-coupled Dy–Dy unit in an octahedral LF ($B_0^4 = 2\,000\,\text{cm}^{-1}$; LF ground state Γ_6).

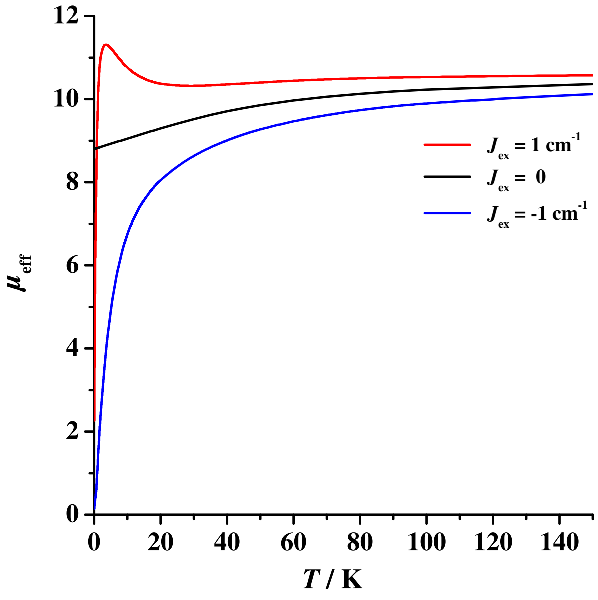

Fig. 37: Exchange-coupled dinuclear Dy unit in a cubical/tetrahedral LF ($B_0^4 = -2\,000\,\text{cm}^{-1}$; LF ground state $\Gamma_8^{(1)}$).

Results: For LF ground state Γ_6 (Fig. 36) $J_{\text{ex}} > 0$ enhances μ_{eff} in the whole temperature range while for $J_{\text{ex}} < 0$ μ_{eff} diminishes. For LF ground state Γ_8 (Fig. 37) it is remarkable that for $J_{\text{ex}} > 0$ μ_{eff} drops steeply from 11.3 to 2.2 far below $\mu_{\text{eff}} = 8.9$ of the uncoupled Dy-Dy pair, caused by a very weak magnet contribution of the ground triplet.

4.5.8 Dy^{3+}–Dy^{3+} (cyl)

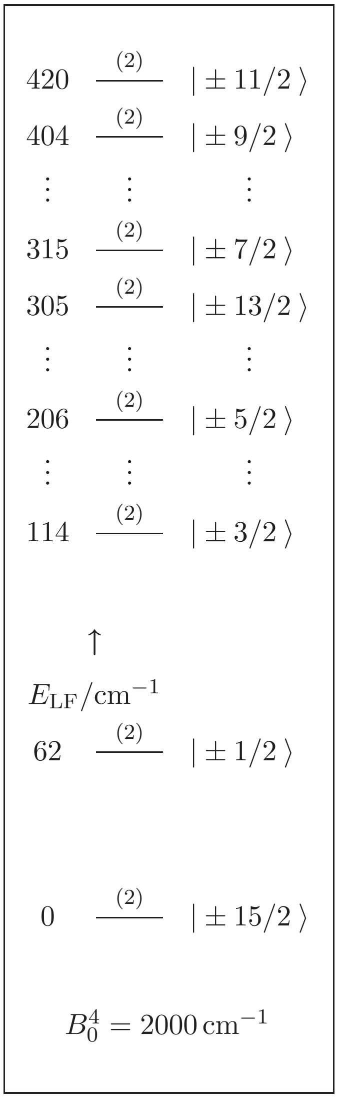

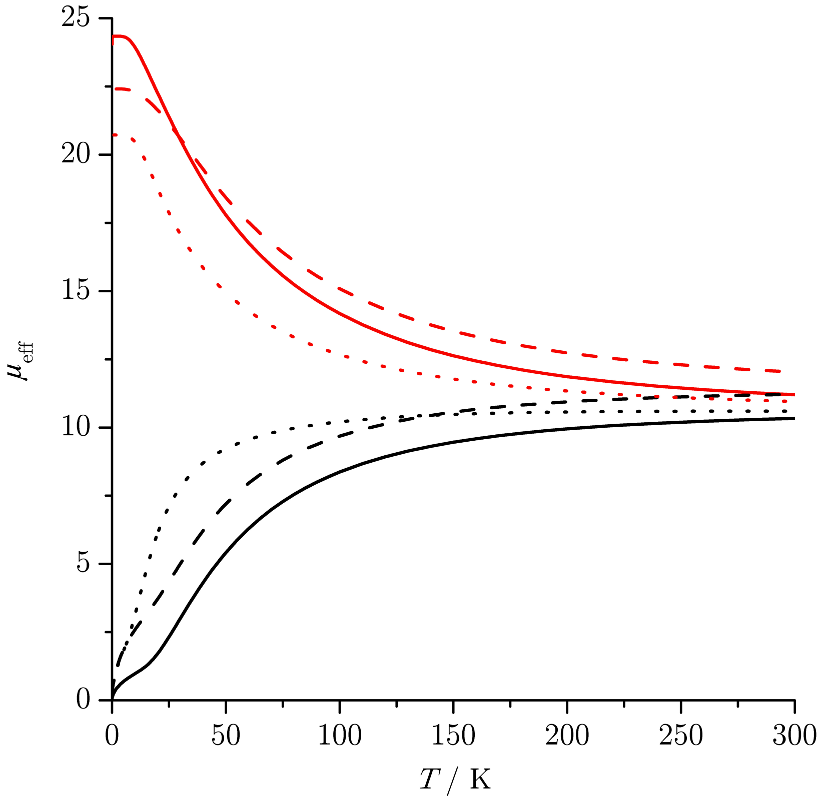

Fig. 38: Exchange-coupled dinuclear Dy unit in cylindrical LF ($B_0^4 = 2\,000\,\mathrm{cm}^{-1}$; LF ground state $|J \pm M_J\rangle$: $|15/2\ \pm 15/2\rangle$).

	$J_{\mathrm{ex}}/\mathrm{cm}^{-1}$	$\mu_{\mathrm{eff}}^{\parallel}$	$\mu_{\mathrm{eff}}^{\perp}$	
Dy–Dy(cyl)	+1	━━	━━	
Dy(cyl)–Cr	+5	━ ━	━ ━	see 4.6.5
Tb(cyl)–Cr	+5	······	······	see 4.6.5

4.5.9 Ln–Ln pair: Temporary résumé of μ_{eff} for $J_{\mathrm{ex}} > 0$ (rating +/–)

Ln^{3+}	**μ_{eff}** [a]				
	Ce^{3+}	**Nd^{3+}**	**Sm^{3+}**	**Tb^{3+}**	**Dy^{3+}**
free ion	2.54	3.62	0.84	9.72	10.64
cub	– 2.3	+/– 3.8	– – 0.48	– – TIP	+ 11.2
cyl	**++** **5.2**	[b]	[b]	+ 12.7	**++** **24.0**

1. Cubic Ln systems are no good candidates for large μ_{eff};
2. Particularly Sm and Tb are unsuitable in cubic LF;
3. Dy in cylindrical LF is an excellent candidate.

---

[a] At $T = 2\,\mathrm{K}$. [b] Examination is still pending.

4.6 Heterodinuclear transition metal–lanthanide systems

4.6.1 p($^2P_{1/2}$)–s($^2S_{1/2}$) molecule

As an introduction, the spin-spin-coupling H_{ex} within a p^1–s^1 unit is considered, where the six states of p^1 are split by H_{SO} into the quartet $^2P_{3/2}$ and the doublet $^2P_{1/2}$. We assume $H_{\text{SO}} \gg H_{\text{ex}}$ and restrict the calculations to $^2P_{1/2}$–$^2S_{1/2}$. The corresponding basis functions $|JM_J\rangle = |\frac{1}{2} \pm\frac{1}{2}\rangle$ of the multiplet $^2P_{1/2}$ are given in Table 30[25].

Table 30: $^2P_{1/2}$ functions $|JM_J\rangle = |\frac{1}{2} \pm\frac{1}{2}\rangle$ of the spin-orbit coupled p^1 system

ψ	$\lvert M_L\, M_S\rangle$	$\lvert J\, M_J\rangle$	$M_J = M_L + M_S$	J	
ψ_3	$-\sqrt{\frac{2}{3}}\,\lvert 1\ -\frac{1}{2}\rangle + \sqrt{\frac{1}{3}}\,\lvert 0\ \frac{1}{2}\rangle$	$\lvert \frac{1}{2}\ \frac{1}{2}\rangle$	$\frac{1}{2}$	$\frac{1}{2}$	$^2P_{1/2}$
ψ_5	$\sqrt{\frac{2}{3}}\,\lvert -1\ \frac{1}{2}\rangle - \sqrt{\frac{1}{3}}\,\lvert 0\ -\frac{1}{2}\rangle$	$\lvert \frac{1}{2}\ -\frac{1}{2}\rangle$	$-\frac{1}{2}$		

Since the calculations are restricted to the ground multiplet $J = 1/2$, $\hat{H}_{\text{ex}}$ can be applied in the form

$$\begin{aligned} \hat{H}_{\text{ex}} &= -2J_{\text{ex}}\underbrace{(g_J-1)}_{\text{De Gennes}}\hat{\boldsymbol{J}}\cdot\hat{\boldsymbol{S}} = -2(g_J-1)J_{\text{ex}}\left(\hat{J}_z\hat{S}_z + \hat{J}_x\hat{S}_x + \hat{J}_y\hat{S}_y\right) \\ &= -2(g_J-1)J_{\text{ex}}\left[\hat{J}_z\hat{S}_z + \tfrac{1}{2}\left(\hat{J}_+\hat{S}_- + \hat{J}_-\hat{S}_+\right)\right] \end{aligned} \tag{131}$$

with the advantage, that for the p system the basis functions $|J\,M_J\rangle$ can be used.

Basis functions of p–s: $|\,M_J\,M_S\,\rangle$, M_J referring to the p electron and M_S to the s electron

According to $g_{1/2} = \frac{2}{3}$ for $^2P_{1/2}$ (see eq. (2)), the De Gennes factor is $g_{1/2} - 1 = -\frac{1}{3}$, and $(g_J - 1)\boldsymbol{J}$ is the component $\boldsymbol{S}_J$ of $\boldsymbol{S}$ in direction of $\boldsymbol{J}$.

H-Matrix of operator (131):

$M_J M_S$	$\lvert \frac{1}{2}\ \frac{1}{2}\rangle$	$\lvert -\frac{1}{2}\ \frac{1}{2}\rangle$	$\lvert \frac{1}{2}\ -\frac{1}{2}\rangle$	$\lvert -\frac{1}{2}\ -\frac{1}{2}\rangle$
$\langle \frac{1}{2}\ \frac{1}{2}\rvert$	$\frac{1}{6}J_{\text{ex}}$			
$\langle -\frac{1}{2}\ \frac{1}{2}\rvert$		$-\frac{1}{6}J_{\text{ex}}$	$\frac{1}{3}J_{\text{ex}}$	
$\langle \frac{1}{2}\ -\frac{1}{2}\rvert$		$\frac{1}{3}J_{\text{ex}}$	$-\frac{1}{6}J_{\text{ex}}$	
$\langle -\frac{1}{2}\ -\frac{1}{2}\rvert$				$\frac{1}{6}J_{\text{ex}}$

(132)

Evaluation of the diagonal element H_{11}:

$$-2(-\tfrac{1}{3})J_{\text{ex}}\langle \tfrac{1}{2}\ \tfrac{1}{2}\,|\,\hat{J}_z\hat{S}_z\,|\,\tfrac{1}{2}\ \tfrac{1}{2}\rangle = (\tfrac{2}{3})J_{\text{ex}}(\tfrac{1}{2})\,(\tfrac{1}{2}) = \tfrac{1}{6}J_{\text{ex}}$$

Tab. 31: Functions and exchange energies of the $J = \frac{1}{2}$, $S = \frac{1}{2}$ system

Function	E
$\frac{1}{\sqrt{2}}\left(\lvert \frac{1}{2}\ -\frac{1}{2}\rangle - \lvert -\frac{1}{2}\ \frac{1}{2}\rangle\right)$	$-\frac{1}{2}J_{\text{ex}}$
$\lvert \frac{1}{2}\ \frac{1}{2}\rangle$ $\frac{1}{\sqrt{2}}\left(\lvert \frac{1}{2}\ -\frac{1}{2}\rangle + \lvert -\frac{1}{2}\ \frac{1}{2}\rangle\right)$ $\lvert -\frac{1}{2}\ -\frac{1}{2}\rangle$	$\frac{1}{6}J_{\text{ex}}$

---

[25] The complete set of basis functions of $^2P_{1/2}$ and $^2P_{3/2}$ is given Table 6.

Evaluation of the off-diagonal element H_{23}:

$$(\tfrac{2}{3})J_{\mathrm{ex}}\left\langle -\tfrac{1}{2}\ \tfrac{1}{2}\,\middle|\,(\tfrac{1}{2})\hat{J}_{-}\hat{S}_{+}\,\middle|\,\tfrac{1}{2}\ -\tfrac{1}{2}\right\rangle = (\tfrac{2}{3})J_{\mathrm{ex}}(\tfrac{1}{2})(1)(1) = \tfrac{1}{3}J_{\mathrm{ex}}$$

Result: Compared to the singlet-triplet splitting of an exchange-coupled s^1–s^1 molecule, the situation is inverted for a p^1–s^1 molecule if strong spin-orbit coupling within the p^1 system is taken into consideration: In the case of antiferromagnetic exchange coupling ($J_{\mathrm{ex}} < 0$), the triplet state is lowest in energy.

4.6.2 $\mathbf{Gd^{3+}}$–$\mathbf{Cu^{2+}}(\boldsymbol{S} = \mathbf{1/2})$

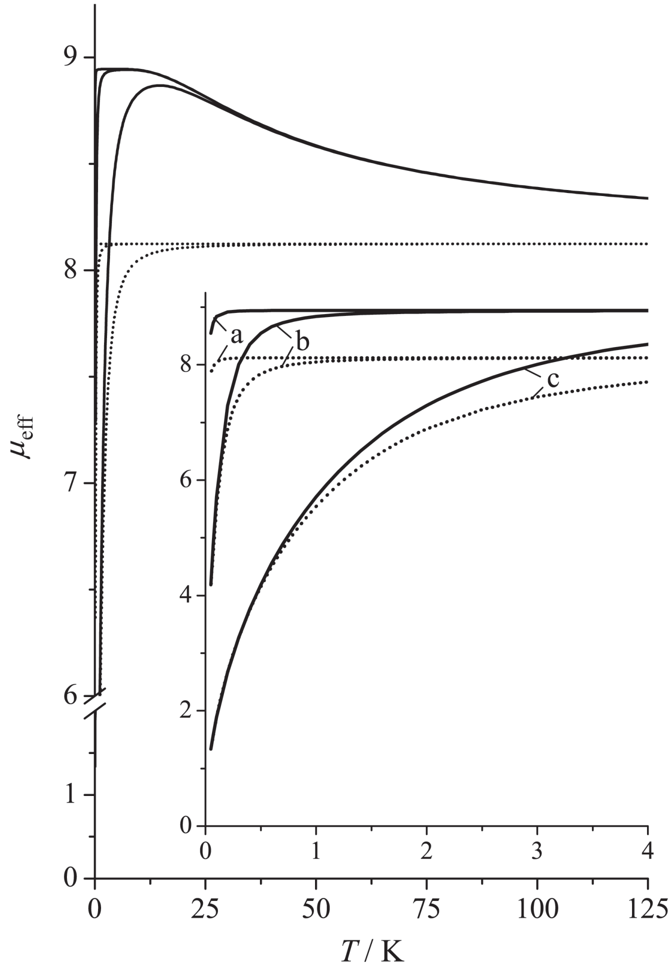

Fig. 39: μ_{eff} *vs.* T plot of a ferromagnetically coupled and an uncoupled Gd^{3+}–Cu^{2+} unit as a function of the applied field: $J_{\text{ex}} = 5\,\text{cm}^{-1}$ (solid lines), $J_{\text{ex}} = 0$ (dotted lines); $g_{\text{Gd}} = g_{\text{Cu}} = 2$; $B_0 = 0.01$ (a), 0.1 (b), 1.0 T (c).

The solid lines in Fig. 39 refer to a heterodinuclear Gd^{3+}–Cu^{2+} complex ($S_{\text{Gd}} = 7/2$; $S_{\text{Cu}} = 1/2$) of ferromagnetically coupled spins with the exchange parameter $J_{\text{ex}} = 5\,\text{cm}^{-1}$. Solely for $\boldsymbol{B}_0 = 0.01\,\text{T}$ (a) the expected plateau at $\mu_{\text{eff}} = 8.94$ is obtained at $T \leq 2\,\text{K}$ except for $T \leq 0.2\,\text{K}$. In order to adjust J_{ex} by fitting procedures to corresponding experimental data, it is justified to apply a susceptibility equation valid for $\boldsymbol{B}_0 \to 0$ (Van Vleck approach). For measurements with the stronger field 0.1 T (b) and all the more 1 T (c) deviations are obvious, which are not adequately described by the simple model. They could be misinterpreted, however, as an additional antiferromagnetic intermolecular spin-spin coupling. A similar problem arises if a corresponding uncoupled system is considered (Fig. 39, dotted lines). A straight line parallel to the T axis is obtained at $\mu_{\text{eff}} = 8.13$ for $\boldsymbol{B}_0 \to 0$ (curve a) while increasing deviations from this reference line to lower values are again obvious with increasing field (b, c), falsely interpreted as an intramolecular spin-spin coupling of antiferromagnetic nature. Hence, either the measurements are carried out at very weak applied fields or the extended susceptibility formula is used as in the given model calculations.

4.6.3 Ce^{3+}(cub)–Cu^{2+}($S = 1/2$)

After discussion of the p^1–s^1 case under the influence of $H_{\mathrm{SO}} + H_{\mathrm{ex}}$, we pass to the f^1–s^1 system perturbed by $H_{\mathrm{SO}} + H_{\mathrm{LF}} + H_{\mathrm{ex}}$. To clarify the computational procedures, the low-temperature magnetic behaviour of a system consisting of a $4\mathrm{f}^1$ ion, exchange-coupled to a pure spin system with $S = \frac{1}{2}$, is described with restricted basis functions. After switching on H_{SO} and $H_{\mathrm{LF}}^{\mathrm{oct}}$ acting on the Ce^{3+} ion, only the ground doublet Γ_7 (E'') is considered for spin-spin coupling with the ${}^2S_{1/2}$ system (represented here by $\mathrm{Cu}^{2+}[3\mathrm{d}^9]$). The procedure is outlined by three steps:

$$\begin{array}{ccc} 4\mathrm{f}^1 & \xrightarrow{H_{\mathrm{SO}}} & \boxed{{}^2F_{5/2}} + {}^2F_{7/2} \\ {}^2F_{5/2} & \xrightarrow{H_{\mathrm{LF}}^{\mathrm{oct}}} & \boxed{\Gamma_7} + \Gamma_8 \\ \Gamma_7 \otimes \Gamma_6 & \xrightarrow{H_{\mathrm{ex}}} & \boxed{\Gamma_2 \oplus \Gamma_5} \end{array}$$

The wave functions of the Ce^{3+} doublet Γ_7 are given in Tab. 32. The state is assumed to be thermally isolated (similar to ${}^2P_{1/2}$ of the p–s molecule (see section 4.6.1) on account of $H_{\mathrm{SO}} > H_{\mathrm{LF}}(\mathrm{oct}) \gg H_{\mathrm{ex}}$) and exchange-coupled to the $S = \frac{1}{2}$ pure spin system.

Table 32: Doublet wavefunctions of ${}^2F_{5/2}$ perturbed by a cubic ligand field

$\vert\Gamma\bar{M}\rangle$		$\vert M_J\rangle$	
$\vert E''\alpha''\rangle$	$=$	$\sqrt{\frac{1}{6}}\,\vert\frac{5}{2}\rangle - \sqrt{\frac{5}{6}}\,\vert-\frac{3}{2}\rangle$	Γ_7
$\vert E''\beta''\rangle$	$=$	$\sqrt{\frac{1}{6}}\,\vert-\frac{5}{2}\rangle - \sqrt{\frac{5}{6}}\,\vert\frac{3}{2}\rangle$	

Application of $\hat{H}_{\mathrm{ex}}$ (eq. (131)) with $g_J = \frac{6}{7}$ produces the 4×4 matrix given in scheme (133) which is similar to scheme (132), apart from the signs of the matrix elements:

$$\begin{array}{r|cccc} M_J M_S & \left|E''\alpha'',\frac{1}{2}\right\rangle & \left|E''\beta'',\frac{1}{2}\right\rangle & \left|E''\alpha'',-\frac{1}{2}\right\rangle & \left|E''\beta'',-\frac{1}{2}\right\rangle \\ \hline \left\langle E''\alpha'',\frac{1}{2}\right| & -\frac{5}{42}J_{\mathrm{ex}} & & & \\ \left\langle E''\beta'',\frac{1}{2}\right| & & \frac{5}{42}J_{\mathrm{ex}} & -\frac{5}{21}J_{\mathrm{ex}} & \\ \left\langle E''\alpha'',-\frac{1}{2}\right| & & -\frac{5}{21}J_{\mathrm{ex}} & \frac{5}{42}J_{\mathrm{ex}} & \\ \left\langle E''\beta'',-\frac{1}{2}\right| & & & & -\frac{5}{42}J_{\mathrm{ex}} \end{array} \tag{133}$$

Evaluation of the diagonal element H_{11} (De Gennes factor: $(g_J - 1) = \frac{6}{7} - 1 = -\frac{1}{7}$):

$$-2(-\tfrac{1}{7})J_{\mathrm{ex}}\left\langle E''\alpha'',\tfrac{1}{2}\right|\hat{J}_z\hat{S}_z\left|E''\alpha'',\tfrac{1}{2}\right\rangle = (\tfrac{2}{7})\left[(\tfrac{1}{6})(\tfrac{5}{2})(\tfrac{1}{2}) + (\tfrac{5}{6})(-\tfrac{3}{2})(\tfrac{1}{2})\right]J_{\mathrm{ex}} = -\tfrac{5}{42}J_{\mathrm{ex}}$$

Results:

$E_{\mathrm{singlet}} = \frac{15}{42}J_{\mathrm{ex}}$ $\qquad$ $E_{\mathrm{triplet}} = -\frac{5}{42}J_{\mathrm{ex}}$ $\qquad$ $\Delta E = E_{\mathrm{triplet}} - E_{\mathrm{singlet}} = -\frac{10}{21}J_{\mathrm{ex}}$

Simulation calculations: For $J_{\mathrm{ex}} > 0$, the triplet state Γ_5 is the ground state while for $J_{\mathrm{ex}} < 0$ the singlet Γ_2 has the lowest energy (as is predicted for the restricted basis).

Figs. 40 and 41 exhibit the corresponding μ_{eff} *vs.* T plots and Figs. 42 and 43 the χ_{m}^{-1} *vs.* T plots[26]. Inspecting Fig. 40 it is remarkable that at $T > 5\,\text{K}$ the antiferromagnetic spin-spin coupling yields higher μ_{eff} values than the ferromagnetic spin-spin coupling. This finding is the consequence of the fact that corresponding to Hund's third rule J is $L - S$ and that for a spin-spin coupling of antiferromagnetic nature the spin parts of the J–S dinuclear unit cancel to a certain degree, so that the orbital part is enhanced. As opposed to that, the spin-spin coupling of ferromagnetic nature leads to a further weakening of the orbital part of the 4f^1 configuration. The fact that the μ_{eff} values of the uncoupled Ce–Cu unit at $T < 2\,\text{K}$ are larger than the μ_{eff} values of both coupled systems is the consequence of the reduction of orbital parts according to the exchange splitting.

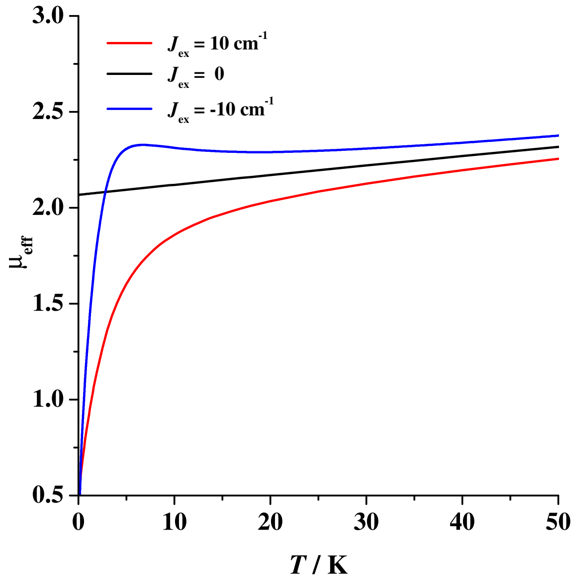

Fig. 40: μ_{eff} *vs.* T plot of an exchange-coupled Ce^{3+}–$\text{Cu}^{2+}(S = \frac{1}{2})$ unit; Ce in octahedral LF ($B_0^4 = 1\,100\,\text{cm}^{-1}$).

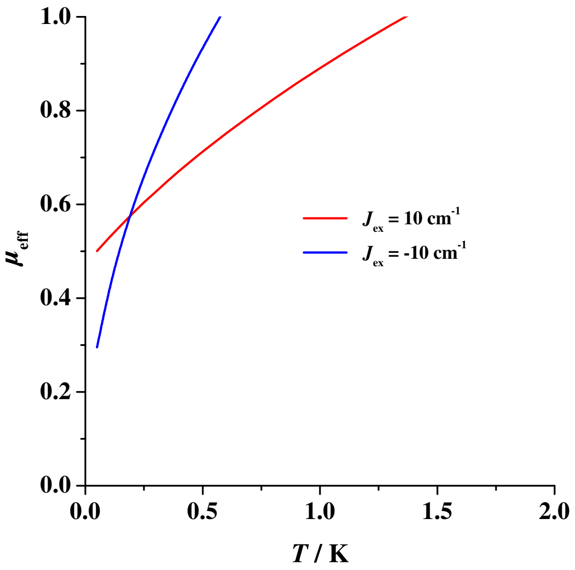

Fig. 41: μ_{eff} *vs.* T plot of an exchange-coupled Ce^{3+}–$\text{Cu}^{2+}(S = \frac{1}{2})$ unit at T <1.5 K; Ce in octahedral LF ($B_0^4 = 1\,100\,\text{cm}^{-1}$).

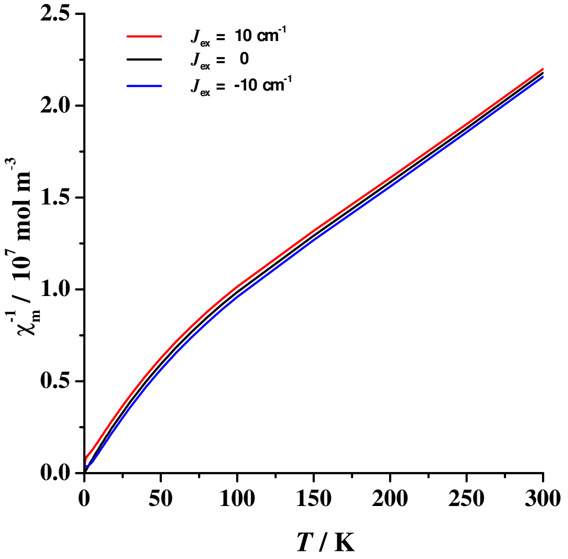

Fig. 42: χ_{m}^{-1} *vs.* T plot of the exchange-coupled Ce^{3+}(oct)–$\text{Cu}^{2+}(S = \frac{1}{2})$ unit.

Notice that, apart from the lowest temperatures, the spin-spin coupling produces small parallel shifts of the χ_{m}^{-1}–T curve of the uncoupled system (Fig. 42, black line). The shifts are described by

$$\left(\chi_{\text{m}}^{-1}\right)' = \chi_{\text{m}}^{-1} - \lambda_{\text{MF}}$$

where $\left(\chi_{\text{m}}^{-1}\right)'$ corresponds with the shifted curve and λ_{MF} is the molecular field parameter.

---

[26] The data presented in Figs. 40 – 43 have been calculated with the full basis set of 14 × 2 = 28 functions (using the computer program CONDON).

Fig. 43 displays that at $T < 5\,\mathrm{K}$ the blue curve ($J_{\mathrm{ex}} < 0$) tends to temperature independent paramagnetism (TIP), whereas the red curve ($J_{\mathrm{ex}} > 0$) exhibits Curie paramagnetism.

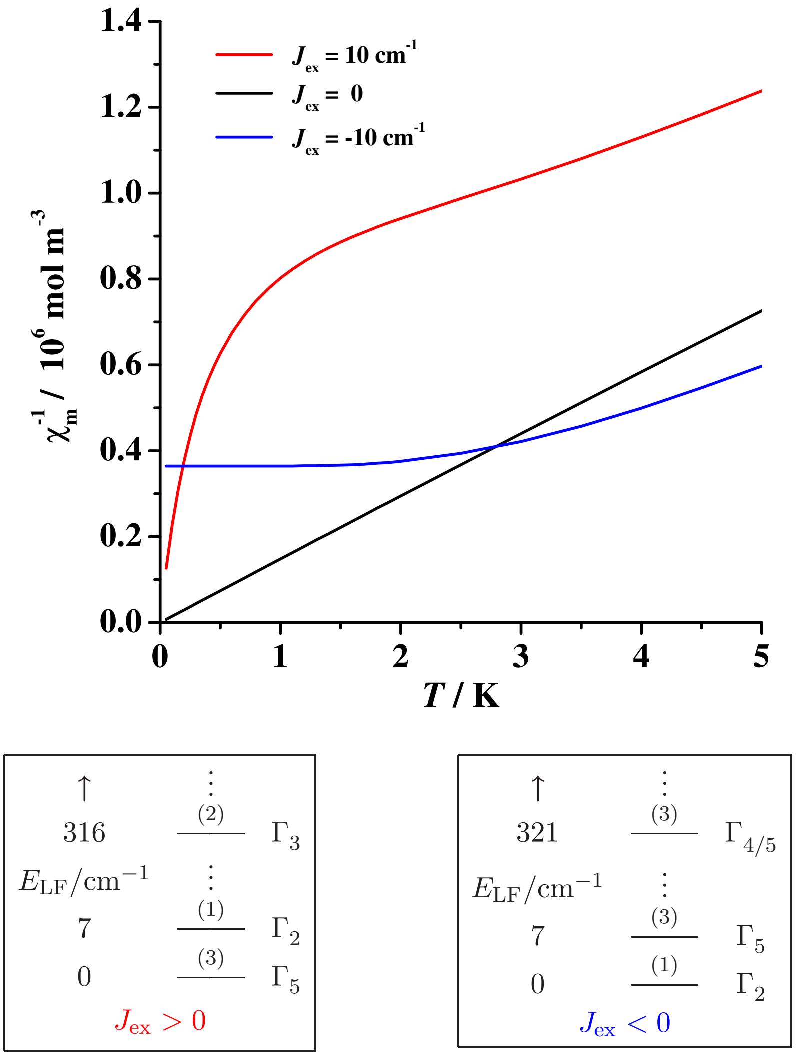

Fig. 43: $\left(\chi_{\mathrm{m}}^{-1}\right)$ *vs.* T plot of an exchange-coupled Ce^{3+}(oct)–Cu^{2+}($S = \frac{1}{2}$) unit, showing the crossing of the red and blue curve around 0.2 K and the energy splitting of the two lowest states Γ_5 and Γ_2 due to H_{ex}.

In Fig. 43 the black reference curve of the uncoupled system follows Curie's law in a good approximation on account of the thermally isolated states Γ_7(Ce) and Γ_6(Cu). Both states show linear χ_{m}^{-1}–T behaviour (apart from a very small 2^{nd} order Zeeman contribution of Γ_7).

4.6.4 Nd^{3+}(cub)–Cu^{2+}($S = 1/2$) and Nd^{3+}(cub)–Cr^{3+}($S = 3/2$)

Figs. 44 and 45 exhibit the μ_{eff} *vs.* T plots of the heterodinuclear species Nd–($S = \frac{1}{2}$) (Cu^{2+}) and Nd–($S = \frac{3}{2}$) (Cr^{3+}), respectively, in cubic LF. Inspecting both Figures it is remarkable that, similar to the Ce-Cu system (Figs. 40 – 43) the antiferromagnetic spin-spin coupling leads to higher μ_{eff} values than the ferromagnetic coupling on account of the fact that the residual component of the spin-spin coupling strengthens the orbital part of the lanthanide's moment.

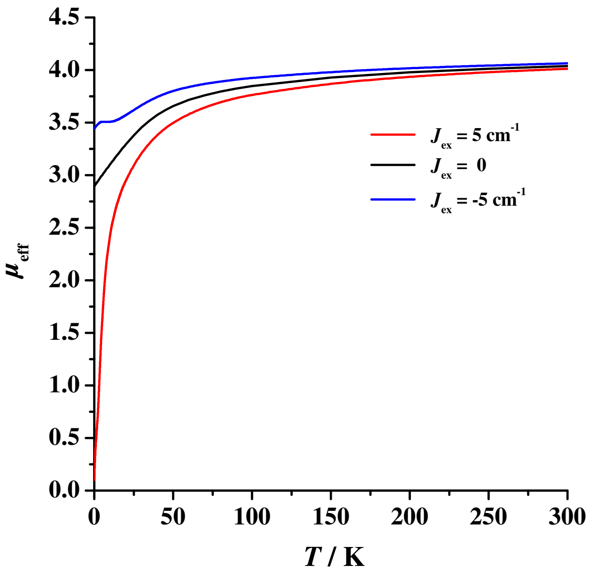

Fig. 44: μ_{eff} *vs.* T diagram of an exchange-coupled Nd^{3+}–Cu^{2+} unit with Nd in a cubic LF ($B_0^4 = 2\,000\,\text{cm}^{-1}$) and Cu regarded as a pure spin system $S = \frac{1}{2}$.

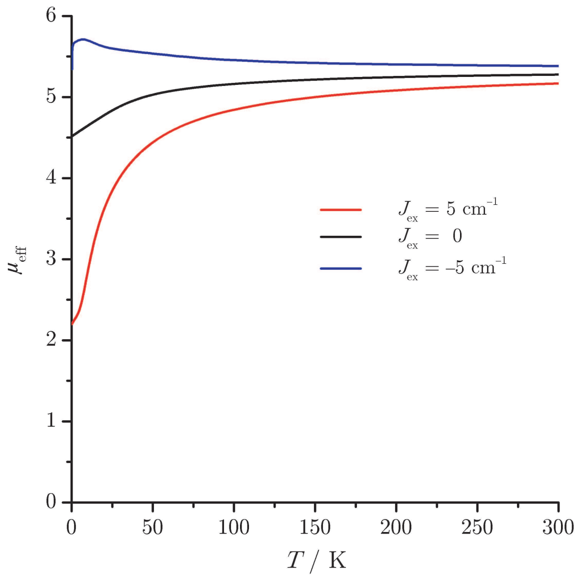

Fig. 45: μ_{eff} *vs.* T diagram of an exchange-coupled Nd^{3+}–Cr^{3+} unit with Nd in a cubic LF ($B_0^4 = 2\,000\,\text{cm}^{-1}$) and Cr regarded as a pure spin system $S = \frac{3}{2}$.

4.6.5 Dy^{3+}(cub)–Cu^{2+}($S = \frac{1}{2}$),Dy^{3+}(cyl)–Cr^{3+}($S = \frac{3}{2}$),Tb^{3+}(cyl)–Cr^{3+}($S = \frac{3}{2}$)

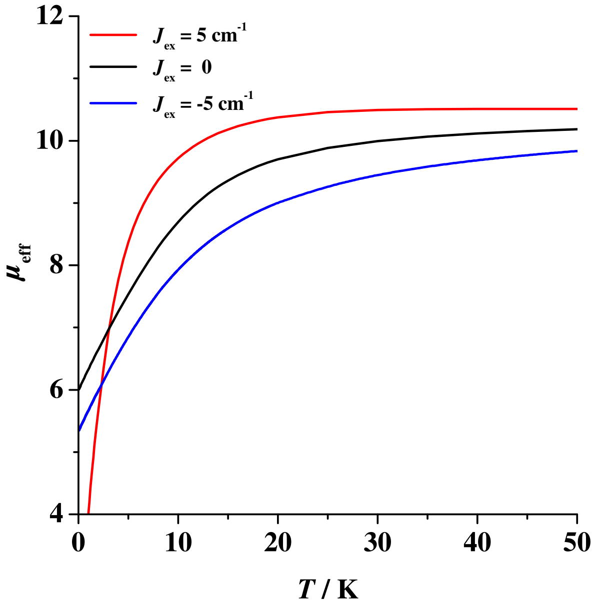

Fig. 46: μ_{eff} *vs.* T diagram of an exchange-coupled Dy^{3+}–Cu^{2+} unit where Dy is in a cubic LF ($B_0^4 = 2\,000\,\text{cm}^{-1}$) whereas Cu is regarded as a pure spin system $S = \frac{1}{2}$.

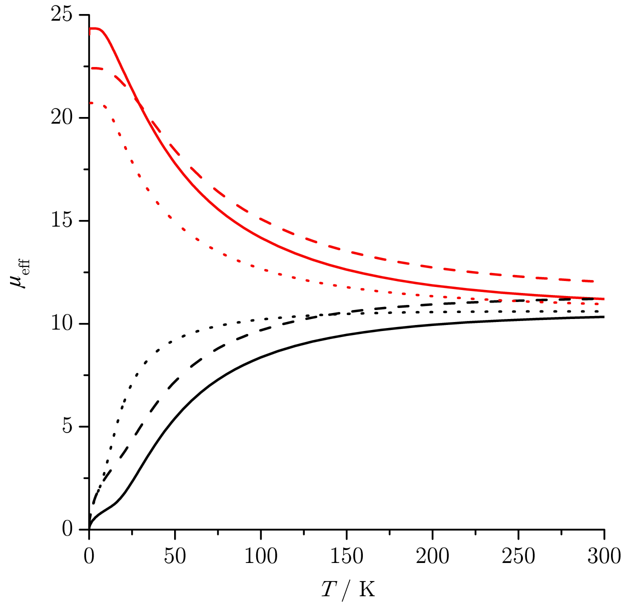

Fig. 47: Dy–Dy(cyl): ━━ $\mu_{\text{eff}}^{\|}$ ━━ $\mu_{\text{eff}}^{\perp}$
Dy(cyl)–Cr: ━ ━ $\mu_{\text{eff}}^{\|}$ ━ ━ $\mu_{\text{eff}}^{\perp}$
Tb(cyl)–Cr: ⋯⋯ $\mu_{\text{eff}}^{\|}$ ⋯⋯ $\mu_{\text{eff}}^{\perp}$

4.6.6 Gd^{3+}–V^{3+}

The 4f ion (Gd^{3+}, $^8S_{7/2}$) is regarded as a pure spin system, unaffected by ligands, zero-field splitting ignored. The electronic situation of the transition metal ion (for example V^{3+}) depends on H_{LF} and H_{SO}, demonstrated in Figure 48.

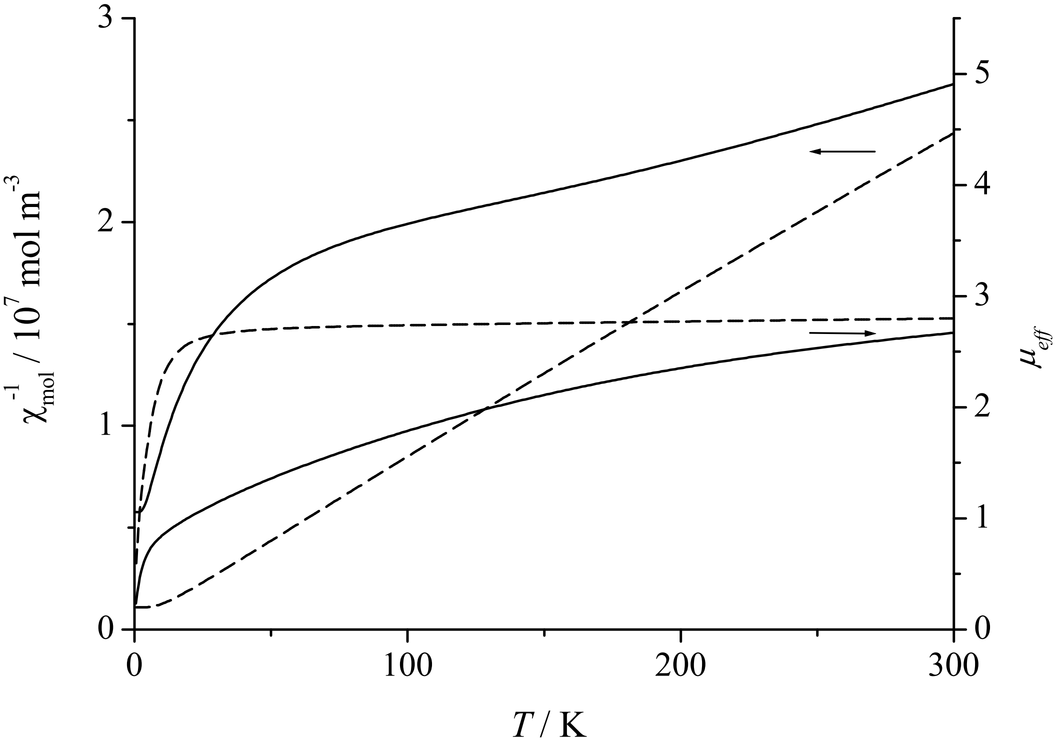

Fig. 48: μ_{eff} *versus* T and χ_{m}^{-1} *versus* T diagrams showing the predicted magnetic behaviour of $V^{3+}[3d^2]$ ion in octahedral (solid lines) and orthorhombic surrounding (dashed lines); parameter values [6]: Racah parameters $B = 861\,\mathrm{cm}^{-1}$, $C = 4\,165\,\mathrm{cm}^{-1}$, $\zeta = 209\,\mathrm{cm}^{-1}$, $B_0^4 = 25\,000\,\mathrm{cm}^{-1}$ for the octahedral coordination, $B_0^2 = -34\,000$, $B_2^2 = -16\,000$, $B_0^4 = 3\,500$, $B_2^4 = 1\,800$, $B_4^4 = 2\,300$ cm^{-1} for orthorhombic symmetry.

While the octahedral system shows between 100 K and 300 K nearly temperature independent paramagnetism, the orthorhombic one approximates to a Curie paramagnet with only slightly varying μ_{eff}. The two situations differ distinctly in the orbital contributions to the magnetic moment. The expected magnetic properties of the V^{3+}–Gd^{3+} unit is given in Figures 49 and 50).

If V^{3+} is octahedrally coordinated, μ_{eff} in the uncoupled situation ($J_{\mathrm{ex}} = 0$) is temperature dependent owing to the loss of magnetic activity of vanadium with decreasing temperature (see the solid reference line in Figure 49, $\mu_{\mathrm{eff}} = 8.37$ (300 K) $\rightarrow$ 8.05 (50 K)). When T approaches zero solely the magnetism of Gd^{3+} contributes. The uncoupled system with vanadium in orthorhombic symmetry, however, exhibits a temperature independent μ_{eff}, except for $T \leq 25$ K. This is the consequence of the nearly total quenching of orbital contributions of vanadium's valence electrons owing to the low-symmetric ligand field. In consequence, the transition metal ion behaves in a wide temperature range as a pure spin system $S = 1$.

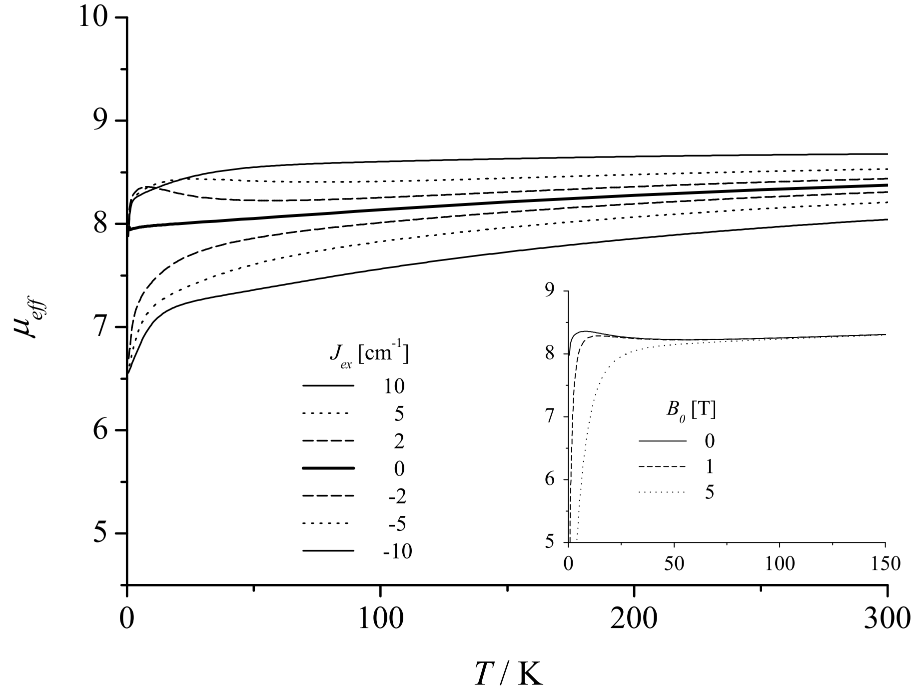

Fig. 49: μ_{eff} *versus* T diagram ($B_0 = 0$) showing the predicted magnetic behaviour of an exchange-coupled 3d^2(oct)–4f^7 species where $J_{\text{ex}} = 0, \pm2, \pm5, \pm10$ cm^{-1}; insert: model calculations for $J_{\text{ex}} = 2\,\text{cm}^{-1}$ and $B_0 = 0$, 1, and 5 T.

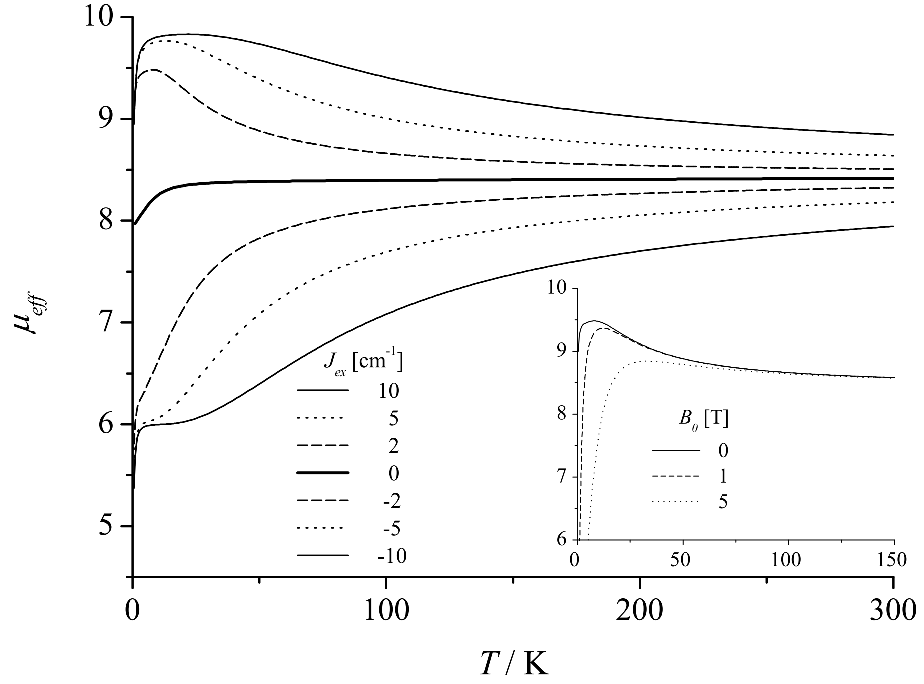

Fig. 50: μ_{eff} *versus* T diagram ($B_0 = 0$) showing the predicted magnetic behaviour of an exchange-coupled 3d^2(rhomb)–4f^7 species where $J_{\text{ex}} = 0, \pm2, \pm5, \pm10$ cm^{-1}; insert: model calculations for $J_{\text{ex}} = 2\,\text{cm}^{-1}$ and $B_0 = 0$, 1, and 5 T.

Switching on the intramolecular spin-spin coupling J_{ex} we see a distinct dependence of the magnetic properties on the sign of J_{ex} and the transition metal's symmetry: Regarding first the cubic case with a ferromagnetic coupling ($J_{\mathrm{ex}} > 0$), μ_{eff} increases, for antiferromagnetic coupling ($J_{\mathrm{ex}} < 0$) μ_{eff} decreases compared to the reference line. However, in contrast to pure spin systems, where we expect a plateau at low temperature, the course is more complicated reflecting the reduction of vanadium's paramagnetism. If the transition metal site has only orthorhombic symmetry significant alterations are ascertained in the course of μ_{eff} *versus* T: At low temperature plateaus become apparent at $\mu_{\mathrm{eff}} \approx 9.9$ and 5.9 for positive and negative J_{ex} corresponding to systems with total spin $S = 9/2$ and 5/2, respectively. The decrease of μ_{eff} at the lowest temperatures is again due to small orbital contributions of vanadium's electronic system.

Problems

9. The Bleaney-Bowers formula, eq. (127), approaches for high temperature the Curie-Weiss law $\chi_{\mathrm{m}} = C/(T-\theta)$. Determine the relation between J_{ex} and θ. Is the result in agreement with the relation $\theta = (2S(S+1)/3k_{\mathrm{B}})\sum_i z_i J_{\mathrm{ex}}$?
10. What magnetic behaviour is obtained, if in the Bleaney-Bowers formula, eq. (127), J_{ex} is set to 0?
11. What are the electronic ($4\mathrm{f}^N$) and the LF symmetry relevant preconditions for building up a homodinuclear Ln molecule with large μ_{eff} and high magnetic anisotropy?
12. Magnetochemical results are often presented as χ_{m}–T, χ_{m}^{-1}–T or μ_{eff}–T diagrams. What type of diagram is suited for (a) Curie paramagnetism, (b) intramolecular ferromagnetic interactions, (c) intramolekular antiferromagnetic interactions, (d) diamagnetic behaviour, (e) TUP behaviour?
13. To reliably characterise magnetic properties measurements at different field strength are essential. What is the reason?
14. A frequent mistake in magnetochemical investigations is the application of too strong magnetic fields. Why may this be unfavourable?
15. To evaluate the paramagnetic part of the susceptibility of a compound with macrocyclic ligands, the problem may occur that the incremental method for the diamagnetic correction is not as precise as necessary. What is to be done?
16. For a polynuclear complex one observes at high temperature Curie-Weiss behaviour with $\theta > 0$ and in the low-temperature region field-dependent susceptibilities. What magnetic collective effect can be expected?
17. With decreasing temperature the μ_{eff} data of a homodinuclear compound increase weakly and then, after passing a maximum at low temperature, steeply drop. (i) What is the reason for this behaviour? (ii) What model (susceptibility expression) should be tried to simulate the behaviour?
18. You notice that the paramagnetic properties of a homodinuclear molecular compound is not satisfactorily described with the corresponding eq. (128). What simple extensions of the model are in principle possible?

5 Solutions

1. Verify the Russell-Saunders ground multiplets for Nd^{2+} and Er^{3+} given in Table 2.

   $\mathrm{Nd}^{2+}[4\mathrm{f}^4]$: $L = 6,\ S = 2,\ J = 4 \Longrightarrow {}^5I_4$.
   $\mathrm{Er}^{3+}[4\mathrm{f}^{11}]$: $L = 6,\ S = 3/2,\ J = 15/2 \Longrightarrow {}^5I_{15/2}$.

2. Evaluate the susceptibility equation for a free p^1 system perturbed by spin-orbit coupling. (Hint: Apply eq. (3); note that for the single-electron system $\lambda_{LS} \equiv \zeta$.)

$$
\begin{aligned}
g_{1/2} &= 1 + \frac{\left(\frac{1}{2}\right)\left(\frac{3}{2}\right) + \left(\frac{1}{2}\right)\left(\frac{3}{2}\right) - 2}{2\left(\frac{1}{2}\right)\left(\frac{3}{2}\right)} = \tfrac{2}{3} \\
g_{3/2} &= 1 + \frac{\left(\frac{3}{2}\right)\left(\frac{5}{2}\right) + \left(\frac{1}{2}\right)\left(\frac{3}{2}\right) - 2}{2\left(\frac{3}{2}\right)\left(\frac{5}{2}\right)} = \tfrac{4}{3} \\
\Lambda_{1/2} &= \left(\tfrac{2}{3}\right)^2\left(\tfrac{1}{2}\right)\left(\tfrac{3}{2}\right) + 2\left(\tfrac{2}{3} - 1\right)\left(\tfrac{2}{3} - 2\right)\tfrac{k_\mathrm{B}T}{\zeta} = \tfrac{1}{3} + \tfrac{8\,k_\mathrm{B}T}{9\,\zeta} \\
\Lambda_{3/2} &= \left(\tfrac{4}{3}\right)^2\left(\tfrac{3}{2}\right)\left(\tfrac{5}{2}\right) + 2\left(\tfrac{4}{3} - 1\right)\left(\tfrac{4}{3} - 2\right)\tfrac{k_\mathrm{B}T}{\zeta} = \tfrac{20}{3} - \tfrac{4\,k_\mathrm{B}T}{9\,\zeta}
\end{aligned}
$$

$$
\begin{aligned}
\chi_\mathrm{m} &= \mu_0 \frac{N_\mathrm{A}\mu_\mathrm{B}^2}{3k_\mathrm{B}T} \times \frac{\mathrm{Z}}{\mathrm{N}}, \quad \text{where} \\
\mathrm{Z} &= 2\left(\tfrac{1}{3} + \tfrac{8\,k_\mathrm{B}T}{9\,\zeta}\right)\exp\left(-\tfrac{3\,\zeta}{8\,k_\mathrm{B}T}\right) + 4\left(\tfrac{20}{3} - \tfrac{4\,k_\mathrm{B}T}{9\,\zeta}\right)\exp\left(-\tfrac{15\,\zeta}{8\,k_\mathrm{B}T}\right) \\
\mathrm{N} &= 2\exp\left(-\tfrac{3\,\zeta}{8\,k_\mathrm{B}T}\right) + 4\exp\left(-\tfrac{15\,\zeta}{8\,k_\mathrm{B}T}\right)
\end{aligned}
$$

$$
\boxed{\chi_\mathrm{m} = \mu_0 \frac{N_\mathrm{A}\mu_\mathrm{B}^2}{3k_\mathrm{B}T}\,\frac{\left[\dfrac{1}{3} + \dfrac{8\,k_\mathrm{B}T}{9\,\zeta} + \left(\dfrac{40}{3} - \dfrac{8\,k_\mathrm{B}T}{9\,\zeta}\right)\exp\left(-\dfrac{3\,\zeta}{2\,k_\mathrm{B}T}\right)\right]}{\left[1 + 2\,\exp\left(-\dfrac{3\zeta}{2k_\mathrm{B}T}\right)\right]}} \tag{134}
$$

   To verify eq. (134), it is recommended to develop the susceptibility equation for the borderline case $\zeta \to 0$ (use the approximation $\exp \pm x \approx 1 \pm x$). For an uncoupled system the relation $\mu = \sqrt{L(L+1) + 4S(S+1)}\,\mu_\mathrm{B}$ holds, so that for the p^1 system ($L = 1$, $S = 1/2$) the permanent magnetic moment $\mu = \sqrt{5}\,\mu_\mathrm{B}$ and the susceptibility equation $\chi_\mathrm{m} = \mu_0\,5N_\mathrm{A}\mu_\mathrm{B}^2/(3k_\mathrm{B}T)$ must be the results.

3. Use the spherical harmonics in Table 3 and construct the real functions $\mathrm{d}_{x^2-y^2}$ and d_{xy} with the help of eqs. (8). Verify the results with the data given in Table 4.

$$
\begin{aligned}
\tfrac{1}{\sqrt{2}}\left[\psi_{n,l,m_l} + \psi_{n,l,-m_l}\right] &= \tfrac{1}{\sqrt{2}}\left[\sqrt{\tfrac{15}{32\pi}}\,\sin^2\theta\,(\cos 2\phi + \mathrm{i}\sin 2\phi + \cos 2\phi - \mathrm{i}\sin 2\phi)\right] \\
&= \sqrt{\tfrac{15}{16\pi}}\,\sin^2\theta\cos 2\phi = \mathrm{d}_{x^2-y^2} \\
\tfrac{1}{\sqrt{2}}\left[\psi_{n,l,m_l} - \psi_{n,l,-m_l}\right] &= \tfrac{1}{\mathrm{i}\sqrt{2}}\left[\sqrt{\tfrac{15}{32\pi}}\,\sin^2\theta\,(\cos 2\phi + \mathrm{i}\sin 2\phi - \cos 2\phi + \mathrm{i}\sin 2\phi)\right] \\
&= \sqrt{\tfrac{15}{16\pi}}\,\sin^2\theta\sin 2\phi = \mathrm{d}_{xy}
\end{aligned}
$$

4. Calculate the matrix elements $\langle l, m_l|\hat{l}_q|l, m_l'\rangle$ (where q stands for $z, +, -$): (a) $\langle 0,0|\hat{l}_z|0,0\rangle$, (b) $\langle 2,2|\hat{l}_+|2,1\rangle$, (c) $\langle 2,2|\hat{l}_+^2|2,0\rangle$, (d) $\langle 2,0|\hat{l}_+\hat{l}_-|2,0\rangle$. (Hint: Apply eqs. (20))

   (a) $\langle 0,0|\hat{l}_z|0,0\rangle = 0$ (b) $\langle 2,2|\hat{l}_+|2,1\rangle = \sqrt{2\cdot 3 - 1\cdot 2}\,\hbar\,\underbrace{\langle 2,2|2,2\rangle}_{1} = 2\,\hbar$

   (c) $\langle 2,2|\hat{l}_+^2|2,0\rangle = \sqrt{6}\,\hbar\langle 2,2|\hat{l}_+|2,1\rangle = 2\sqrt{6}\,\hbar^2\,\underbrace{\langle 2,2|2,2\rangle}_{1} = 2\sqrt{6}\,\hbar^2$

   (d) $\langle 2,0|\hat{l}_+\hat{l}_-|2,0\rangle = \sqrt{6}\,\hbar\langle 2,0|\hat{l}_+|2,-1\rangle = \sqrt{6+(-1+1)}\,\hbar\,\sqrt{6}\,\hbar\,\underbrace{\langle 2,0|2,0\rangle}_{1} = 6\,\hbar^2$

5. The 14 microstates $|m_l m_s\rangle$ of an f^1 system ($l = 3$, $s = \frac{1}{2}$) yield under the influence of spin-orbit coupling 14 eigenstates $|jm_j\rangle$ which, apart from the states $|\frac{7}{2}\ \pm\frac{7}{2}\rangle$ are linear combinations of two microstates each. Use Table 7 to evaluate the vector coupling coefficients for the coupled states $|\frac{5}{2}\ \frac{1}{2}\rangle$, $|\frac{5}{2}\ -\frac{1}{2}\rangle$, $|\frac{7}{2}\ \frac{3}{2}\rangle$, and $|\frac{7}{2}\ -\frac{3}{2}\rangle$. Control your results with the entries of Table 8.

   $\left|\,\frac{5}{2}\,\frac{1}{2}\,\right\rangle = a\,\left|\,1\,-\frac{1}{2}\,\right\rangle + b\,\left|\,0\,\frac{1}{2}\,\right\rangle$
   Assignments: $j = \frac{5}{2}$, $m = m_j$, $j_1 = l = 3$, $m_2 = m_s = \pm\frac{1}{2}$ $(j_2 = s = \frac{1}{2})$
   $a = \sqrt{\frac{j_1+m+\frac{1}{2}}{2j_1+1}} = \sqrt{\frac{3+\frac{1}{2}+\frac{1}{2}}{7}} = \sqrt{\frac{4}{7}}$ $b = -\sqrt{\frac{j_1-m+\frac{1}{2}}{2j_1+1}} = -\sqrt{\frac{3-\frac{1}{2}+\frac{1}{2}}{7}} = -\sqrt{\frac{3}{7}}$ [27]
   $\left|\,\frac{5}{2}\,-\frac{1}{2}\,\right\rangle = a\,\left|-1\,\frac{1}{2}\,\right\rangle + b\,\left|\,0\,-\frac{1}{2}\,\right\rangle$
   $a = -\sqrt{\frac{j_1-m+\frac{1}{2}}{2j_1+1}} = -\sqrt{\frac{3+\frac{1}{2}+\frac{1}{2}}{7}} = -\sqrt{\frac{4}{7}}$ $b = \sqrt{\frac{j_1+m+\frac{1}{2}}{2j_1+1}} = \sqrt{\frac{3-\frac{1}{2}+\frac{1}{2}}{7}} = \sqrt{\frac{3}{7}}$
   $\left|\,\frac{7}{2}\,\frac{3}{2}\,\right\rangle = a\,\left|\,2\,-\frac{1}{2}\,\right\rangle + b\,\left|\,1\,\frac{1}{2}\,\right\rangle$
   Assignments: $j = \frac{7}{2}$, $m = m_j$, $j_1 = l = 3$, $m_2 = m_s = \pm\frac{1}{2}$ $(j_2 = s = \frac{1}{2})$
   $a = \sqrt{\frac{j_1-m+\frac{1}{2}}{2j_1+1}} = \sqrt{\frac{3-\frac{3}{2}+\frac{1}{2}}{7}} = \sqrt{\frac{2}{7}}$ $b = \sqrt{\frac{j_1+m+\frac{1}{2}}{2j_1+1}} = \sqrt{\frac{3+\frac{3}{2}+\frac{1}{2}}{7}} = \sqrt{\frac{5}{7}}$
   $\left|\,\frac{7}{2}\,-\frac{3}{2}\,\right\rangle = a\,\left|-2\,\frac{1}{2}\,\right\rangle + b\,\left|-1\,-\frac{1}{2}\,\right\rangle$
   $a = \sqrt{\frac{j_1+m+\frac{1}{2}}{2j_1+1}} = \sqrt{\frac{3-\frac{3}{2}+\frac{1}{2}}{7}} = \sqrt{\frac{2}{7}}$ $b = \sqrt{\frac{j_1-m+\frac{1}{2}}{2j_1+1}} = \sqrt{\frac{3+\frac{3}{2}+\frac{1}{2}}{7}} = \sqrt{\frac{5}{7}}$

6. What levels (multiplets J) may arise from the terms (a) ^1S, (b) ^2P, (c) ^3P, (d) ^3D, (e) ^4D? How many states (distinguished by the quantum number M_J) belong to each level?

   (a) ^1S: $J = 0$ (1 state)
   (b) ^2P: $J = \frac{1}{2}$ (2), $J = \frac{3}{2}$ (4)
   (c) ^3P: $J = 0$ (1), $J = 1$ (3), $J = 2$ (5)
   (d) ^3D: $J = 1$ (3), $J = 2$ (5), $J = 3$ (7)
   (e) ^4D: $J = \frac{1}{2}$ (2), $J = \frac{3}{2}$ (4), $J = \frac{5}{2}$ (6), $J = \frac{7}{2}$ (8)

7. Determine the crystal field overall splitting (CFOS) for the Dy^{3+} ion in $\mathrm{Cs_2NaDyCl_6}$ on the basis of Fig. 35. Apply eqs. (102) and (103) as well as the entries in Table 23 and take the B_0^4 and B_0^6 values for Dy from Table 16.

$$\beta_J\tilde{F}(4)B_0^4 \;=\; Wx = -\left(\frac{8}{135\,135}\right)\left(\frac{15}{2}\right)\times 1\,614\,\mathrm{cm}^{-1} = -0.7166\,\mathrm{cm}^{-1}$$

---

[27] According to the phase convention one has to change the sign of a and b (*cf.* Example 2.3).

$$\begin{aligned}\gamma_J \tilde{F}(6) B_0^6 &= W(1-|x|) = \left(\frac{4}{3\,864\,861}\right)\left(\frac{3465}{4}\right) \times 148\,\mathrm{cm}^{-1} = 0.1327\,\mathrm{cm}^{-1} \\ \frac{x}{1-|x|} &= -5.401 \qquad \Longrightarrow \qquad x = -0.8438, \quad W = 0.8493\end{aligned}$$

On account of $W > 0$ the E_{LF}/W axis points upwards. Consequently, the LF ground state at $x = -0.8438$ is Γ_6. The corresponding LF state of highest energy is $\Gamma_8^{(3)}$. The energy separation $\Delta E_{\mathrm{LF}}/W$ between $\Gamma_8^{(3)}$ and Γ_6 is 490 cm^{-1}, so that CFOS $= \Delta E_{\mathrm{LF}} = 490 \times 0.8493\,\mathrm{cm}^{-1} = 416\,\mathrm{cm}^{-1}$, in agreement with the data given in ref. [26], p. 2591.

8. In which respect does the magnetic susceptibility of a mononuclear lanthanide systems with Ln point symmetry (i) $\mathrm{O_h}$, (ii) $\mathrm{D_{\infty h}}$, (iii) $\mathrm{D_{2h}}$ differ?

   (i) $\mathrm{O_h}$: isotropic (cubic) system ($\chi_x = \chi_y = \chi_z$)
   (ii) $\mathrm{D_{\infty h}}$: anisotropic (cylindrical) system ($\chi_x = \chi_y \neq \chi_z$)
   (iii) $\mathrm{D_{2h}}$: anisotropic (orthorhombic) system ($\chi_x \neq \chi_y \neq \chi_z$)

9. The Bleaney-Bowers formula, eq. (127), approaches at high temperature the Curie-Weiss law $\chi_{\mathrm{m}} = C/(T-\theta)$. Determine the relation between J_{ex} and θ. Is the result in agreement with the relation $\theta = [2S(S+1)/3k_{\mathrm{B}}] \sum_i z_i J_{\mathrm{ex},i}$?

$$\begin{aligned}\chi_{\mathrm{m}} &= \mu_0 \frac{N_{\mathrm{A}}\mu_{\mathrm{B}}^2 g^2}{3k_{\mathrm{B}}T} \frac{1}{\left[1 + \frac{1}{3}\exp\left(\frac{-2J_{\mathrm{ex}}}{k_{\mathrm{B}}T}\right)\right]} \qquad\qquad (\exp \pm x \approx 1 \pm x \quad \text{for} \quad x \to 0) \\ &\approx \mu_0 \frac{N_{\mathrm{A}}\mu_{\mathrm{B}}^2 g^2}{3k_{\mathrm{B}}} \frac{1}{T\left(\frac{4}{3} - \frac{2J_{\mathrm{ex}}}{3k_{\mathrm{B}}T}\right)} = \frac{\mu_0 N_{\mathrm{A}}\mu_{\mathrm{B}}^2 g^2}{T\left(4k_{\mathrm{B}} - \frac{2J_{\mathrm{ex}}}{T}\right)} = \frac{\mu_0 N_{\mathrm{A}}\mu_{\mathrm{B}}^2 g^2}{3k_{\mathrm{B}}\left(T - \frac{J_{\mathrm{ex}}}{2k_{\mathrm{B}}}\right)}\left(\frac{3}{4}\right) \\ \theta &= \frac{J_{\mathrm{ex}}}{2k_{\mathrm{B}}}; \qquad [2S(S+1)/3k_{\mathrm{B}}] \sum_i z_i J_{\mathrm{ex},i} = \frac{J_{\mathrm{ex}}}{2k_{\mathrm{B}}} \quad \text{for} \quad S = \tfrac{1}{2}, i = 1, z_i = 1\end{aligned}$$

10. What magnetic behaviour is obtained, if in the Bleaney-Bowers formula, eq. (127), J_{ex} is set to 0?

$$\chi_{\mathrm{m}} = \mu_0 \frac{N_{\mathrm{A}}\mu_{\mathrm{B}}^2 g^2}{3k_{\mathrm{B}}T} \frac{1}{\left[1 + \frac{1}{3}\exp\left(\frac{-2J_{\mathrm{ex}}}{k_{\mathrm{B}}T}\right)\right]} \xrightarrow{J_{\mathrm{ex}}=0} \chi_{\mathrm{m}} = \frac{N_{\mathrm{A}}\mu_{\mathrm{B}}^2 g^2}{3k_{\mathrm{B}}T}\left(\frac{3}{4}\right) \qquad \text{Curie law}$$

11. What are the electronic ($4\mathrm{f}^N$) and LF symmetrical preconditions for building up a homodinuclear Ln molecule with large μ_{eff} and high magnetic anisotropy?

    (i) Ln from the second half of the Ln series (on account of free ion ground states with $J = L + S$);
    (ii) Ln with half-integer J (nonmagnetic LF ground states of the Ln ion are ruled out);
    (iii) Ln with large S and large L;
    (iv) anisotropic LF, for example unique axis anisotropy (cylindrical, hexagonal, tetragonal)

12. Magnetochemical results are often presented as χ_m–T, χ_m^{-1}–T or μ_{eff}–T plots. What type of diagram is suited for molecular systems showing (a) Curie paramagnetism, (b) intramolecular ferromagnetic interactions, (c) intramolekular antiferromagnetic interactions, (d) diamagnetic behaviour, (e) TUP behaviour?

    (a) χ_m^{-1}–T (b) μ_{eff}–T (c), (d), (e) χ_m–T

13. To reliably characterise magnetic properties measurements at different field strength are essential. What is the reason?

    To furnish proof of (i) ferromagnetic impurities, (ii) magnetic ordering effects

14. A frequent mistake in magnetochemical investigations is the application of too strong magnetic fields. Why may this be unfavourable?

    Weak magnetic ordering effects may be overlooked.

15. To evaluate the paramagnetic part of the susceptibility of a compound with macrocyclic ligands, the problem may occur that the incremental method for the diamagnetic correction is not as precise as necessary. What is to be done?
    Measurement of the magnetic susceptibility of the ligand.

16. For a polynuclear complex one observes at high temperature Curie-Weiss behaviour with $\theta > 0$ and in the low-temperature region field-dependent susceptibilities. What magnetic collective effect can be expected?
    Ferromagnetism

17. With decreasing temperature the μ_{eff} data of a homodinuclear compound increase weakly and then, after passing a maximum at low temperature, steeply drop. (i) What is the reason for this behaviour? (ii) What model (susceptibility expression) should be tried to simulate the behaviour?
    (i) Intramolecular spin-spin coupling of ferromagnetic nature, intermolecular spin-spin coupling of antiferromagnetic nature.
    (ii) Consideration of a molecular field parameter λ_{MF}: $\chi_m^{-1} = (\chi_m')^{-1} - \lambda_{\text{MF}}$

18. You notice that the paramagnetic properties of a homodinuclear molecular compound is not satisfactorily described with the corresponding eq. (128). What simple extensions of the model are in principle possible?
    (i) Addition of a TIP term χ_0;
    (ii) Consideration of intermolecular exchange interactions by a molecular field parameter λ_{MF}.

6 Appendix 1

6.1 Magnetic quantities

Table 33: Definitions, units and conversion factors [5]

Quantity		SI	CGS-emu	Factor[a]
μ_0	Permeability of vacuum	$\mu_0 = 4\pi \times 10^{-7}$ H/m[b]	1	
$\boldsymbol{B}$	Magnetic induction	$\boldsymbol{B} = \mu_0(\boldsymbol{H} + \boldsymbol{M})$ T = Vs/m^2	$\boldsymbol{B} = \boldsymbol{H}^{(\mathrm{ir})} + 4\pi \boldsymbol{M}$ G	10^{-4} T/G
$\boldsymbol{H}$	Magnetic field strength	$\boldsymbol{H}$ A/m	Oe	$\frac{10^3}{4\pi}$ (A m^{-1})/Oe
$\boldsymbol{B}_0$	”Magnetic field”	$\boldsymbol{B}_0 = \mu_0 \boldsymbol{H}$ T = Vs/m^2	G	10^{-4} T/G
$\boldsymbol{M}$	Magnetization	$\boldsymbol{M}$ A/m	G	10^3 (A/m)/G
$\boldsymbol{m}$	Magnetic dipole moment	$\boldsymbol{m} = \boldsymbol{M}V$ Am^2 = J/T	$\boldsymbol{m} = \boldsymbol{M}V$ G cm^3	10^{-3} Am^2/Gcm^3
$\boldsymbol{m}/\mu_\mathrm{B}$		1	1	1
μ_B	Bohr magneton	$\mu_\mathrm{B} = e\hbar/(2m_\mathrm{e})$ Am^2	$\mu_\mathrm{B} = e\hbar/(2m_\mathrm{e})$ Gcm^3	10^{-3} Am^2/Gcm^3
$\boldsymbol{\sigma}$	specific magnetic dipole moment[d]	$\boldsymbol{\sigma} = \boldsymbol{M}/\rho^c$ Am^2/kg	$\boldsymbol{\sigma} = \boldsymbol{M}/\rho$ Gcm^3/g	$1\ \frac{\mathrm{Am^2/kg}}{\mathrm{Gcm^3/g}}$
$\boldsymbol{M}_\mathrm{m}$	Molar magnetization[f]	$\boldsymbol{M}_\mathrm{m} = \boldsymbol{M}M/\rho^e$ Am^2/mol	$\boldsymbol{M}_\mathrm{m} = \boldsymbol{M}M/\rho$ Gcm^3/mol	10^{-3} Am^2/Gcm^3
$\boldsymbol{\mu}_\mathrm{a}$	Atomic magnetic dipole moment[g]	$\boldsymbol{\mu}_\mathrm{a} = \boldsymbol{M}_\mathrm{m}/(N_\mathrm{A}\mu_\mathrm{B})$ Am^2	$\boldsymbol{\mu}_\mathrm{a} = \boldsymbol{M}_\mathrm{m}/(N_\mathrm{A}\mu_\mathrm{B})$ Gcm^3	
$\mu_\mathrm{a}/\mu_\mathrm{B}$		1	1	1
χ	Magnetic volume susceptibility	$\boldsymbol{M} = \chi \boldsymbol{H}$ 1	$\boldsymbol{M} = \chi^{(\mathrm{ir})} \boldsymbol{H}^{(\mathrm{ir})}$ 1	4π
χ_g	Magnetic mass susceptibility	$\chi_\mathrm{g} = \chi/\rho$ m^3/kg	$\chi_\mathrm{g}^{(\mathrm{ir})} = \chi^{(\mathrm{ir})}/\rho$ cm^3/g	$\frac{4\pi}{10^3}\ \frac{\mathrm{m^3/kg}}{\mathrm{cm^3/g}}$
χ_m	Molar magnetic susceptibility	$\chi_\mathrm{m} = \chi\, M/\rho$ m^3/mol	$\chi_\mathrm{m}^{(\mathrm{ir})} = \chi^{(\mathrm{ir})}\, M/\rho$ cm^3/mol	$4\pi/10^6$ m^3/cm^3
μ_eff	Effective Bohr magneton number [2]	$[3k_\mathrm{B}/\mu_0 N_\mathrm{A} \mu_\mathrm{B}^2]^{1/2} [\chi_\mathrm{m} T]^{1/2}$ 1	$[3k_\mathrm{B}/\mu_0 N_\mathrm{A} \mu_\mathrm{B}^2]^{1/2} [\chi_\mathrm{m} T]^{1/2}$ 1	1

---

[a] Multiplicative factor applied to the value in CGS-emu units to obtain the value in SI units.

[b] H = Henry; H/m = Vs/(Am).

[c] ρ = mass density.

[d] Specific magnetization; $\boldsymbol{\sigma}^s$ = specific saturation magnetization.

[e] M = molar mass.

[f] $\boldsymbol{M}_\mathrm{m}^\mathrm{s}$ = molar saturation magnetization.

[g] $\boldsymbol{\mu}_\mathrm{a}^\mathrm{s}$ = atomic magnetic saturation moment.

- The legal SI units are not generally accepted. The CGS-emu system is still widely used in magnetochemistry. Therefore, use magnetic quantities which are independent of the two systems, e. g., μ_{eff} or μ_{eff}^2 instead of $\chi_{\mathrm{m}}T$.

- Do not mix the systems, e. g., use G (Gauss) instead of T (Tesla) in the CGS-emu system.

- Use $\boldsymbol{B}_0 = \mu_0 \boldsymbol{H}$ in graphical representations (conversion factor 10^{-4} T/Oe).

6.2 Energy equivalents and conversion factors

Tab. 34: Energy equivalents and conversion factors

	J	eV	s^{-1}	cm^{-1}	K	T	kJ/mol
1 J	1	6.24151×10^{18}	1.50919×10^{33}	5.03411×10^{22}	7.24292×10^{22}	1.07828×10^{23}	6.02214×10^{20}
1 eV	1.0218×10^{-19}	1	2.1799×10^{14}	8.6554×10^{3}	1.6045×10^{4}	1.72760×10^{4}	9.64853×10^{1}
1 s^{-1}	6.62607×10^{-34}	4.13567×10^{-15}	1	3.33564×10^{-11}	4.79922×10^{-11}	7.14477×10^{-11}	3.99031×10^{-13}
1 cm^{-1}	1.98645×10^{-23}	1.23984×10^{-4}	2.99792×10^{10}	1	1.43877	2.14195	1.19626×10^{-2}
1 K	1.38066×10^{-23}	8.61739×10^{-5}	2.08367×10^{10}	6.95039×10^{-1}	1	1.48874	8.31451×10^{-3}
1 T	9.27402×10^{-24}	5.78839×10^{-5}	1.39963×10^{10}	4.66864×10^{-1}	6.71710×10^{-1}	1	5.58494×10^{-3}
1 kJ/mol	1.66054×10^{-21}	1.03642×10^{-2}	2.50607×10^{12}	8.35933×10^{1}	1.20272×10^{2}	1.79053×10^{2}	1

7 Appendix 2: Matrix elements of operator equivalents

Tab. 35: Matrix elements of the operator equivalents $\tilde{O}_0^4$ [20]

J	$\tilde{F}(4)^{a)}$	$\langle M_J \vert\vert M_J \rangle$								
		$\pm\frac{1}{2}$	$\pm\frac{3}{2}$	$\pm\frac{5}{2}$	$\pm\frac{7}{2}$	$\pm\frac{9}{2}$	$\pm\frac{11}{2}$	$\pm\frac{13}{2}$	$\pm\frac{15}{2}$	
$\frac{5}{2}$	15/2	2	−3	1	–	–	–	–	–	
$\frac{7}{2}$	15/2	9	−3	−13	7	–	–	–	–	
$\frac{9}{2}$	21/2	18	3	−17	−22	18	–	–	–	
$\frac{11}{2}$	15	28	12	−13	−33	−27	33	–	–	
$\frac{13}{2}$	15/2	108	63	−13	−92	−132	−77	143	–	
$\frac{15}{2}$	15/2	189	129	23	−101	−201	−221	−91	273	
		0	±1	±2	±3	±4	±5	±6	±7	±8
4	15/2	18	9	−11	−21	14	–	–	–	–
5	105/2	6	4	−1	−6	−6	6	–	–	–
6	15/2	84	64	11	−54	−96	−66	99	–	–
7	3/2	756	621	251	−249	−704	−869	−429	1001	–
8	105/2	36	31	17	−3	−24	−39	−39	−13	52

[a)] In ref. [20] the respective products $\tilde{F}(4) \times \tilde{O}_0^4$ etc. are listed.

Tab. 36: Matrix elements of the operator equivalents $\tilde{O}_{\pm 4}^4$ [20]

J	$\tilde{F}(44)$	$\langle M_J \vert\vert M_J - 4 \rangle$						
		$\langle\frac{5}{2}\vert\vert -\frac{3}{2}\rangle$	$\langle\frac{7}{2}\vert\vert -\frac{1}{2}\rangle$	$\langle\frac{9}{2}\vert\vert\frac{1}{2}\rangle$	$\langle\frac{11}{2}\vert\vert\frac{3}{2}\rangle$	$\langle\frac{13}{2}\vert\vert\frac{5}{2}\rangle$	$\langle\frac{15}{2}\vert\vert\frac{7}{2}\rangle$	
$\frac{5}{2}$	$3\sqrt{35/2}$	$\sqrt{5}$	–	–	–	–	–	
$\frac{7}{2}$	$3\sqrt{35/2}$	$5\sqrt{3}$	$\sqrt{35}$			–	–	
$\frac{9}{2}$	$21\sqrt{5/2}$	$5\sqrt{3}$	$5\sqrt{2}$	$3\sqrt{2}$	–	–	–	
$\frac{11}{2}$	$3\sqrt{35}$	35	$3\sqrt{105}$	$5\sqrt{21}$	$\sqrt{165}$	–	–	
$\frac{13}{2}$	$3\sqrt{35/2}$	$42\sqrt{5}$	$35\sqrt{6}$	$15\sqrt{22}$	$15\sqrt{11}$	$\sqrt{715}$		
$\frac{15}{2}$	$3\sqrt{35/2}$	$42\sqrt{15}$	$10\sqrt{231}$	$15\sqrt{77}$	$5\sqrt{429}$	$\sqrt{5005}$	$\sqrt{1365}$	
		$\langle 2\vert\vert -2\rangle$	$\langle 3\vert\vert -1\rangle$	$\langle 4\vert\vert 0\rangle$	$\langle 5\vert\vert 1\rangle$	$\langle 6\vert\vert 2\rangle$	$\langle 7\vert\vert 3\rangle$	$\langle 8\vert\vert 4\rangle$
4	$3\sqrt{35/2}$	15	$5\sqrt{7}$	$\sqrt{70}$	–	–	–	–
5	$3\sqrt{35/2}$	35	$5\sqrt{42}$	$3\sqrt{70}$	$\sqrt{210}$	–	–	–
6	$3\sqrt{35/2}$	70	$21\sqrt{10}$	$15\sqrt{14}$	$5\sqrt{66}$	$3\sqrt{55}$	–	–
7	$3\sqrt{35/2}$	126	$70\sqrt{3}$	$5\sqrt{462}$	$15\sqrt{33}$	$5\sqrt{143}$	$\sqrt{1001}$	–
8	$3\sqrt{35/2}$	210	$6\sqrt{1155}$	$15\sqrt{154}$	$5\sqrt{1001}$	$\sqrt{15\,015}$	$5\sqrt{273}$	$2\sqrt{455}$

Tab. 37: Matrix elements of the operator equivalents $\tilde{O}_0^6$ [20]

J	$\tilde{F}(6)$	$\langle M_J\|\|M_J\rangle$								
		$\pm\frac{1}{2}$	$\pm\frac{3}{2}$	$\pm\frac{5}{2}$	$\pm\frac{7}{2}$	$\pm\frac{9}{2}$	$\pm\frac{11}{2}$	$\pm\frac{13}{2}$	$\pm\frac{15}{2}$	
$\frac{5}{2}$	0	0	0	0	–	–	–	–	–	
$\frac{7}{2}$	315/4	−5	9	−5	1	–	–	–	–	
$\frac{9}{2}$	315	−8	6	10	−11	3	–	–	–	
$\frac{11}{2}$	945/2	−20	4	25	11	−31	11	–	–	
$\frac{13}{2}$	135	−200	−25	185	227	−11	−319	143	–	
$\frac{15}{2}$	3465/4	−75	−25	45	87	59	−39	−117	65	
		0	±1	±2	±3	±4	±5	±6	±7	±8
4	315/4	−20	1	22	−17	4	–	–	–	–
5	315/2	−40	−12	36	29	−48	15	–	–	–
6	945/2	−40	−20	22	43	8	−55	22	–	–
7	945/4	−200	−125	50	197	176	−55	−286	143	–
8	3465/4	−120	−85	2	93	128	65	−78	−169	104

Tab. 38: Matrix elements of the operator equivalents $\tilde{O}_{\pm4}^6$ [20]

J	$\tilde{F}(64)$	$\langle M_J\|\|M_J-4\rangle$						
		$\langle\frac{5}{2}\|\|-\frac{3}{2}\rangle$	$\langle\frac{7}{2}\|\|-\frac{1}{2}\rangle$	$\langle\frac{9}{2}\|\|\frac{1}{2}\rangle$	$\langle\frac{11}{2}\|\|\frac{3}{2}\rangle$	$\langle\frac{13}{2}\|\|\frac{5}{2}\rangle$	$\langle\frac{15}{2}\|\|\frac{7}{2}\rangle$	
$\frac{5}{2}$	0	0	–	–	–	–	–	
$\frac{7}{2}$	$45\sqrt{14}/4$	$-7\sqrt{3}$	$3\sqrt{35}$	–	–	–	–	
$\frac{9}{2}$	$315\sqrt{2}/4$	$-16\sqrt{3}$	$6\sqrt{2}$	$30\sqrt{2}$	–	–	–	
$\frac{11}{2}$	$135\sqrt{7}/2$	−63	$-\sqrt{105}$	$13\sqrt{21}$	$7\sqrt{165}$	–	–	
$\frac{13}{2}$	$135\sqrt{14}/2$	$-56\sqrt{5}$	$-21\sqrt{6}$	$13\sqrt{22}$	$46\sqrt{11}$	$6\sqrt{715}$	–	
$\frac{15}{2}$	$495\sqrt{14}/4$	$-42\sqrt{15}$	$-6\sqrt{231}$	$3\sqrt{77}$	$7\sqrt{429}$	$3\sqrt{5005}$	$5\sqrt{1365}$	
		$\langle2\|\|-2\rangle$	$\langle3\|\|-1\rangle$	$\langle4\|\|0\rangle$	$\langle5\|\|1\rangle$	$\langle6\|\|2\rangle$	$\langle7\|\|3\rangle$	$\langle8\|\|4\rangle$
4	$135\sqrt{14}/4$	−14	$-\sqrt{7}$	$2\sqrt{70}$	–	–	–	–
5	$45\sqrt{14}/4$	−168	$-13\sqrt{42}$	$12\sqrt{70}$	$15\sqrt{210}$	–	–	–
6	$135\sqrt{14}/4$	−168	$-35\sqrt{10}$	$8\sqrt{14}$	$21\sqrt{66}$	$28\sqrt{55}$	–	–
7	$45\sqrt{14}/4$	−1260	$-546\sqrt{3}$	$-6\sqrt{462}$	$147\sqrt{33}$	$126\sqrt{143}$	$45\sqrt{1001}$	–
8	$495\sqrt{14}/4$	−252	$-6\sqrt{1155}$	$-6\sqrt{154}$	$3\sqrt{1001}$	$2\sqrt{15\,015}$	$19\sqrt{273}$	$12\sqrt{455}$

References

[1] A. F. Williams, *A Theoretical Approach to Inorganic Chemistry*, Springer, Berlin (1979).

[2] J. H. Van Vleck, *Electric and Magnetic Susceptibilities*, Oxford University Press, Oxford 1932.

[3] E. U. Condon, G. H. Shortley, *The Theory of Atomic Spectra*, University Press, Cambridge 1970; p. 179.

[4] A. Abragam, B. Bleaney, Electron Paramagnetic Resonance of Transition Ions, Clarendon Press, Oxford 1970; p. 289.

[5] (a) S. Hatscher, H. Schilder, H. Lueken, W. Urland: Practical Guide to Measurements and Interpretation of Magnetic Properties (IUPAC Technical Report), *Pure Appl. Chem.* **2005**, *77*, 497 - 511; (b) German version: *Angew. Chem.* **2006**, *118*, 8283 - 8240.

[6] J. S. Griffith, *The Theory of Transition-Metal Ions*, Cambridge University Press, Cambridge, 1971.

[7] H. Lueken, *Magnetochemie*, Teubner, Stuttgart, Leipzig 1999.

[8] H. L. Schläfer, G. Gliemann, *Einführung in die Ligandenfeldtheorie*, Akad. Verlagsges., Wiesbaden 1980; engl. edition: *Basic Principles of Ligand Field Theory*, Wiley-Interscience, New York 1969.

[9] P. W. Atkins, R. S. Friedman, *Molecular Quantum Mechanics*, 4th ed., Oxford University Press, Oxford 2005.

[10] H. Bethe, Termaufspaltung in Kristallen, *Ann. Phys.* **1929**, *5*, 133 - 208; further publication of this article in: Symmetry in chemical theory, Benchmark papers in inorganic chemistry, vol. 4, ed. J. P. Fackler, Jr., Dowden, Hutchinson, Ross, Inc. 1973 (ISBN: 0-87933-018-X).

[11] C. J. Ballhausen, *Ligand Field Theory*, McGraw-Hill, New York 1962.

[12] H. Schilder, H. Lueken, Computerized magnetic studies on d, f, d–d, f–f, and d–S, f–S systems under varying ligand and magnetic fields *J. Magn. Magn. Mater.* **2004**, *281*, 17- 26.

[13] P. A. Tanner, V. V. Ravi Kanth Kumar, C. K. Jayasankar, M. F. Reid, Analysis of spectral data and comparative energy level parametrizations for Ln^{3+} in cubic elpasolite crystals, *J. Alloys Comp.* **1994**, *215*, 349 - 370.

[14] M. J. Reisfeld, G. A. Crosby, Analysis of the absorption spectrum of cesium uranium(V) hexafluoride, *Inorg. Chem.* **1965**, *4*, 65 - 70.

[15] C. Görller-Walrand, K. Binnemans, *Rationalization of Crystal-Field Parametrization*, in K. A. Gschneidner, Jr., L. Eyring, *Handbook on the Physics and Chemistry of Rare Earths*, Elsevier, Amsterdam 1996, vol. 23, ch. 155, p. 121 - 283.

[16] K. R. Lea, M. J. M. Leask, W. P. Wolf: The Raising of Angular Momentum Degeneracy of f-Electronic Terms by Cubic Crystal Fields, *J. Phys. Chem. Solids*, **1962**, *23*, 1381 - 1405.

[17] D. Smith, J. H. M. Thornley, The use of operator equivalents, *Proc. Phys. Soc.* **1966**, *89*, 779.

[18] K. W. H. Stevens, Matrix elements and operator equivalents connected with the magnetic properties of rare earth ions, *Proc. Phys. Soc. A [London]* **1952**, *65*, 209.

[19] R. J. Elliott, K. W. H. Stevens, *Proc. Roy. Soc. A [London]* **1953**, *218*, 553.

[20] R. J. Birgeneau, Tables of matrix elements of Racah tensor operator equivalents, *Can. J. Phys.* **1967**, *45*, 3761 - 3771.

[21] M. Hutchings, Point-charge calculations of energy levels of magnetic ions in crystalline electric fields, *Solid State Phys.* **1964**, *16*, 227.

[22] A. J. Kassman, Relationships between the coefficients of the tensor operator and operator equivalent methods, *J. Chem. Phys.* **1970**, *53*, 4118 - 4119.

[23] R. J. Elliott, K. W. H. Stevens, The Theory of magnetic resonance experiments on salts of the rare earths *Proc. Phys. Soc.* **1953**, *A 218*, 553.

[24] H. Lueken, M. Meier, G. Klessen, W. Bronger, J. Fleischhauer, *J. Less-Common Met.* **1979**, *63*, P35 - P44.

[25] A. Schröder, R. van den Berg, H. von Löhneysen, H. Lueken, *Solid state commun.* **1988**, *65*, 99 - 101.

[26] C. A. Morrison, R. P. Leavitt, and D. E. Wortman, *J. Chem. Phys.* **1980**, *73*, 2580 - 2598.